Neurobiology Underlying Modulatory Action
of
Prefrontal Corticotropin Releasing Factor Neurons
on
Sustained Attention

by

Spencer Cooke

A dissertation submitted in partial fulfillment

of the requirements for the degree of

Doctor of Philosophy

(Neuroscience)

at the

UNIVERSITY OF WISCONSIN-MADISON

2026

Date of final oral examination: April 16, 2026

This dissertation is approved by the following members of the Final Oral Committee:

Craig W. Berridge, Professor, Psychology

Lauren Riters, Associate Professor, Integrative Biology

Brian A. Baldo, Associate Professor, Psychiatry

Ari Rosenberger, Assistant Professor, Neuroscience

Corinna Burger, Professor, Neurology

Acknowledgements

There are so many experiences, emotions, and events that define the journey to a PhD. The immense joy and gratitude I feel after having spent the better part of the last decade working towards this achievement is difficult to express, and none of it would be possible without the countless people and acts of kindness that made my journey possible.

I would like to start by thanking my mentor Craig Berridge, through whose example and close mentorship I have become the scientist I am today. Your scientific approach and attention to detail will remain standards that I will continue to strive towards in my career.

I am thankful for my committee members; Drs. Ari Rosenber, Brian Baldo, Corrinna Burger, and Lauren Riters, who have been an invaluable source of information and introduced me to novel perspectives that propelled my research to the next level.

To our lab manager Andrea Martin, I am so grateful for your amazing depth of knowledge in things both technical and general as well as you sense of humor. Working with you has made long days not only bearable but also a blast. To Shannon Nicole, I am forever grateful for your invaluable help with tissue collection and imaging. To Rob Spencer, I am thankful for your foundational work setting up so many of the systems and equipment that allow our lab to function in addition to your great jokes and tireless work ethic. To the students that I have mentored with over the years; Greta Missbach, Jaylene Muñoz, Jenna Kiraly, Nicole Sitgler, Julia Xiong, and Jane Liu, thank you for your patience, your consistency, and your dedication as we both learned and grew together.

To my close friends, Wilder Rees, Dr. Iskander Said, Gabe Oswalt, Hunter Roth, Adam Hunter, Sean Carter, Ben Steele, James Hollingsworth, Dr. Kurt Berckmueller, Dr. Anna Belford, Dr. Jacob Gluski, Dr. Bikalpa Ghimire, and Dr. Brandon Polzin, thank you for the laughs you have provided that have made this journey infinitely lighter.

To my family, my mom; Ann Stabolepszy, my dad; Christopher Cooke, my brother; Malcolm Cooke, my cousin; Andrew Kikawa, my aunt; Eve Kikawa, and my uncle; Brent Kikawa. Thank you for always being a sunny oasis and an endless fountain of support during my PhD journey.

And finally, to my partner and fellow PhD traveler, Candice Malone, I cannot thank you enough for your unending understanding, support, and advice that has been my north star during my PhD. All the hard days and long nights were worth it just for having met you.

Table of Contents

Abstract

The prefrontal cortex (PFC) supports higher cognitive processes that are dysregulated in multiple psychopathologies. Development of treatments for this form of cognitive dysfunction is hindered by our limited understanding of the neurobiology of PFC-dependent cognition. Prior studies demonstrate the medial PFC of rats contains a dense population of corticotropin-releasing factor (CRF) neurons. Activation of caudal dorsomedial PFC (dmPFC) CRF neurons disrupts both working memory and sustained attention via differing projection pathways. A series of studies was conducted to better understand the neurobiology of CRF-dependent cognitive actions. We observed heterogeneity in the neurochemical identity of caudal dmPFC CRF neurons: glutamatergic CRF (CRF_{Glu}) neurons comprise a majority (85%), while the remaining were identified as GABAergic (CRF_{GABA}). Caudal dmPFC CRF_{GABA} neuronal activation impaired working memory but not sustained attention, while CRF_{Glu} neuronal activation impaired both. The working memory actions of both subpopulations were dependent on caudal dmPFC CRF receptors. The regions involved in the sustained attention actions of CRF_{Glu} neurons are unknown. Anterograde tracing demonstrated the lateral mediodorsal thalamus (MD) receives a remarkably dense innervation from caudal dmPFC CRF neurons. Activation of CRF receptors or caudal dmPFC CRF axons in the lateral MD impaired sustained attention. The sustained attention actions of PFC CRF_{Glu} neurons were associated with reductions in signal-related spiking activity of caudal dmPFC neurons, event-independent increases in theta/alpha and decreases in beta/gamma oscillatory power in the PFC, and an increase in reward-related theta/alpha frontothalamic synchrony. These studies provide novel insight into the neurobiology of higher cognitive function.

Chapter 1

Introduction

I. The PFC and Cognition

The PFC plays a vital role in higher cognitive functions that guide goal-directed behavior, particularly in the presence of distractors and ambiguity. Thus, lesions of the PFC impair performance in tests of working memory, planning, and response selection (Funahashi et al., 1993; Passingham, 1975; Tizard, 1958). These cognitive functions are supported by, or encoded in, the firing patterns of PFC neurons. For example, foundational experiments in monkeys identified the presence of a subpopulations of dorsolateral PFC neurons that display elevated firing during the delay period of working memory tasks (J. M. Fuster & Alexander, 1971; Kojima & Goldman-Rakic, 1982). Similar delay-related neurons were also identified in the medial PFC of rodents (Batuev et al., 1990; Devilbiss et al., 2012; Jung et al., 1998). The sustained nature of delay-related firing is thought to involve recurrent circuitry within the PFC (Datta & Arnsten, 2018; Devilbiss, Jenison, et al., 2012; Goldman-Rakic, 1995; Wang et al., 2013; Wang, 2001). Subsequent studies identified subpopulations of PFC neurons tuned to different goal-related stimuli such as reward and error cues, signals that predict outcomes, and periods of sustained attention (Batuev et al., 1990; Devilbiss et al., 2017; Niki & Watanabe, 1979; Sakurai & Takahashi, 2006; Spencer et al., 2015; Watanabe, 1989, 1990, 1992; Wu et al., 2017). In addition to encoding of cognitive task-relevant information in neural firing, fluctuations in local field potential (LFP) oscillations and oscillatory synchrony have been proposed to reflect information processing in the PFC, and connected regions, during cognitive task performance (Arski et al., 2021; Benchenane et al., 2011).

The PFC supports higher cognitive function via connections with a variety of cortical and subcortical regions. This includes topographically organized projections to the striatum and medial dorsal thalamus (MD). Thus, in rodents, the dorsomedial PFC (dmPFC) preferentially innervates the dorsomedial striatum (dmSTR) and lateral MD and is closely associated with higher cognitive function, while the ventromedial PFC (vmPFC) preferentially targets the ventromedial striatum (vmSTR) and medial MD, and is associated with motivation/reward related processes (Chudasama & Robbins, 2006; Phillips et al., 2021; Voorn et al., 2004). Consistent with this, extensive evidence indicates that inactivation or lesion of the dmSTR or lateral MD lead to cognitive deficits comparable to those seen with manipulations of the dmPFC (O'Callaghan et al., 2014; Wolff & Halassa, 2024). Moreover, dmSTR and MD neurons display working memory-related activity similar to that observed in the PFC (Aosaki et al., 1995; Chiba et al.,

2015; J. M. Fuster & Alexander, 1973; Hupalo, Bryce, et al., 2019; Parnaudeau et al., 2018a; Rikhye et al., 2018; Schmidt et al., 2019; Tanibuchi & Goldman-Rakic, 2003; Y. Watanabe & Funahashi, 2004, 2012). In addition to dorsoventral topography, the rat medial PFC also displays functional and anatomical topography in the rostrocaudal dimension. For example, limited anatomical studies show denser projections from rostral prelimbic PFC areas to rostral portions of the nucleus accumbens and medial MD, while caudal prelimbic PFC sends projections to dorsal nucleus accumbens, caudal dorsal STR, and lateral MD (Gorelova & Yang, 1996; Hoover & Vertes, 2007; Sesack et al., 1989a). Additionally, pharmacological manipulations across dorsal vs. ventral and rostral vs. caudal medial PFC have been observed to elicit different behavioral actions (see below).

II. Catecholamine Modulation of PFC-Dependent Cognition

Extensive evidence indicates that PFC-dependent cognition is modulated by catecholamine signaling within the PFC (Berridge & Arnsten, 2015). Thus, in tests of working memory, both low and high rates of dopamine (DA) D1 receptor activation leads to impairment, while moderate rates of D1 receptor activation supports high levels of performance (A. F. Arnsten et al., 2010, 2012; Vijayraghavan et al., 2007). A similar inverted-U modulation of working memory is observed with norepinephrine (NE). However, in this case optimal performance is dependent on high-affinity postsynaptic α2A receptors while high rates of NE release engage working memory-impairing and lower affinity α1 and β1 receptors (A. F. Arnsten, 2009a; A. F. Arnsten & Pliszka, 2011; Berridge et al., 2012; Paspalas et al., 2013; M. Wang et al., 2007).

These behavioral actions of DA and NE receptors are paralleled by modulatory actions on coding properties of PFC neurons. Thus, α2 receptors have been demonstrated to enhance the signal-to-noise ratio of delay-related signaling by strengthening the activity of delay-tuned neurons, while α1 receptors decrease this ratio by increasing the activity of neurons not tuned to delay (A. F. Arnsten et al., 2010, 2012; Gamo et al., 2010; Vijayraghavan et al., 2007). For DA, moderate levels of D1 receptor activation suppresses the activity of neurons not tuned to delay while high rates of D1 receptor activation enhances the activity of the broader population of PFC neurons (A. F. Arnsten et al., 2012; Vijayraghavan et al., 2007).

Importantly, there exists heterogeneity in the receptor mechanisms regulating distinct PFC-dependent cognitive processes. Thus, while NE α1 receptors impair working memory, they facilitate both focused and flexible attention (Lapiz & Morilak, 2006; Spencer & Berridge, 2019). Consistent with the above-described functional topography of the medial PFC in rodents, the cognitive actions of PFC catecholamines are topographically organized. Thus, dorsoventrally, catecholamines act in the dmPFC, but not vmPFC, to modulate working memory and sustained attention (Spencer & Berridge, 2019; Arnsten et al., 1999) while, rostrocaudally, NE acts in the caudal, but not rostral, dmPFC to modulate sensory gating (Alsene et al., 2011).

III. Corticotropin Releasing Factor and Regulation of Cognition

Corticotropin releasing factor (CRF) is a 41-amino acid neuropeptide released by the hypothalamus to regulate the pituitary-adrenal axis and the secretion of corticosteroids in stress (Deussing & Chen, 2018; Klavdieva, 1995). Following the isolation and characterization of CRF in 1981 (Vale et al., 1981), it was discovered that CRF-synthesizing neurons and axons are found in a variety of extrahypothalamic brain structures (Bale & Vale, 2004; Bloom et al., 1982; Deussing & Chen, 2018; Fink, 1981; Saffran et al., 1955; Vale et al., 1981). These include the central nucleus of the amygdala, the bed nucleus of the stria terminalis, and much of neocortex (Olschowka et al., 1982; Swanson et al., 1983a). Within the cortex, CRF neurons are observed widely, and are particularly dense in the PFC. In rodents, CRF neurons are found throughout the rostrocaudal extent of the medial PFC and across layers II, III, and V-VI (Charlton et al., 1987; Sakanaka et al., 1987).

CRF binds to two receptors: $CRFR_1$ and $CRFR_2$ (Bale & Vale, 2004). Both receptors are G-protein coupled receptors linked to either G_s, G_q, G_i, or G_o intracellular signaling (Grammatopoulos et al., 2001). In the rat, $CRFR_1$ mRNA is present throughout the PFC, while $CRFR_2$ mRNA is expressed in very low levels (De Souza et al., 1985; Lovenberg et al., 1995a; Potter et al., 1994). As $CRFR_1$ has a tenfold greater affinity for CRF than $CRFR_2$, $CRFR_1$ is considered the primary CRF receptor of the rodent PFC (Perrin et al., 1995). Interestingly, in primates, both $CRFR_1$ and $CRFR_2$ are found in the frontal cortex (Chalmers et al., 1995; Kostich et al., 1998; Van Pett et al., 2000).

PFC CRF and Cognition. Despite intense study of CRF in subcortical circuits, the actions of PFC CRF have been largely overlooked for most of the past half-century. Limited studies demonstrate that CRF acts within rodent PFC to modulate stress related behavior and physiology (George et al., 2012; Meng et al., 2011a). However, until recently, the role of PFC CRF in higher cognition was unknown. A series of recent studies by our lab demonstrate that both CRF neurons and receptors within the PFC modulate higher cognitive function (Berridge et al., 2022; Hupalo et al., 2021; Hupalo, Martin, et al., 2019; Hupalo & Berridge, 2016). To examine the cognitive actions of PFC CRF neurons, we developed a dual viral approach in which the first virus encoded Cre-recombinase under the control of the CRF promoter (AAV8-CRFp) while the second virus encoded excitatory (hM3Dq) or inhibitory (hM4Di) DREADD receptors and a reporter protein, mCherry, in a Cre-dependent manner (AAV8-DIO-hM3Dq/hM4Di). In male rats we observed that chemogenetic activation of caudal dmPFC CRF neurons impaired working memory performance (Figure 1). Working memory impairment was not observed when control virus lacking the DREADD transgene was infused into the caudal dmPFC (Figure 1) or when CRF neurons in the rostral dmPFC or ventromedial (rostral or caudal) PFC were activated (Hupalo et al., 2019). Working memory impairment elicited by activation of caudal dmPFC CRF neurons was dependent on local (caudal dmPFC) CRF receptors in a PKA-dependent manner (Figure 2) and was associated with a robust degradation in PFC neuronal coding of key task events (delay, reward; Figure 3; Hupalo et al., 2019).

Additional studies demonstrated that activation and suppression of caudal dmPFC CRF neurons also impaired and improved, respectively, performance in an operant signal detection task of PFC-dependent sustained attention (Figure 4; Hupalo et al., 2021). However, despite the similar actions of caudal dmPFC CRF neurons across working memory and sustained attention, these actions were dependent on highly distinct projection pathways. Thus, the working memory impairing actions of caudal dmPFC CRF neurons are dependent on local caudal dmPFC receptors, while the sustained attention effects of these neurons was independent of PFC CRF receptors. Consistent with this, direct activation and blockade of caudal, but not rostral, dmPFC CRF receptors (via local infusions of CRF or an antagonist) impaired and improved working memory, respectively, while having no effect on sustained attention (Figure 5).

Sex-Dependent Working Memory Effects of PFC CRF Neurotransmission. Sex differences exist in certain actions of CRF (Bangasser et al., 2011, 2013; Valentino et al., 2013). We recently demonstrated similar working memory effects of caudal dmPFC CRF receptor and neuronal manipulations between male and female rats when female rats are tested outside of proestrus (Figure 6; Berridge et al., 2022). During the 12- to 18-hour period of proestrus, when ovarian steroids reach peak levels, CRF effects on working memory were not observed. A similar protective effect of high ovarian steroids against the sustained attention-impairing actions of intracerebroventricularly (ICV) administered CRF has been recorded (Cole et al., 2016a).

Translational Relevance. Collectively, these observations indicate that caudal dmPFC CRF neurons modulate PFC cognitive function. Importantly, global blockade of brain CRF receptors via ICV injection improves both working memory and sustained attention in male and female rats (Berridge et al., 2022; Hupalo et al., 2021; Hupalo & Berridge, 2016). The procognitive actions of CRF antagonists are similar to those seen for all ADHD-approved drugs in patients and healthy human and animal subjects (Spencer et al., 2015). Thus, CRF may represent a useful target for the development of novel cognitive enhancers for the treatment of PFC-dependent cognitive dysfunction.

Neurochemical Identity of PFC CRF neurons. While early studies noted the presence of CRF in GABAergic neurons, subsequent studies demonstrated that CRF can also colocalize with glutamate (Dabrowska et al., 2013; Helmeke et al., 2008; Mohila & Onn, 2005). In immunohistochemical studies, we examined the extent to which caudal dmPFC CRF neurons co-express either of these neurotransmitters. We observed that across the rostral/caudal dmPFC and ventromedial PFC ~85% (86 ± 0.8% of 461 neurons; Figure 7a) of medial PFC CRF neurons are glutamatergic (CRF_{Glu}), putative pyramidal projection neurons, while the remaining ~15% are GABAergic (CRF_{GABA}), putative interneurons (14 ± 3.2% of 492 neurons; Figure 7b). In both these immunohistochemical and our prior chemogenetic studies, we observed a surprisingly high density of CRF neurons within the medial PFC not adequately described in the prior literature. This likely reflects the fact that the CRF antibodies used to initially characterize CRF distributions lacked the sensitivity of those currently available. While the antibody we have used has been well-validated (Das et al., 2007; Rajbhandari et al., 2015), to better confirm our immunohistochemical and viral vector observations we developed a fluorescent *in situ*

hybridization (FISH) assay to detect CRF mRNA. We observed strong overlap with FISH and CRF immunoreactivity (~98% ± 1% of 4,454 neurons; Figure 7c)**.** Collectively, these studies unambiguously demonstrate a previously unrealized prominent presence of CRF-synthesizing neurons in the medial PFC that is comprised of both CRF_{Glu} and CRF_{GABA} subpopulations. The fact that the working memory effects of PFC CRF neurons are dependent on local receptors could argue for an involvement of CRF_{GABA} neurons in the regulation of working memory. Given the sustained attention effects of PFC CRF neurons are independent of local release this could suggest an involvement of CRF_{Glu} neurons in the regulation of this cognitive process.

Aims

The above reviewed studies demonstrate that caudal dmPFC CRF neurons regulate distinct PFC-dependent cognitive processes via unique projection pathways. Currently, we lack an understanding of the sustained attention actions of CRF_{Glu} vs. CRF_{GABA} neural networks, the neural pathways associated with PFC CRF neural modulation of sustained attention, and the neural coding effects of PFC CRF neurons in sustained attention. The following aims are designed to address these issues.

1) **Document the extent and expression of GABAergic and glutamatergic CRF neurons within the PFC and characterize the role of caudal dmPFC glutamatergic and GABAergic CRF neurons in working memory and sustained attention performance.**
2) **Examine the projections of PFC-CRF neurons, the actions of CRF receptor activation and blockade in the MD and surrounding regions, and the effect of activating MD projecting PFC-CRF neurons in working memory and sustained attention performance.**
3) **Determine the actions of caudal dmPFC CRF_{Glu} neurons on task-related neurophysiological activity within the dmPFC → MD circuit in sustained attention-tested animals.**

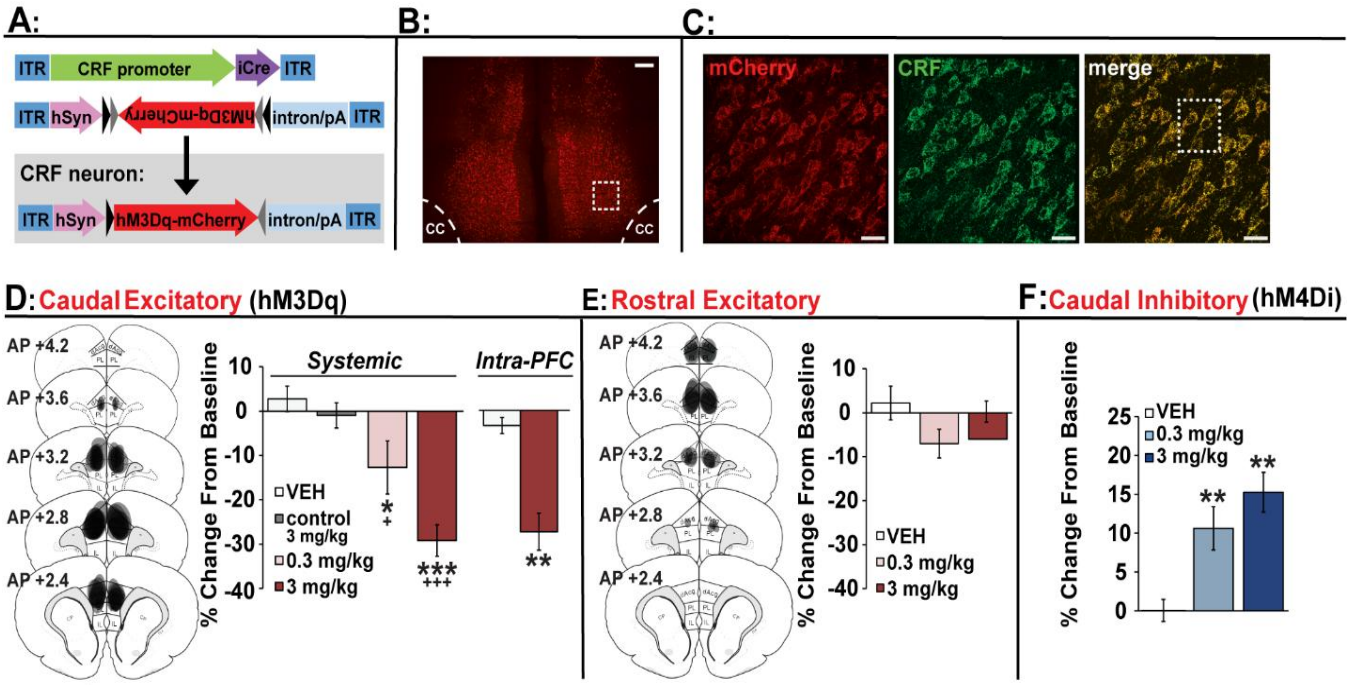

Figure 1: Chemogenetic activation of caudal dmPFC CRF neurons impairs working memory. A) Schematic of dual viral vector system used to activate (*AAV8 CRF-Cre + hSyn-Dio-hM3Dq*) or inhibit (*CRF-Cre + hSyn-Dio-hM4Di*) CRF neurons in the PFC. **B)** Photomicrograph depicting mCherry expression in the caudal dmPFC from a CRF- hM3Dq-treated animal; scale bar = 200 µm; cc: corpus callosum. **C)** Collapsed 30 µm z-stack from inset in *B*, demonstrating mCherry colocalization (red) with CRF-ir cells (green) and extensive overlap of the 2 signals (yellow); scale bar = 30 µm. Additional studies demonstrated the DREADD agonist, CNO, elicits Fos-ir in mCherry-positive cells in animals treated with the excitatory DREADD virus (hM3Dq) but not viral controls (Hupalo et al., 2019). **D)** Effects of chemogenetic **activation** of CRF neurons in the **caudal** dmPFC. *Schematics*: hM3Dq viral spread (AP +3.2 to +2.2) from *all animals tested*. *Bar graphs:* CNO dose-dependently impairs task performance relative to vehicle (n = 7) and CNO-treated viral control animals (n = 7; 'control 3 mg/kg'). *Similar effects were observed with CNO infusion into the caudal dmPFC (Intra-PFC).* **E)** Chemogenetic **activation** of CRF neurons in the ***rostral*** dmPFC (AP +4.2 to +3.2) has no significant effects on task performance. **F)** Chemogenetic **suppression** of CRF neurons in the ***caudal*** dmPFC **improves** task performance. Bars represent mean ± SEM percent change in accuracy relative to baseline. *, **, *** P < .05, .01, .001 vs. vehicle; $^{+}$, $^{+++}$ P < .05, .001 vs. viral controls. Data from Hupalo et al., 2019.

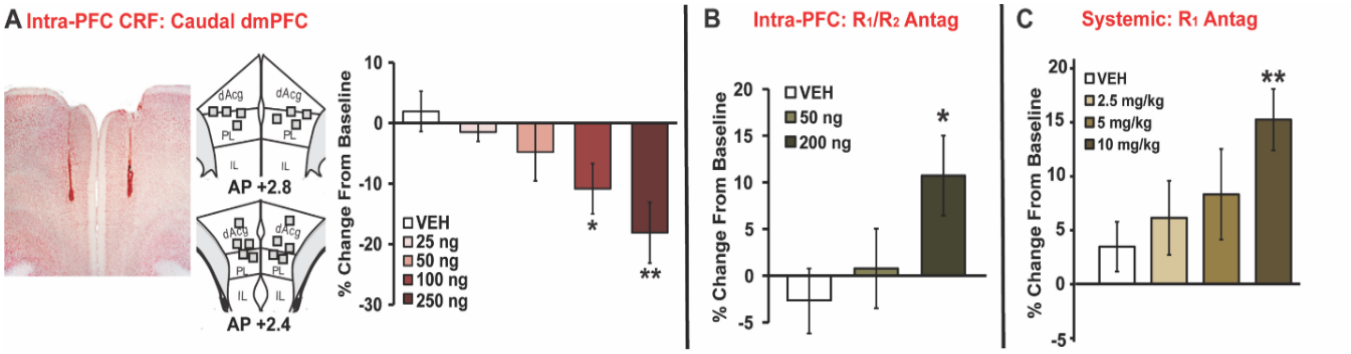

Figure 2. Working memory effects of PFC CRF receptors. A) Intra-***caudal dmPFC CRF*** infusion dose-dependently impairs working memory (see Hupalo & Berridge, 2016 for mapping data). Photomicrograph of needle tract in 1 animal; Schematics indicate infusion sites. Bar graph depicts %change from baseline (Vehicle, 25ng, 50ng, 100ng, 250ng CRF/500 nl). **B)** Intra-caudal dmPFC infusion of non-selective CRF antagonist (D-Phe-CRF) and systemic administration of an R1-selective CRF antagonist. **C)** improve working memory. Treatments were given 20 min. prior to testing. **Note:** we minimize damage to the dorsal PFC using small (33 ga.) needles and only implanting cannula ~200 µm past the dura. Needle tracts represent largest extent of damage in the PFC. From Hupalo & Berridge, 2016.

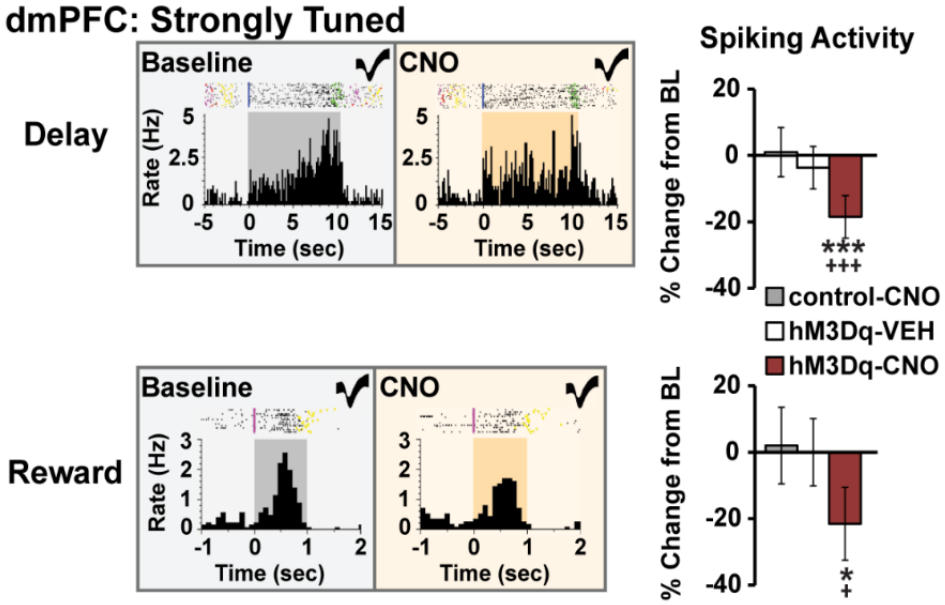

Figure 3: Caudal dmPFC CRF neuronal activation degrades task-related activity of dmPFC neurons. Recording arrays were implanted into the caudal dmPFC following bilateral infusions of the excitatory DREADD (hM3Dq) or control viral vectors. >3 weeks later, animals were treated with vehicle (VEH) or 3 mg/kg CNO. Shown are exemplar peri-event time histograms (PETHs) for a putative pyramidal neurons strongly tuned to **delay** (*top row*) or **reward** (*bottom row*). Bar graphs depict effects of vehicle or CNO on task-related spiking activity. CNO **suppressed** delay- (n=24-54/group) and reward-related (n=11- 24/group) activity. Weaker to no effects were observed in the dmSTR (see 32). *, *** P < .05, .001 vs vehicle, $^{+}$, $^{+++}$ P < .05, 0.001 vs. virus control.

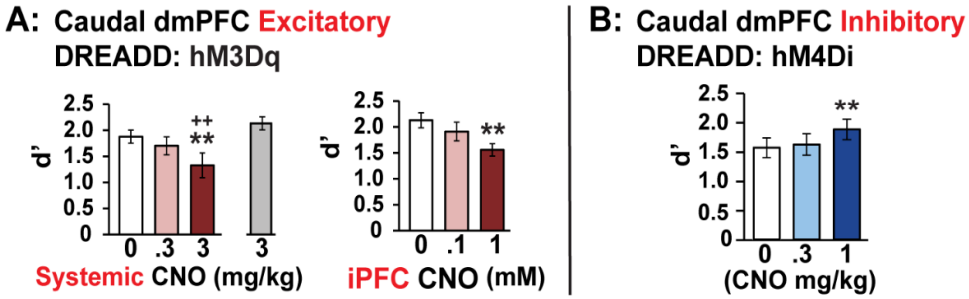

Figure 4: Sustained Attention effects of caudal dmPFC CRF neuronal activation. Depicted are the sustained attention impairing (*A*) and improving (*B*) effects of activating or inactivating caudal dmPFC CRF neurons as measured by d prime. **A)** Activation of caudal dmPFC CRF neurons via systemic CNO impairs sustained attention at the highest dose (~30% decrease relative to vehicle treatment (0 CNO). This effect was not seen in viral control animals (grey bar), nor when activating rostral dmPFC or vmPFC CRF neurons (data not shown, see Hupalo et al., 2021). **B)** Inhibition of caudal dmPFC CRF neurons improved sustained attention relative to vehicle (~20% increase), comparable to relevant seen with clinically relevant doses of methylphenidate (Ritalin; Spencer et al., 2015). ** P < .01 vs vehicle, $^{++}$ P < .01 vs control. Data from Hupalo et al., 2021.

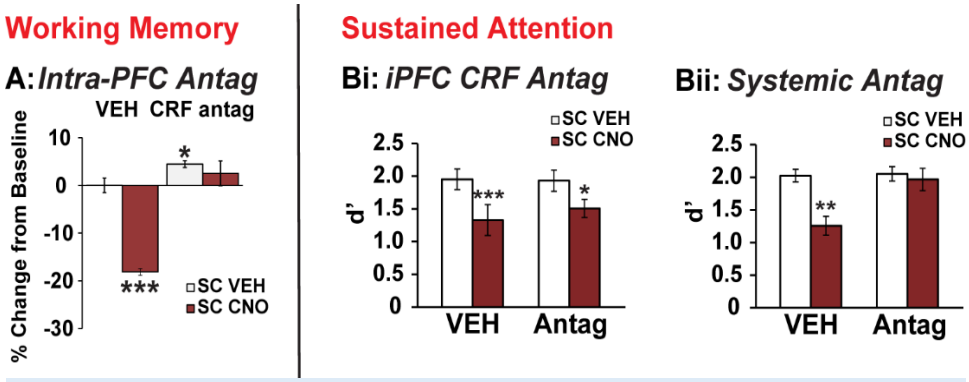

Figure 5: Working Memory, *but not Sustained Attention*, effects of caudal dmPFC CRF neurons are dependent on local CRF Receptors. **A)** Animals received either a vehicle (VEH) or CRF antagonist, D-Phe-CRF (100 ng/500nl bilaterally) into the caudal dmPFC prior to systemic (sc) vehicle or CNO. Intra-PFC antagonist, but not vehicle, impairment seen with CNO., **B)** Intra-PFC infusion of the CRF antagonist did ***NOT*** block the sustained attention impairing effects antagonist did ***NOT*** block the sustained attention impairing effects of the CRF antagonist did ***NOT*** block the sustained attention impairing effects of CNO (**Bi**), while systemic administration of a CRF antagonist did (**Bii**; NBI35965, 1 mg/kg). *, *** P < .05, 001 vs. vehicle. From Hupalo et al, 2019; 2021.

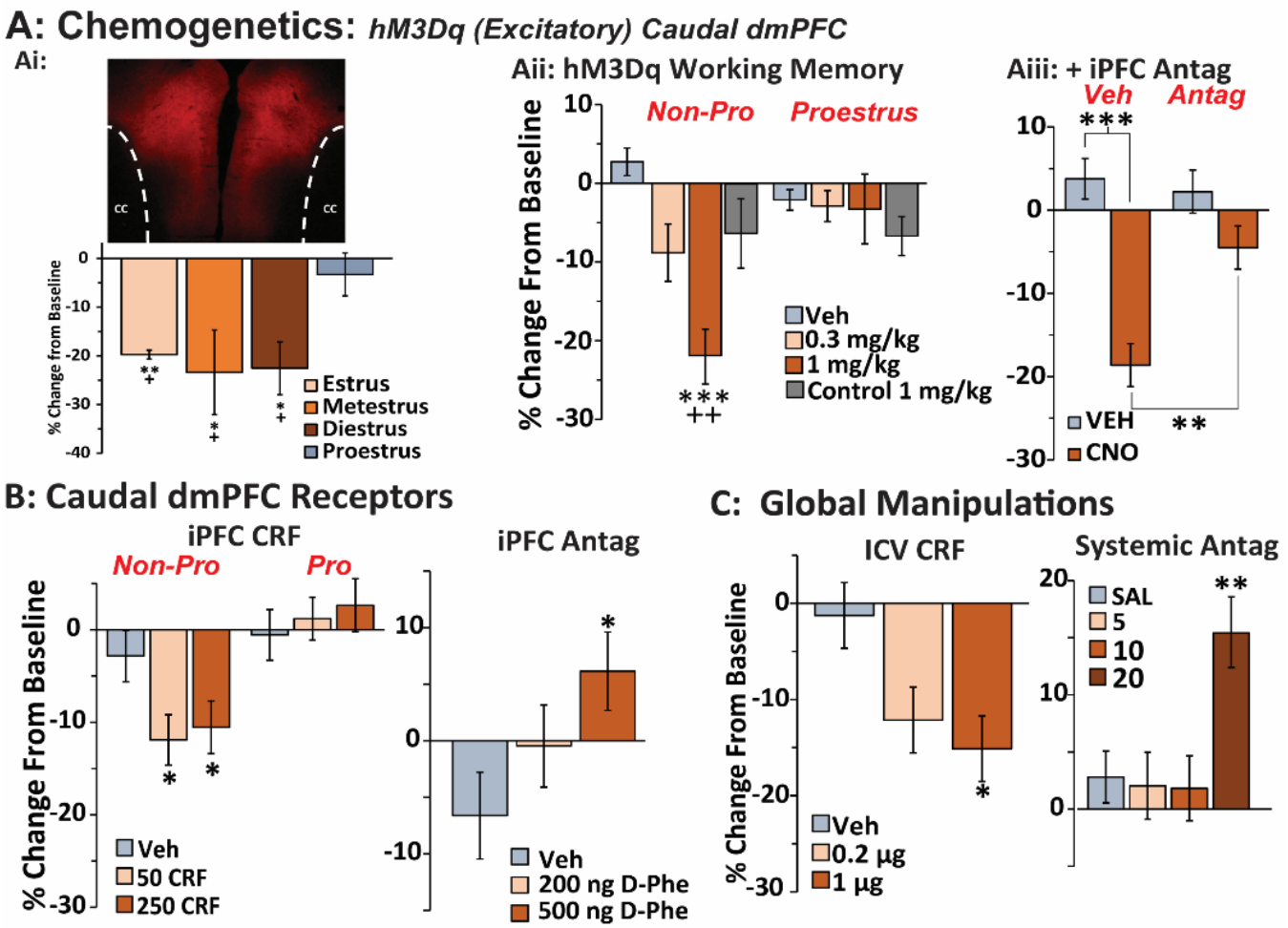

Figure 6. Working memory actions of PFC CRF manipulations *in Females*. Ai) *Top:* Photomicrograph of hM3Dq viral expression in caudal dmPFC. *Bottom:* Preliminary analyses indicated 1mg/kg CNO impaired working memory in estrus, metestrus and diestrus but not proestrus (n = 4-7). * = P < .05 vs. baseline; $^{+}$ = P < .05 vs. proestrus. **Aii)** CNO (0.3, 1.0 mg/kg, s.c.) dose-dependently impaired working memory *outside of proestrus* but not in viral controls lacking this transgene (*Control*). **Aiii)** Working memory impairment by 1mg/kg CNO is prevented by bilateral intra-caudal dmPFC infusion of the CRF antagonist, D- Phe-CRF (100 ng, Antag) but not vehicle (Veh). **B)** *Left:* Bilateral infusion of CRF into the caudal dmPFC (but not rostral, not shown) impaired working memory *outside, but not during, proestrus* (*at a lower dose than males*). *Right*: Systemic administration of R1 antagonist NBI35965, improved working memory at the highest dose of 20 mg/kg. Significant improvement in males was seen at 10 mg/kg. *, **, *** P < .05, .01, .001 vs vehicle, $^{++}$ P < .01 vs. viral controls. From Berridge et al, 2022.

Chapter 2

Neurochemical and Circuit Heterogeneity of Cognition-Modulating Prefrontal Corticotropin-Releasing Factor Neurons

Spencer K. Cooke, Andrea J. Martin, Robert C. Spencer, Shannon E. Nicol, and Craig W. Berridge

Published in *Biological Psychiatry*, March 2025.

Background: Impairment of prefrontal cortex (PFC)-dependent cognition is associated with multiple psychiatric disorders. Development of more effective treatments for this form of cognitive dysfunction is hindered by our limited understanding of the neurobiology underlying PFC-dependent cognition. We previously identified a robust population of corticotropin releasing factor (CRF) neurons in the caudal dorsomedial PFC (dmPFC) of rats that impair both working memory and sustained attention. Although the working memory actions of these neurons involved local CRF release, the sustained attention actions were not. These results suggest potential heterogeneity within this population of CRF neurons, including the potential existence of both GABAergic (CRF_{GABA}) interneurons and glutamatergic (CRF_{Glu}) CRF projection neurons.

Methods: Immunohistochemical analyses first identified both CRF_{GABA} and CRF_{Glu} neurons in the caudal dmPFC. Intersectional viral vector chemogenetic approaches were then used to assess the effects of activating caudal dmPFC CRF_{Glu} and CRF_{GABA} neurons on working memory and sustained attention in males and females (tested outside of proestrus).

Results: CRF_{Glu} neurons comprised a majority (85%) of caudal dmPFC CRF neurons, while remaining were identified as CRF_{GABA} neurons. For both females and males, activation of caudal dmPFC CRF_{GABA} neurons impaired working memory but not sustained attention, while activation of CRF_{Glu} neurons impaired both working memory and sustained attention. Interestingly, the working memory actions of both CRF_{GABA} and CRF_{Glu} neurons were dependent on local CRF receptors.

Conclusion: These results advance our understanding of the neurobiology of PFC-dependent cognition and potential mechanisms through which cognitive dysfunction could arise.

Introduction

The prefrontal cortex (PFC) supports 'executive' cognitive processes that guide goal-directed behavior, including working memory and sustained attention (J. Fuster, 2015; Goldman-Rakic, 1996; Spencer & Berridge, 2019). While PFC-dependent cognitive dysfunction is associated with a diversity of psychiatric disorders (Millan et al., 2012), treatment for this is currently constrained by a limited understanding of the neurobiology that supports PFC-dependent cognition. Recent studies identify an important role of PFC corticotropin-releasing factor (CRF) neurons in higher cognitive function (Berridge et al., 2022; Hupalo et al., 2021; Hupalo, Martin, et al., 2019; Maltese et al., 2025). For example, chemogenetic activation of CRF neurons in the caudal dorsomedial PFC (dmPFC) impairs PFC-dependent working memory in rats, while inhibition of these neurons improves working memory (Hupalo, Martin, et al., 2019). The working memory effects of caudal dmPFC CRF neurons involve local receptors (Hupalo, Martin, et al., 2019; Hupalo & Berridge, 2016). Largely comparable working memory effects of caudal dmPFC CRF neurons are observed across males and females, with the exception of proestrus, during which CRF-dependent cognitive impairment was not observed (Berridge et al., 2022). Caudal dmPFC CRF neurons exert similar modulatory actions on PFC-dependent sustained attention (Hupalo et al., 2021). In contrast to working memory, these effects were not dependent on local CRF receptors, consistent with the fact that direct activation of caudal dmPFC CRF receptors had no effect on sustained attention (Hupalo et al., 2021; Hupalo & Berridge, 2016). Thus, while caudal dmPFC CRF neurons similarly regulate working memory and sustained attention, these actions involve distinct projection pathways.

The differential circuitry underlying the cognitive actions of caudal dmPFC CRF neurons suggests heterogeneity within this neuronal population. Outside the PFC, CRF has been observed in both GABAergic and glutamatergic neurons (Fudge et al., 2022; Tagliaferro & Morales, 2008; Valentino et al., 2001). As GABA neurons often act locally, the dependency of the working memory actions of PFC CRF neurons on local CRF receptors (Hupalo, Martin, et al., 2019) could suggest an involvement of GABAergic CRF interneurons, although alternative possibilities exist. Consistent with this, studies with transgenic mice indicate a majority of medial PFC CRF neurons are GABAergic (Chen et al., 2020; de León Reyes et al., 2023). However, the rich density of medial PFC CRF neurons we observed previously

in outbred rats, many displaying features of glutamatergic pyramidal neurons, suggests these neurons are unlikely to be largely GABAergic (5–7; unpublished observations). Thus, the extent to which caudal dmPFC CRF neurons of animals used in our earlier studies are glutamatergic or GABAergic and whether such subpopulations impact higher cognition are currently unknown. To address these issues, we first examined the degree to which caudal dmPFC CRF neurons express immunohistochemical markers for GABA or glutamate in male and female Sprague-Dawley rats. We observed both glutamatergic (CRF_{Glu}) and GABAergic (CRF_{GABA}) neurons in differing proportions within the caudal dmPFC (85% and 15%, respectively). Additional studies examined the cognitive actions of these neuronal subpopulations utilizing an intersectional viral approach to chemogenetically activate CRF_{GABA} or CRF_{Glu} neurons in working memory- and sustained attention-tested males and females (outside proestrus; 7).

Methods and Materials

Animals.

Male and female Sprague-Dawley rats (8-12 weeks; Charles River, Wilmington, Massachusetts) were pair-housed on a 13/11-hour light/dark cycle (lights on 0600). Food was restricted 4-7 days following arrival (males, 15-19 grams/day; females, 10-13 grams/day). Animals were handled extensively prior to training. Training/testing was conducted between 0800-1600 hours (5-7 days/week). All testing in females occurred outside proestrus. Facilities and procedures were in accordance with the National Institutes of Health and approved by an Institutional Animal Care and Use Committee.

Immunohistochemical analyses and cell counting.

Animals were anesthetized, transcardially perfused and 40-μm thick sections collected. Immunohistochemical staining and cell counting were performed as previously described (Hupalo, Martin, et al., 2019). Washed tissue sections were incubated with one of the following primary antibodies: mouse anti-GAD67 (1:20000; EMD Millipore, Darmstadt, Germany, #MAB5406), mouse anti-CaMKIIα (1:2000; Abcam, Waltham, MA, #ab22609), guinea pig anti-CRF (1:1000; Bachem, Torrance, CA, #t-5007), rabbit anti-c-Fos (1:8000; EMD Millipore, #F7799), mouse anti-c-Fos (1:8000; Biosensis, Thebarton, South Australia, #M-1752-100) or rabbit-anti hemagglutinin (HA; 1:2000; Cell Signaling Technology, Danvers, MA, #3724s). Sections were incubated with the following secondary antibodies: donkey anti-mouse (1:500; Life Technologies, Carlsbad, CA, #A21202, AF488), goat anti-guinea pig (1:200; Life Technologies, # A11075, AF488), donkey anti-rabbit (1:500; Life Technologies, #A10042, AF568) or donkey anti-rabbit (1:200; Life Technologies, #A21206, AF488). In the case of HA, double immunolabeling was performed by staining first for HA and then for either CaMKIIα, GAD67 or c-fos. 3-4 60X images were collected per section with a confocal microscope (3-5 tissue sections/animal). Cells were counted only if there was a clear nucleus and when fluorescence was clearly observed in the cytoplasm or nucleus (for Fos-ir). The percentage of double-labeled cells was averaged for each animal and then averaged across animals.

Working memory testing.

Animals were trained in a delayed non-match to position T-maze task of spatial working memory in which animals alternate maze arm entry to receive a sucrose reward (45 mg pellet/trial) as previously described (Berridge et al., 2006; Spencer et al., 2012). External spatial cues were masked and white noise (60 dB) played above the center of the maze. Between trials, animals were placed in a start box at the base of the maze, prevented from exiting by a removable gate. Following pretraining and surgery, animals were trained with 20-trials/session and the introduction of a 10-second delay between trials. As accuracy improves with repeated testing, delays were increased in 10-second intervals when needed to maintain an accuracy range of 75-95% (delay range: 10-40 seconds). Treatments were given when accuracy across the 2 prior days did not differ by greater than 10%. Results were analyzed as percent change from baseline. Baseline was defined as the average performance of the 2 days prior to treatment.

Sustained attention testing.

Animals were trained in an operant-based signal detection task of sustained attention with 60dB white noise as described previously (Bushnell, 1998; Hupalo et al., 2021). Across 100-trials, animals pressed the right lever if they detected a brief LED signal of varying duration (7 signal lengths, range=0.125-1.0-second, with replacement) that occurred randomly on one-half of the trials ("signal trials") and pressed the left lever if no light was detected ("no-signal trials"). Levers were projected after a trial. Correct responses on signal trials ("hit") and no-signal trials were rewarded (45-mg sucrose pellet/trial, Bio-Serv, Frenchtown, NJ) and were followed by 5-second house light illumination. Incorrect presses on signal trials and no-signal trials ("false alarms") resulted in lever retraction and a 5-second blackout. Upon failure to respond within 5-seconds of lever projection ("omission"), lever retraction and a 5-second blackout ensued. Trials were separated by a variable inter-trial interval averaging 14-seconds (minimum of 5-seconds). Once animals achieved three consecutive days of ^{3}70% correct, they underwent surgery. Following recovery, animals resumed testing until pre-surgery performance levels were achieved.

Measures of performance included probability of hits (number of hits/number of signal trials) and false alarms (false alarms/no-signal trials), number of omissions, response latency, as well as the stimulus detectability measure, d', defined as Z(N)-Z(SN), where N=1-probability false alarms and

SN=1-probability hits. Treatments were replicated. For each replication round, drug effects were assessed relative to vehicle (Bushnell, 1998; Hupalo et al., 2021).

Surgery and Viral Infusions.

Animals were anesthetized with isoflurane and placed in a stereotaxic device (flat skull). A cocktail of two viruses was infused into the caudal dmPFC for expression of designer receptors exclusively activated by designer drugs (DREADDs; A+2.5; L±0.8; V±2.85). The first virus was always AAV8-CRF-Cre ($1.3x10^{13}$ gc/mL; Vector Biolabs, Malvern, PA). To visualize all CRF neurons, the second virus was AAV8-hSyn-DIO-hM4Di-mCherry (premixed 1:2, 1.7 µL/hemisphere, $2.9x10^{13}$ gc/mL, Addgene; 5). To activate CRF_{GABA} neurons the second virus was AAV8-Dlx-DIO-hM3Dq-mCherry (premixed 1:1; 2.2 µL/hemisphere; $2.9x10^{13}$ gc/mL; Vector Biolabs). To activate CRF_{Glu} neurons, the second virus was AAV8-CaMKIIα(1.3)-DIO-hM3Dq-woodchuck hepatitis virus post-transcriptional regulatory element (WPRE)-HA (premixed 1:2, 1.7 µL/hemisphere, $1.5x10^{13}$ gc/mL, Vector Biolabs). The reporter protein, HA, was used due to plasmid crowding associated with the inclusion of WPRE. Viral controls lacked the DREADD transgene. Viruses were infused bilaterally at a rate of 0.25 µL/min via 33ga. stainless-steel injectors that were left in place for at least 4-minutes following infusion. Viruses were allowed to incubate for at least 3-weeks prior to testing. The extent of reporter protein expression was mapped as described previously (Hupalo, Martin, et al., 2019).

Subsets of animals that received CRF_{GABA} and CRF_{Glu} viral cocktails and were tested in working memory were bilaterally implanted with 25ga. cannulae inserted ~200 mm below the dura over the caudal dmPFC (A+2.5; L±0.8).

Drugs and treatments.

The DREADD agonist, CNO (clozapine-N-oxide dihydrochloride, Tocris, Bristol, UK), was dissolved in 0.9% saline and administered subcutaneously 45-minutes before testing. Doses were based on previous observations (Berridge et al., 2022; Hupalo et al., 2021; Hupalo, Martin, et al., 2019) and limited pilot studies. Where appropriate, the CRF antagonist, D-Phe-CRF_{12-41} (human/rat, Bachem, Torrance, CA), dissolved in 0.9% saline, was infused bilaterally into the caudal dmPFC via 33ga.

stainless-steel infusion needles (2.5 mm projection; 0.5 mL at 0.25 µL/minute; 5). All treatments were separated by at least 1-day.

Vaginal cytology.

Daily vaginal cytology tracked estrus cycle stage (Berridge et al., 2022). Estrus stage was first estimated from wet samples collected within 1-hour prior to behavioral testing. If samples suggested an animal was outside proestrus, testing ensued. Dried samples were later stained (Harris' Hematoxylin Protocol, National Diagnostics, 2011) to confirm cycle stage. Results were analyzed only if stained samples confirmed testing occurred outside proestrus.

Statistical Analyses.

Behavioral data were analyzed using a linear mixed-effects model in JMP® Pro Version 12.2.0 (SAS Institute Inc., Cary, NC). Treatment, and sex where applicable, were fixed effect factors and animal was a random effect factor. For sustained attention round of replication was included as a fixed effect covariate (Dixon, 2016). Multiple comparisons of either treatment or the treatment*sex interaction using Holm-Bonferroni corrected t-tests were used to make planned comparisons between CNO treatment levels and vehicle in hM3Dq treated animals. Corrected p-values are reported. The effects of CNO in viral controls were compared to hM3Dq animals using planned comparison t-tests.

Results

Neurochemical identity of PFC CRF neurons.

Immunohistochemical studies first examined whether caudal dmPFC CRF neurons co-express markers of GABA (GAD67-ir) or glutamate (CaMKIIα-ir). CRF neurons were identified using our previously characterized viral cocktail that selectively expresses DREADDs/mCherry in CRF neurons (Hupalo, Martin, et al., 2019). This approach was used given mCherry expression can be more robust than CRF-ir, facilitating accurate cell counting. Our prior study demonstrated that virtually all (94±5%) virus-labeled neurons colocalized CRF-ir (Hupalo, Martin, et al., 2019). The CRF antibody used in this study had been validated via immunoadsorption (Das et al., 2007, p. 200). However, for the current study we examined the extent to which labeling from this antibody overlaps with mRNA expression using *in situ* hybridization (Supplemental Methods). We observed nearly complete (99±1%) overlap between CRF-ir and CRF mRNA expression (Figure S1), further supporting the use of mCherry expression to identify CRF neurons. In the caudal dmPFC, we observed GAD67-ir in 14±7% of mCherry-positive neurons in males (Figure 1A; n=492 cells, 4-animals) and 16±6% of mCherry-positive neurons in females (n=667 cells, 3-animals). Additionally, we observed CaMKIIα-ir in 86±6% of mCherry-positive neurons in males (Figure 1B; n=461 cells, 3-animals) and in 85±5% of mCherry-positive neurons in females (n=719 cells, 3-animals). Given these observations, we developed chemogenetic viral vector approaches to selectively activate caudal dmPFC CRF_{GABA} and CRF_{Glu} neurons.

Cognitive actions of caudal dmPFC CRF_{GABA} neurons.

Viral validation. Three weeks following CRF_{GABA} viral cocktail infusion into the caudal dmPFC robust mCherry expression was observed within a radius of ~500 μm, filling the majority of the caudal dmPFC with minimal spread beyond (Figure 2A-C). Immunohistochemical analyses demonstrated viral expression was selective for CRF_{GABA} neurons (Figure 2Ai-Aii). Specifically, of mCherry-expressing neurons, 93±5% colocalized GAD67-ir (n=897 cells, 3-males, 3-females), while 87±6% colocalized CRF-ir (n=510 cells, 3-males, 2-females). Of CRF-ir neurons, 16±2% expressed mCherry (n=2821, 3-males, 2-females). mCherry was observed in 80±7% of GAD67-ir neurons (n=677 cells, 2-males, 3-

females). Additional studies assessed whether the DREADD agonist, CNO, activates CRF_{GABA} neurons as measured by Fos-ir. In CRF_{GABA}-hM3Dq treated animals, 6 mg/kg CNO (maximally impairing dose used in working memory studies) elicited clearly visible Fos-ir in 51±5% of 1324 mCherry-expressing cells (3-male and 4-female animals; Figure 2Aiii). Prior studies observed virtually no Fos-ir in CNO-treated viral control animals under identical conditions (Hupalo, Martin, et al., 2019).

Working Memory. To assess the working memory actions of CRF_{GABA} neurons, males and females received the CRF_{GABA}-hM3Dq virus cocktail bilaterally in the caudal dmPFC and were later tested following treatment with vehicle or varying doses of CNO (Table 1A for group size). We observed a significant effect of treatment ($F_{3,62}$=8.818, p<0.0001) but not sex ($F_{1,23}$=0.757, p=0.393) or a significant treatment*sex interaction ($F_{3,62}$=0.12, p=0.95). Specifically, chemogenetic activation of caudal dmPFC CRF_{GABA} neurons dose-dependently impaired working memory performance (Figures 2D, S2), with maximum impairment at 6 mg/kg CNO relative to vehicle (males, t_{56}=-3.420, p=0.004; females, t_{57}=-3.100, p=0.009) and 6 mg/kg CNO-treated viral controls (males, t_{16}=4.31, p<0.001; females, t_{20}=2.150, p=0.04). These effects were not associated with significant effects on run time (males, vehicle: 249±40s; 6 mg/kg CNO: 258±40s; $F_{(1, 10)}$=0.0533, p=0.8221; females, vehicle: 165±7s; 6 mg/kg CNO: 164±7s; $F_{(1, 12.7)}$=0.0115, p=0.9164).

Sustained Attention. In contrast to working memory, there was not a significant effect of treatment ($F_{2,66}$=0.713, p=0.494; Figures 2E, S2; Table 1B for group size), sex ($F_{1,13}$=0.000093, p=0.992) or a significant sex*treatment interaction ($F_{2,66}$=0.348, p=0.707) for sustained attention as measured by d'. In general, there were no significant effects of treatment, sex, or sex*treatment interactions on additional measures of sustained attention performance (see Table 2).

Cognitive actions of caudal dmPFC *CRF_{Glu}* neurons.

Viral validation. Three weeks following CRF_{Glu}-hM3Dq viral infusion into the caudal dmPFC there was robust expression of the reporter protein, HA, that was limited to a radius of ~500 μm (Figure 3A-C). Of HA-expressing neurons, 97±1% colocalized CaMKIIα-ir (*n*=1079 cells, 3-males, 3-females), while

100% colocalized CRF-ir (*n*=1368 cells, 3-males, 3-females; Figure 3Ai-Aii). Additionally, 95±2% of CaMKIIα-ir neurons colocalized HA-ir (*n*=1108 cells, 3-males, 3-females) while 88±3% CRF-ir neurons colocalized HA-ir (*n*=1562 cells, 3-males, 3-females). In CRF-CaMKIIα-hM3Dq treated animals (males, n=2; females, n=4), 3 mg/kg CNO administered in the home cage (highest dose used for working memory) activated PFC CRF_{Glu} neurons, as measured by Fos-ir (62±5% of 1089 neurons; Figure 3Aiii).

Working Memory. Males and females received bilateral intra-caudal dmPFC CRF_{Glu}-hM3Dq virus cocktail and were later tested in working memory following vehicle or varying doses of CNO (Table 1A for group size). CNO elicited a dose-dependent impairment in working memory ($F_{3,42}$=10.410, p<0.0001; Figures 3D, S3) in the absence of a significant effect of sex ($F_{1,14}$=0.003, p=0.960) or a significant treatment*sex interaction ($F_{3,42}$=0.624, p=0.603). Maximum impairment was observed at 3 mg/kg CNO relative to vehicle (males, t_{42}=-2.690, p=0.031; females, t_{42}=-4.480, p<0.0003) or CNO-treated viral controls (males, t_{14}=-2.960, p=0.010; females, t_{14}=-2.640, p=0.020). These effects were not associated with significant effects on run time (males, vehicle: 223±28s; 3 mg/kg CNO: 277±28s; $F_{(1, 7)}$=3.5175, p=0.1028; females, vehicle: 216±54s; 3 mg/kg CNO: 252±54s; $F_{(1, 7)}$=0.2456, p=0.6354).

Sustained Attention. In contrast to CRF_{GABA} neuronal activation, CNO dose-dependently impaired sustained attention as measured by d' ($F_{3,115}$=17.26, *p*<0.0001; Figures 3E, S3; Table 1B for group size), with 6 mg/kg eliciting maximal impairment relative to vehicle (male, t_{110}=--4.08, *p*<0.0003; female, t_{118}=-5.75, *p*<0.0003) and viral controls (male, t_{16}=-2.33, p=.017; female, t_{14}=-3.05, p=0.004). Decreases in d' were associated with significant increases in false alarms and response latency, and not consistent changes in omissions (Table 2B). There was not a significant sex*treatment interaction on the majority of sustained attention measures. However, we did observe small, yet significant, interactions on omissions ($F_{3,116}$=4.42, *p*=0.0056), for which females displayed an overall greater number, and response latency ($F_{3,13177}$=13.55, *p*<0.0001), for which females had higher values overall.

Are caudal dmPFC CRF receptors involved in the working memory effects of CRF_{GABA} and CRF_{Glu} neurons?

Prior studies demonstrated the working memory-impairing, but not sustained attention-impairing, effects of caudal dmPFC CRF neurons are dependent on local CRF receptors (Hupalo et al., 2021; Hupalo, Martin, et al., 2019). Thus, additional studies examined whether the working memory effects of caudal dmPFC CRF_{GABA} and/or CRF_{Glu} neurons involve local CRF receptors. In the studies above, we observed no sex differences. In our experience, female cognitive testing has been associated with greater animal usage due to less than 100% accuracy in timing treatments outside of proestrus, more variability in day-to-day performance, and consequently, more animal attrition due to infection. Therefore, to minimize animal usage, for these studies all testing was conducted in males (Table 1C for group sizes). Animals treated with the CRF_{GABA}-targeting or CRF_{Glu}-targeting viral cocktails received bilateral intra-caudal dmPFC infusions of either vehicle or the CRF-antagonist, D-Phe-CRF, immediately prior to receiving systemic vehicle or the highest impairing dose of CNO identified in the studies above and were tested 45-minutes later. A dose of D-Phe-CRF (100 ng/hemisphere) was used that was subthreshold for improving working memory on its own, based on previous observations (Hupalo, Martin, et al., 2019; Hupalo & Berridge, 2016) and limited pilot studies.

In CRF_{GABA} animals there was a significant treatment effect ($F_{3,37}$=5.149, p=0.0045). In animals treated bilaterally with intra-PFC vehicle, 6 mg/kg CNO elicited a significant impairment in working memory relative to systemic vehicle treatment (t_{36}=-3.760, p=0.0012; Figures 4A, S4). In contrast, in animals treated bilaterally with intra-PFC infusions of D-Phe CRF, CNO treatment did not differ significantly from vehicle treatment (t_{36}=-1.120, p=0.2715; Figure 4A).

In CRF_{Glu} animals there was a significant treatment effect ($F_{3,25.8}$=15.003, p<0.0001). In animals receiving intra-PFC vehicle, 3 mg/kg CNO elicited a significant impairment in working memory relative to systemic vehicle treatment (t_{24}=-5.84, p=0.0002; Figures 4B, S4). In animals treated with intra-PFC D-Phe-CRF, CNO did not significantly impair performance relative to systemic vehicle treatment (t_{26}=-1.80, p=0.0831; Figure 4B).

Discussion

Our understanding of the neural mechanisms that support PFC-dependent cognition remains limited. Although early studies identified CRF neurons and receptors in the PFC, their role in higher cognitive function has only been explored relatively recently. Our prior studies demonstrate CRF neurons in the caudal dmPFC of rats impair working memory and sustained attention via distinct projection pathways, suggestive of heterogeneity within this neuronal population (Berridge et al., 2022; Hupalo et al., 2021; Hupalo, Martin, et al., 2019). Consistent with this, the current studies observed that the caudal dmPFC contains both CRF_{GABA} and CRF_{Glu} neurons, in varying proportions (~15% and ~85%, respectively). Additional observations demonstrate that CRF_{GABA} neurons impair working memory but not sustained attention, while CRF_{Glu} neurons impair both cognitive processes. The working memory effects of both CRF_{GABA} and CRF_{Glu} neurons were dependent on local CRF receptors. Heterogeneity in caudal dmPFC CRF neurons, their cognitive actions, and circuitry underlying these actions may allow for a more fine-tuned and context-dependent regulation of goal-directed behavior.

Robust and heterogeneous population of PFC CRF neurons.

While early anatomical studies indicated a prominent population of CRF neurons within the PFC, details of this distribution were typically lacking (see 20,21). Additionally, many of these studies were limited by the use of antibodies less sensitive than those available today, including those directed against ovine CRF that display different properties than those directed against rat/human CRF (Rivier et al., 1983; Skofitsch & Jacobowitz, 1985). The current and recent studies (Berridge et al., 2022; Hupalo et al., 2021; Hupalo, Martin, et al., 2019) have identified CRF-expressing neurons in the medial PFC of adult outbred rats using antibodies directed against rat CRF, *in situ* hybridization, and viral vectors expressing CRF-dependent Cre-recombinase. These differing methods provide a remarkably consistent picture of a highly dense population of CRF neurons distributed throughout the medial PFC spanning layers II/III and V/VI. The current studies demonstrate that within the caudal dmPFC ~85% of CRF neurons are glutamatergic and ~15% are GABAergic. While these studies did not analyze the distribution of CRF_{Glu} and CRF_{GABA} neurons throughout the medial PFC, we have observed a similar density and distribution of CRF neurons throughout this region (Berridge et al., 2022; Hupalo et al.,

2021; Hupalo, Martin, et al., 2019). Thus, it seems likely a similar pattern of CRF_{Glu} and CRF_{GABA} neurons exists more broadly within the medial PFC.

The current results are in apparent contradiction with previous studies in transgenic *Crh-IRES-Cre;Ai14;Gad67-GFP* mice that indicated the majority of medial PFC CRF neurons are GABAergic and more densely located in layers II/III (Chen et al., 2020; de León Reyes et al., 2023). However, it should be noted that these studies did not validate the accuracy of this mouse line for identification of CRF or GABA neurons either immunohistochemically or with *in situ* hybridization. This is a concern given evidence indicates the *Crh-IRES-Cre* mouse line (used to create the crossed *IRES-Cre;Ai14;Gad67-GFP* line) fails to label a sizeable proportion of CRF-ir neurons (Chen et al., 2020; Taniguchi et al., 2011; Y. Wang et al., 2021). Future studies will need to examine the extent to which CRF_{Glu} and CRF_{GABA} neurons exist in the PFC of other rat/mouse strains and other species, particularly primates.

Differing patterns of cognitive action of CRF_{Glu} and CRF_{GABA} neurons.

The current studies demonstrate that CRF_{GABA} neurons impact working memory but not sustained attention, adding to growing evidence for different neural mechanisms within the PFC regulating working memory vs. certain forms of attention (sustained attention and flexible attention; 3,5,26–28), but not other forms (selective attention; 29). In contrast to CRF_{GABA} neurons, CRF_{Glu} neuronal activation impaired both working memory and sustained attention. Prior studies demonstrated the working memory, but not the sustained attention, effects of non-selective activation of caudal dmPFC CRF neurons are dependent on local receptors. The current studies further demonstrate the working memory effects of both caudal dmPFC CRF_{Glu} and CRF_{GABA} neurons involve local receptors. In rodents, CRF1 receptors are the dominant receptor in the PFC (Van Pett et al., 2000). These receptors are expressed by a majority of PFC pyramidal neurons and to a lesser extent GABAergic neurons (Gallopin et al., 2006). During the delay interval of working memory tasks, PFC pyramidal neurons display sustained discharge (Goldman-Rakic, 1995). This activity is posited to maintain goal-related information in the absence of sensory signals (Goldman-Rakic, 1995, 1999) and is influenced by GABAergic interneurons (Rao et al., 2000). Elevated protein kinase-A (PKA) signaling in PFC pyramidal neurons impairs working memory (Runyan et al., 2005; Taylor et al., 1999) and degrades delay-related activity (M. Wang et al., 2007).

Consistent with these observations, our prior studies demonstrate the working memory impairing effects of non-selectively activating caudal dmPFC CRF neurons are PKA-dependent and are associated with a robust suppression of delay-related activity of dmPFC pyramidal neurons (Hupalo, Martin, et al., 2019). These actions could well reflect, at least in part, actions of CRF1 receptors on pyramidal neurons. Selective involvement of PFC CRF receptors and/or CRF_{GABA} neurons in working memory, but not sustained attention, could reflect the fact that these neurons/receptors interfere with the maintenance of mental representations required for working memory but not sustained attention. The degree to which CRF_{Glu} and CRF_{GABA} neurons impact working memory related activity of PFC neurons remains to be determined.

Given the above-described observations regarding the lack of involvement of local receptors in the sustained attention actions of non-selective activation of caudal dmPFC CRF neurons, it is assumed the sustained attention modulating effects of CRF_{Glu} neurons involve CRF release outside the PFC. We recently observed that caudal dmPFC CRF neurons provide a remarkably dense innervation of the lateral portion of the mediodorsal thalamus (Cooke et al., 2022), a region critically involved in PFC-dependent cognitive function (Parnaudeau et al., 2018b). Moreover, recent studies in our laboratory indicate that CRF receptor activation in the lateral MD impairs sustained attention (Cooke et al., 2022). Thus, caudal dmPFC CRF_{Glu} neurons may influence sustained attention, and potentially working memory, via CRF release within the lateral MD.

Translational relevance

Dysregulated PFC-dependent cognition is associated with multiple psychiatric disorders. The current observations suggest CRF_{Glu} and/or CRF_{GABA} neurons could play a role in the etiology of one or more of these disorders. Independent of etiology, targeting CRF neurotransmission may provide a new approach for the treatment of PFC-dependent cognitive dysfunction. For example, we have demonstrated that CRF receptor blockade globally within the brain improves both working memory and sustained attention (Hupalo et al., 2021; Hupalo & Berridge, 2016), similar to all ADHD-approved treatments (Spencer et al., 2015). The current observations suggest that targeting PFC CRF_{GABA} or CRF_{Glu} neurotransmission could provide for a more fine-grain tuning of PFC-dependent cognition.

Moreover, evidence indicates a prominent role of glutamate and GABA neurotransmission in the regulation of PFC-dependent cognition (Auger & Floresco, 2015; Lewis et al., 2008; Woo et al., 2022; Yuen et al., 2012). The current observations provide additional support for this while also identifying a need to understand the cognitive consequences of CRF-GABA and CRF-glutamate interactions within and outside the PFC.

In primates, PFC pyramidal neurons in deep layer III may be particularly vulnerable in late adolescence when schizophrenia typically manifests (A. F. T. Arnsten & Datta, 2024). Interestingly, these neurons display an enhanced PKA-related transcriptome (A. F. T. Arnsten & Datta, 2024). Moreover, at least within rodents, PFC CRF1 receptors are enriched in layers II/III (Van Pett et al., 2000). Whether PFC layer III pyramidal or GABAergic neurons co-express CRF or its receptors in primates remains to be determined. Additionally, acute and chronic stress impair PFC-dependent cognition in a PKA-dependent manner (A. F. Arnsten, 2009b), consistent with PFC cognitive dysfunction in stress related disorders (A. F. Arnsten, 2009b; Birnbaum et al., 1999; Devilbiss et al., 2017b). Acute stress also increases levels of CRF and CRF1 receptors in the PFC (Meng et al., 2011b; Uribe-Mariño et al., 2016) and PFC CRF1 receptors contribute to stress-related cognitive impairment (Uribe-Mariño et al., 2016). Future studies will need to determine the extent to which stress impacts CRF_{Glu} and CRF_{GABA} neurons and the potential involvement of these neuronal populations in stress-related and other psychiatric disorders.

Acknowledgments

This work was supported by the National Institutes of Health grant MH116526 (CWB) and the Office of the Vice Chancellor for Research and Graduate Education at the University of Wisconsin-Madison with funding from the Wisconsin Alumni Research Foundation (CWB). SKC was partially supported by NINDS T32NS105602 through the Neuroscience Training Program at the University of Wisconsin-Madison. CWB, AJM, and SKC designed the study. AJM, SKC and SEN collected the data, with input from CWB and RCS. AJM, SKC and SEN analyzed the data, with input from CWB and RCS. CWB and SKC wrote the first drafts of the manuscript. All authors assisted in editing. Incomplete versions of the data were presented in an abstract and poster presentation at Society for Neuroscience in 2021 and 2024.

Disclosures

The authors report no biomedical financial interests or potential conflicts of interest.

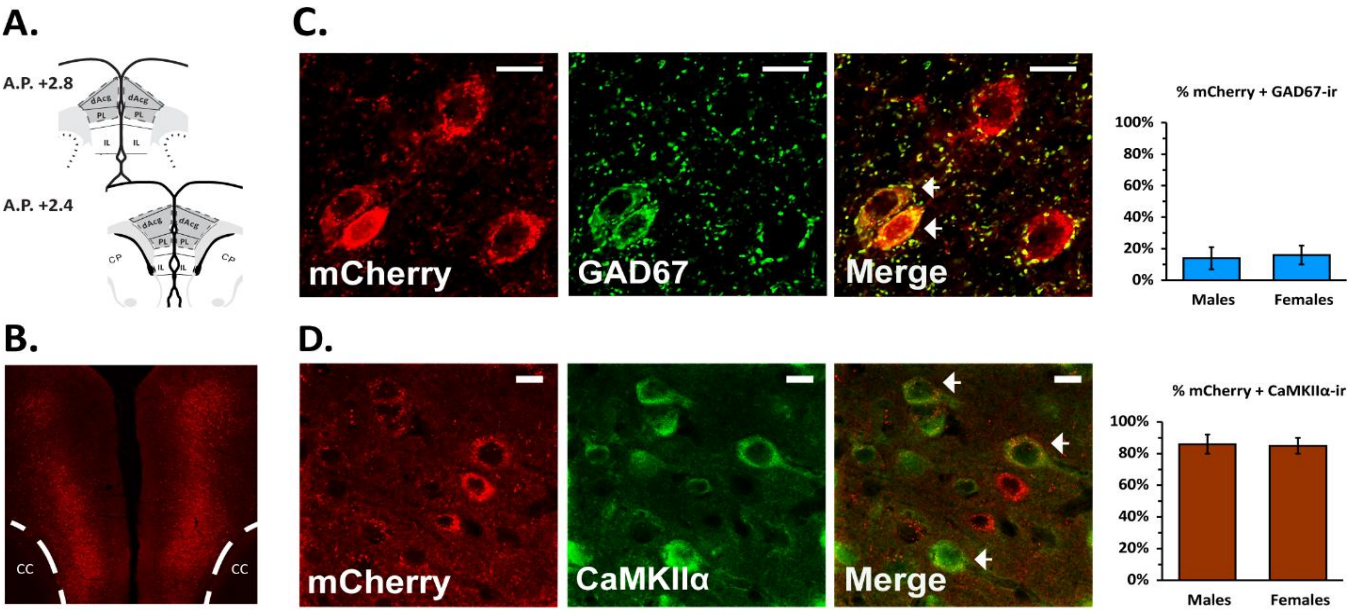

Figure 1. Immunohistochemical identification of CRF_{GABA} and CRF_{Glu} neurons in the caudal dmPFC. A) Schematics depicting the caudal aspect of the dmPFC that prior studies demonstrated contain cognition modulating CRF receptors and neurons. These studies identified a region of the dorsomedial PFC centered at ~AP+2.6 and spanning ~AP+3.0-2.2 that includes the dorsal anterior cingulate and dorsal prelimbic PFC. **B)** Low-power photomicrograph depicting bilateral viral expression (mCherry) within the caudal dmPFC using a 2-viral system that expresses DREADD receptors in CRF neurons. **C)** Collapsed 2-µm z-stack photomicrographs from an animal treated with the CRF-targeting DREADD viral cocktail depicting mCherry expression (left panel, red) and GAD67-ir (middle panel, green) that colocalize in a merged image (right panel). Bar graphs depict the percentage of CRF neurons (mCherry-positive) expressing GAD-67-ir (± SEM) for males and females. Scale bars = 20 µm. Arrows indicate exemplar double-labeled neurons. **D)** Collapsed 2-µm z-stack photomicrographs from an animal treated with the CRF-targeting DREADD viral cocktail depicting mCherry expression (left panel, red) and CamKIIa-ir (middle panel, green) that colocalize in merged image (right panel). Bar graph depicts the percentage of CRF neurons (HA-ir) expressing CamKII-ir (± SEM) for males and females. Scale bars = 20 µm. Arrows indicate exemplar double-labeled neurons.

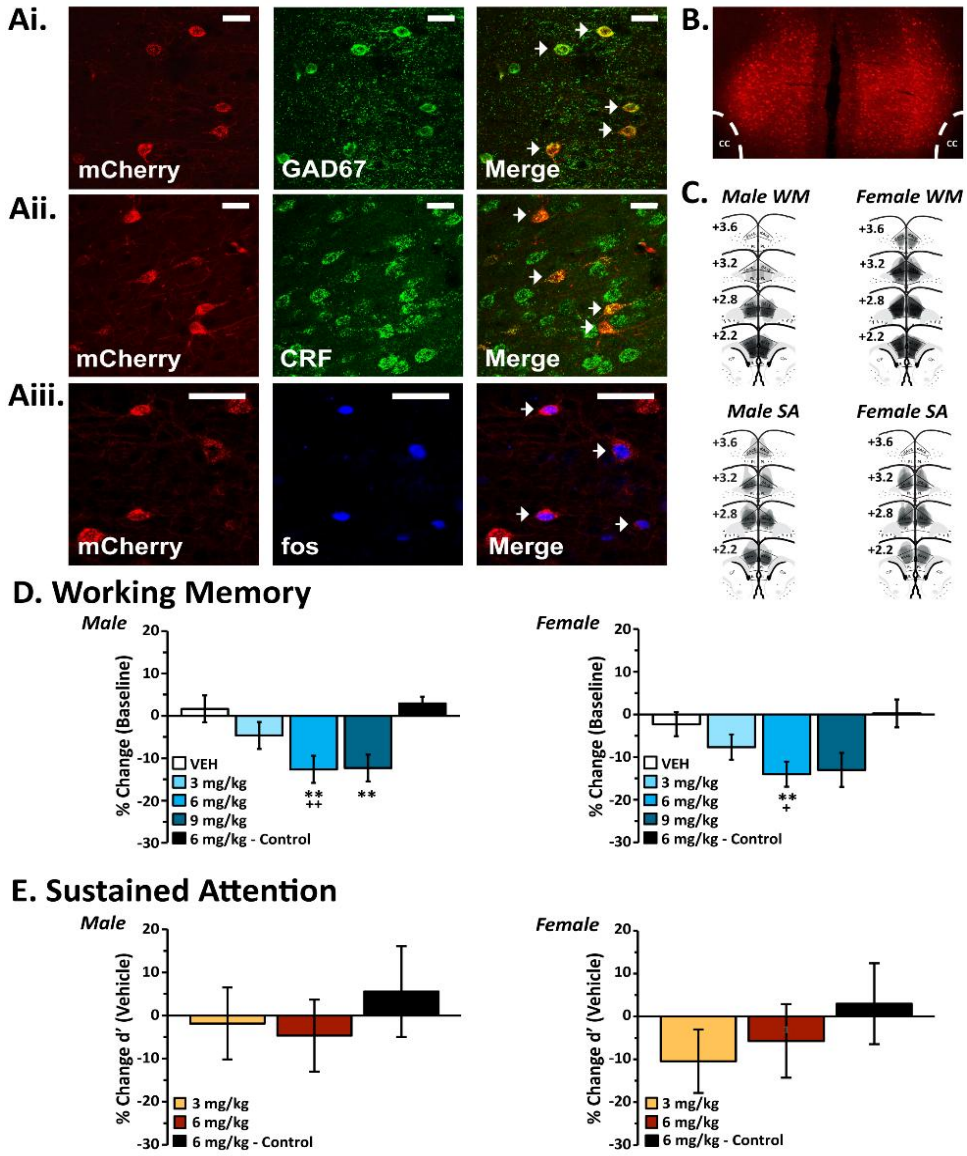

Figure 2. Activation of caudal dmPFC CRF$_{GABA}$ neurons impairs working memory but not sustained attention. Ai) Collapsed 2-µm z-stack photomicrographs from an animal treated with the CRF$_{GABA}$-hM3Dq viral cocktail depicting mCherry expression (left panel, red) and GAD67-ir (middle panel, green) that colocalize when the two images are merged (right panel). **Aii)** Collapsed 2-µm z-stack depicting mCherry expression (left, red) and CRF-ir (middle, green) colocalize when the two images are merged (right). **Aiii)** CNO treatment in CRF$_{GABA}$ animals elicits neuronal activation of mCherry-positive neurons (left, red), as measured by Fos-ir (middle, blue). Arrows indicate exemplar double-labeled neurons. Scale bars = 20 µm. **B)** Low-power photomicrograph of bilateral viral expression within the caudal dmPFC. **C)** Schematics depicting spread of CRF$_{GABA}$-hM3Dq viral expression in the caudal dmPFC from all males (left column) and females (right column) tested in *working memory* (WM, top pair) and sustained attention (SA, bottom pair). **D)** Bar graphs depict the *working memory* effects of vehicle (VEH) and varying doses of CNO in CRF$_{GABA}$ animals as measured by the percent change from baseline. CNO dose-dependently impairs working memory performance in both males and females (outside proestrus) treated with the CRF$_{GABA}$-hM3Dq viral cocktail relative to vehicle and 6 mg/kg CNO-treated viral control animals (Control). **E)** Bar graphs depict the *sustained attention* effects for varying doses of CNO in CRF$_{GABA}$ animals calculated as a percent change in d' from vehicle treatment. CNO did not significantly affect this measure of sustained attention performance in animals treated with the CRF$_{GABA}$-hM3Dq viral cocktail relative to vehicle and 6 mg/kg CNO-treated viral controls. Bars represent mean ± SEM estimated by the linear mixed-effects models. See Figure S2 for individual conditional predicted values and their relationship with raw performance. $^{**}P < 0.01$ vs. vehicle; $^{+,++}p < 0.05$, 0.01 vs. viral controls. cc, corpus callosum; CP, caudate-putamen; dAcg, dorsal anterior cingulate; IL, infralimbic PFC; PL, prelimbic PFC.

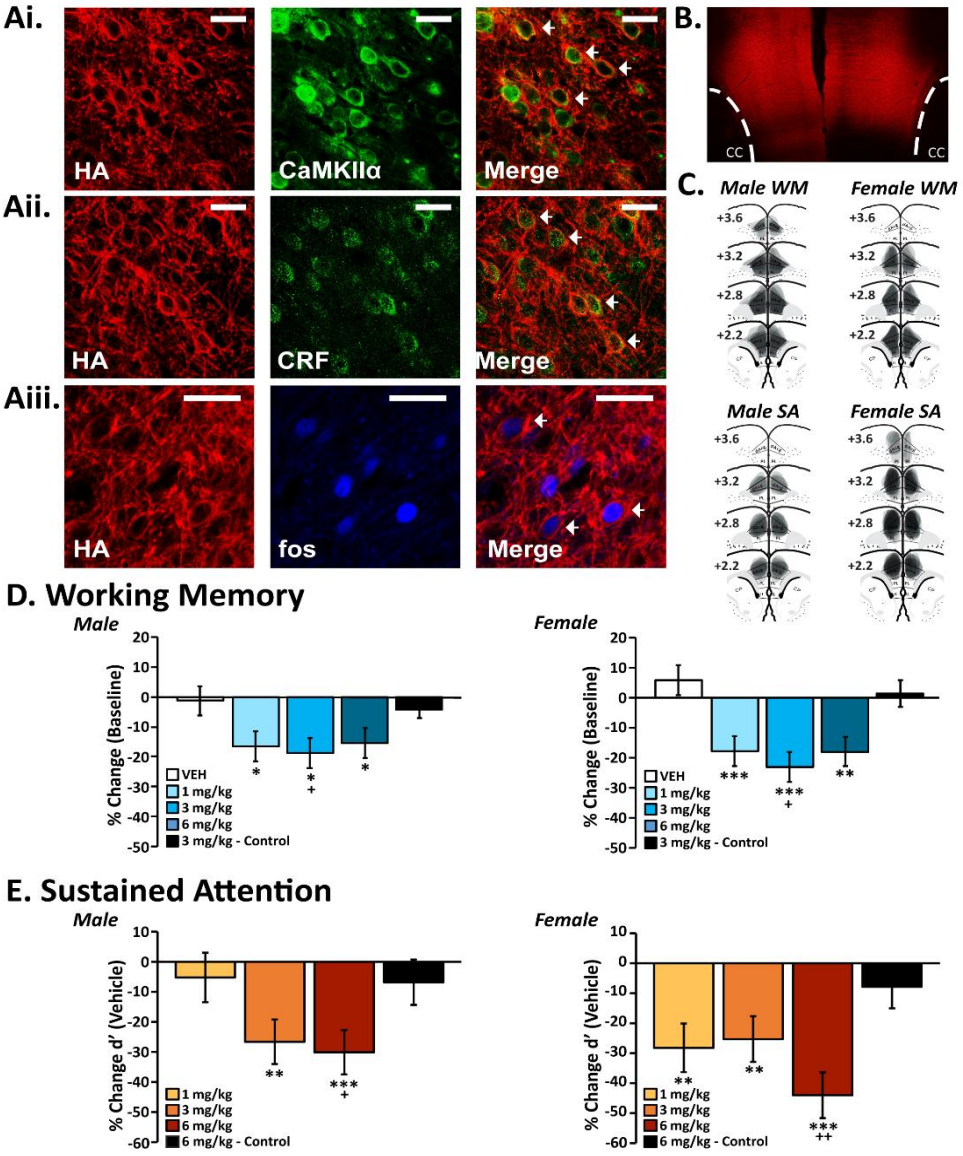

Figure 3. Chemogenetic activation of caudal dmPFC CRF_{Glu} neurons impairs both working memory and sustained attention. Ai) Collapsed 2-µm z-stack photomicrographs from an animal treated with the CRF_{Glu}-hM3Dq viral cocktail animal depicting HA expression (left panel, red) and CaMKIIα -ir (middle, green) that colocalize when the two images are merged (right panel). **Aii)** Collapsed 2-µm z-stack depicting HA expression (left panel, red) that colocalize CRF-ir (middle, green) when the two images are merged (right panel). **Aiii)** CNO treatment in hM3Dq animals elicits neuronal activation of HA-positive neurons, as measured by Fos-ir. Arrows indicate exemplar double-labeled neurons. Scale bars = 20 µm. **B)** Low-power photomicrograph of bilateral viral expression within the caudal dmPFC. **C)** Schematics depicting spread of CRF_{Glu}-hM3Dq viral expression in the caudal dmPFC from all males (left column) and females (right column) tested in *working memory* (WM, top pair) and sustained attention (SA, bottom pair). **D)** Bar graphs depict the *working memory* effects for vehicle (VEH) and varying doses of CNO in CRF_{Glu} animals as measured by the percent change from baseline. CNO dose-dependently impairs working memory performance in both males and females (outside proestrus) treated with the CRF_{Glu}-hM3Dq viral cocktail relative to vehicle and 3 mg/kg CNO-treated viral control animals (Control). **E)** Bar graphs depict the *sustained attention* effects of varying doses of CNO in CRF_{Glu} animals as measured as a percent change in d' from vehicle treatment. CNO significantly impaired sustained attention performance in animals treated with the CRF_{Glu}-hM3Dq viral cocktail relative to vehicle and 6 mg/kg CNO-treated viral controls. Bars represent mean ± SEM estimated by the linear mixed-effects models. See Figure S3 for individual conditional predicted values and their relationship with raw performance. $^{*,**,***}P < 0.05, 0.01, 0.001$ vs. vehicle; $^{+,++}p < 0.05, 0.01$ vs. viral controls. cc, corpus callosum; CP, caudate-putamen; dAcg, dorsal anterior cingulate; IL, infralimbic PFC; PL, prelimbic PFC.

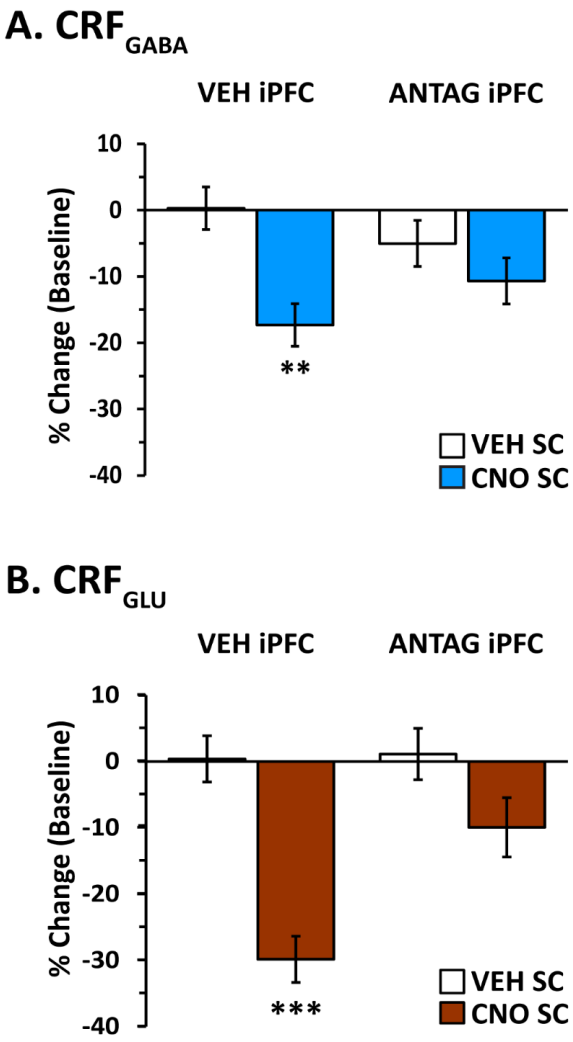

Figure 4. Local CRF receptors contribute to the working memory actions of caudal dmPFC CRF_{GABA} and CRF_{Glu} neurons. Bar graphs depict the effects of bilateral intracaudal dmPFC infusions of a CRF antagonist on the working memory effects of chemogenetic activation of caudal dmPFC CRF_{GABA} and CRF_{Glu} neurons as measured by percentage change in accuracy from baseline. Animals received bilateral infusions of either VEH (VEH iPFC) or the CRF antagonist D-Phe-CRF (ANTAG iPFC) immediately before receiving either subcutaneous VEH (VEH SC) or the highest impairing dose of CNO (CNO SC). Animals were tested 45 minutes later. (A) In animals treated with the CRF_{GABA}-hM3Dq viral cocktail, intracaudal dmPFC CRF antagonist prevented the working memory-impairing effects of CNO. (B) In animals treated with the CRF_{Glu}-hM3Dq viral cocktail, intracaudal dmPFC infusion of the CRF antagonist prevented the working memory **effects** of CNO. Bars represent mean ± SEM percentage change estimated by the linear mixed-effects models. See Figure S4 for individual conditional predicted values and their relationship with raw performance. $**p < .01$, $***p < .001$ vs. VEH. ANTAG, antagonist; CNO, clozapine *N*-oxide; CRF, corticotropin-releasing factor; dmPFC, dorsomedial prefrontal cortex; GABA, gamma-aminobutyric acid; glu, glutamate; iPFC, intra-PFC; SC, subcutaneous; VEH, vehicle.

Table I. Group Sizes for CRF_{GABA} and CRF_{Glu} Working Memory and Sustained Attention Experiments.

A. CRF_{GABA} & CRF_{Glu} Working Memory						
	Male-CRF_{GABA}				**Male-Control**	
Treatment	Saline	3 mg/kg CNO	6mg/kg CNO	9 mg/kg CNO	Saline	6 mg/kg CNO
n	*11*	*11*	*10*	*11*	*8*	*8*
	Female-CRF_{GABA}				**Female-Control**	
Treatment	Saline	3 mg/kg CNO	6 mg/kg CNO	9 mg/kg CNO	Saline	6 mg/kg CNO
n	*14*	*13*	*12*	*13*	*8*	*8*
	Male-CRF_{Glu}				**Male-Control**	
Treatment	Saline	1 mg/kg CNO	3 mg/kg CNO	6 mg/kg CNO	Saline	3 mg/kg CNO
n	*8*	*8*	*8*	*8*	*8*	*8*
	Female-CRF_{GABA}				**Female-Control**	
Treatment	Saline	1 mg/kg CNO	3 mg/kg CNO	6 mg/kg CNO	Saline	3 mg/kg CNO
n	*8*	*8*	*8*	*8*	*8*	*8*

B. CRF_{GABA} & CRF_{Glu} Sustained Attention						
	Male-CRF_{GABA}				**Male-Control**	
Treatment	Saline		3 mg/kg CNO	6 mg/kg CNO	Saline	6 mg/kg CNO
n	*7*		*7*	*7*	*7*	*7*
	Female-CRF_{GABA}				**Female-Control**	
Treatment	Saline		3 mg/kg CNO	6 mg/kg CNO	Saline	6 mg/kg CNO
n	*8*		*8*	*7*	*8*	*8*
	Male-CRF_{Glu}				**Male-Control**	
Treatment	Saline	1 mg/kg CNO	3 mg/kg CNO	6 mg/kg CNO	Saline	6 mg/kg CNO
n	*9*	*7*	*9*	*9*	*9*	*9*
	Female-CRF_{Glu}				**Female-Control**	
Treatment	Saline	1 mg/kg CNO	3 mg/kg CNO	6 mg/kg CNO	Saline	6 mg/kg CNO
n	*12*	*7*	*8*	*8*	*8*	*8*

C. CRF_{GABA} & CRF_{Glu} Working Memory + Intra-PFC CRF Antagonist				
	CRF_{Glu}			
Treatment	CNO SC + VEH iPFC	VEH SC + VEH iPFC	VEH SC + D-Phe iPFC	CNO SC + D-Phe iPFC
n	*12*	*12*	*10*	*8*
	CRF_{GABA}			
Treatment	CNO SC + VEH iPFC	VEH SC + VEH iPFC	VEH SC + D-Phe iPFC	CNO SC + D-Phe iPFC
n	*14*	*14*	*12*	*12*

Shown are the group sizes of working memory and sustained attention tested males and females receiving intra-caudal dmPFC viral cocktails for expressing excitatory DREADD receptors in CRF_{GABA}- and CRF_{Glu}-neurons and the respective viral controls.

Table 2. Effects of Chemogenetic Activation of Caudal dmPFC CRF_{GABA} and CRF_{Glu} Neurons on Select Sustained Attention Performance Variables.

A.

Male CRF_{GABA}			
	Proportion Hits	**Proportion False Alarms**	**Omissions**
Vehicle	60±7%	7±2%	0.17±0.71
3 mg/kg CNO	58±7%	6±2%	1.18±0.71
6 mg/kg CNO	59±7%	8±2%	0.61±0.71
Vehicle-Control	64±5%	12±3%	0.19±1.59
6 mg/kg CNO-Control	62±5%	9±3%	0.88±1.63

Female CRF_{GABA}			
	Proportion Hits	**Proportion False Alarms**	**Omissions**
Vehicle	59±6%	6±2%	0.38±0.64
3 mg/kg CNO	61±6%	11±2%*	1.37±0.67
6 mg/kg CNO	55±7%	5±2%	0.61±0.77
Vehicle-Control	65±4%	13±3%	2.55±1.45
6 mg/kg CNO-Control	67±4%	13±3%	3.62±1.48

B.

Male CRF_{Glu}			
	Proportion Hits	**Proportion False Alarms**	**Omissions**
Vehicle	70±3%	8±4%	0.01±1.35
1 mg/kg CNO	70±4%	9±4%	0.09±1.54

3 mg/kg CNO	72±3%	22±4%**	2.79±1.35**
6 mg/kg CNO	70±3%	21±4%**	0.45±1.35
Vehicle-Control	68±5%	11±3%	0.13±1.52
6 mg/kg CNO-Control	64±5%	12±3%	0.09±1.50

Female CRF_{Glu}			
	Proportion Hits	**Proportion False Alarms**	**Omissions**
Vehicle	71±3%	8±3%	3.41±1.16
1 mg/kg CNO	71±4%	19±4%**	4.78±1.54
3 mg/kg CNO	79±3%	27±4%***	3.94±1.40
6 mg/kg CNO	72±4%	36±4%***	8.73±1.41
Vehicle-Control	72±5%	9±3%	3.22±1.57
6 mg/kg CNO-Control	66±5%	9±3%	6.77±1.61

Response Latency				
	CRF_{GABA}		**CRF_{Glu}**	
	Male	**Female**	**Male**	**Female**
Vehicle	0.72 ± 0.04	0.72 ± 0.04	0.73 ± 0.08	0.79 ± 0.07
1 mg/kg CNO	-	-	0.81 ± 0.08****	0.95 ± 0.07***
3 mg/kg CNO	0.74 ± 0.04	0.71 ± 0.04	1.03 ± 0.08***	1.04 ± 0.07***
6 mg/kg CNO	0.75 ± 0.04	0.66 ± 0.04**	0.98 ± 0.08***	1.29 ± 0.07***

C.

Shown are the mean (± SEM) effects of vehicle and varying doses of CNO on hits, false alarms and response omissions in CRF_{GABA} (A) and CRF_{Glu} (B) male and females. Panels A and B also present the effects of vehicle and the highest dose of CNO (6 mg/kg) in viral control treated animals. Panel C presents the effects of these treatments on reaction time in CRF_{GABA} and CRF_{Glu} males and females. $^{*,**,***,****}P < 0.05, 0.01, 0.001, 0.0001$ vs. saline.

Supplemental Materials

Supplemental methods

In-situ hybridization.

Three 20-nucleotide probes labeled with digoxigenin (MicroSynth, Balgach, Switzerland) were utilized, each targeting different portions of rat CRF mRNA (NCBI GenBank reference sequence: NM_031019.2). Nucleotide sequences were taken from areas predicted to be unfolded (using RNA Webserver), have melting temperatures between 65-75°C, be comprised of 40 to 60% guanine and cytosine and have less than 0.001 affinity to non-CRF mRNA (NCBI BLAST). The three probes best meeting these criteria were: 1) 5'-CAA CCU CAG CCG AUU CUG AU-3', 2) 5'-CGG CUA ACU UUU UCC GCG UG-3', and 3) 5'-GAG AGC CUA UAU ACC CCU UA-3'. The reverse sequences of each probe served as a control ('sense' probes).

Animals were anesthetized, transcardially perfused and 40-µm thick sections collected through the PFC. In situ hybridization was conducted as described previously (Ritchie et al., 2024; Zhao et al., 2013). Briefly, tissue was serially washed with: 1) diethyl pyrocarbonate (DEPC)-treated 0.2 M PBS, 2) 3% H_2O_2; 3) 0.2 M HCl, and 4) 0.25% acetic anhydride. Hybridization occurred at 60°C with a probe concentration of 0.1 µg/mL in hybridization buffer (Ritchie et al., 2024; Zhao et al., 2013) over 18-24 hours. Tissue was washed with gradients of standard citrate saline and unbound oligonucleotide probes were digested with RNAse A (20 µg/mL; Roche, Indianapolis, IN). Probes were visualized using anti-digoxigenin antibodies (1:100; Roche, #11207733910) and tyramide amplification of cyanine 3 (Akoya Biosciences, Marlborough, MA, #NEL744001KT). Immunohistochemical labeling of CRF was conducted immediately following *in situ* hybridization. Tissue sections were washed before incubation with guinea pig anti-CRF (1:1000; Bachem, Torrance, CA, #t-5007). Sections were then incubated with goat anti-guinea pig antibody (1:200; Life Technologies, # A11075, AF488). 3-4 60X images (ImageJ, NIH) were collected per section with a confocal microscope (3-5 tissue sections/animal). Cells were counted only if there was a clear nucleus and were considered double-labeled only when fluorescence was clearly observed in the cytoplasm or nucleus (for Fos-ir) within the same cell. The percentage of double-labeled cells was averaged for each animal and then averaged across animals.

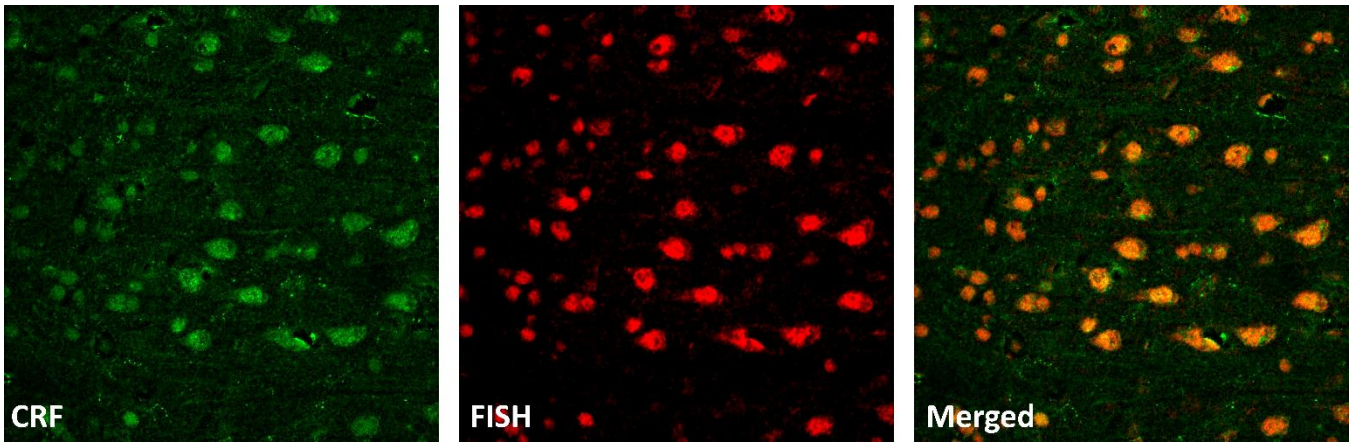

Figure S1. Strong overlap between CRF mRNA and CRF-ir in the caudal dmPFC. Shown are 2-µm-z-stacks from caudal dmPFC tissue sections showing labeling for CRF-ir (left panel, green), CRF mRNA (middle, red) and the overlap of the two (right panel). Cell counts indicated 97 ± 1% of CRF mRNA-containing neurons also co-expressed CRF-ir (n=1541 cells, 2 males, 2 females), while 99 ± 1% of CRF-ir neurons co-expressed CRF mRNA (n=1531 cells, 2 males, 2 females). When combined with earlier observations, these studies demonstrate a robust population of CRF neurons in the medial PFC. Scale bars = 20 µm.

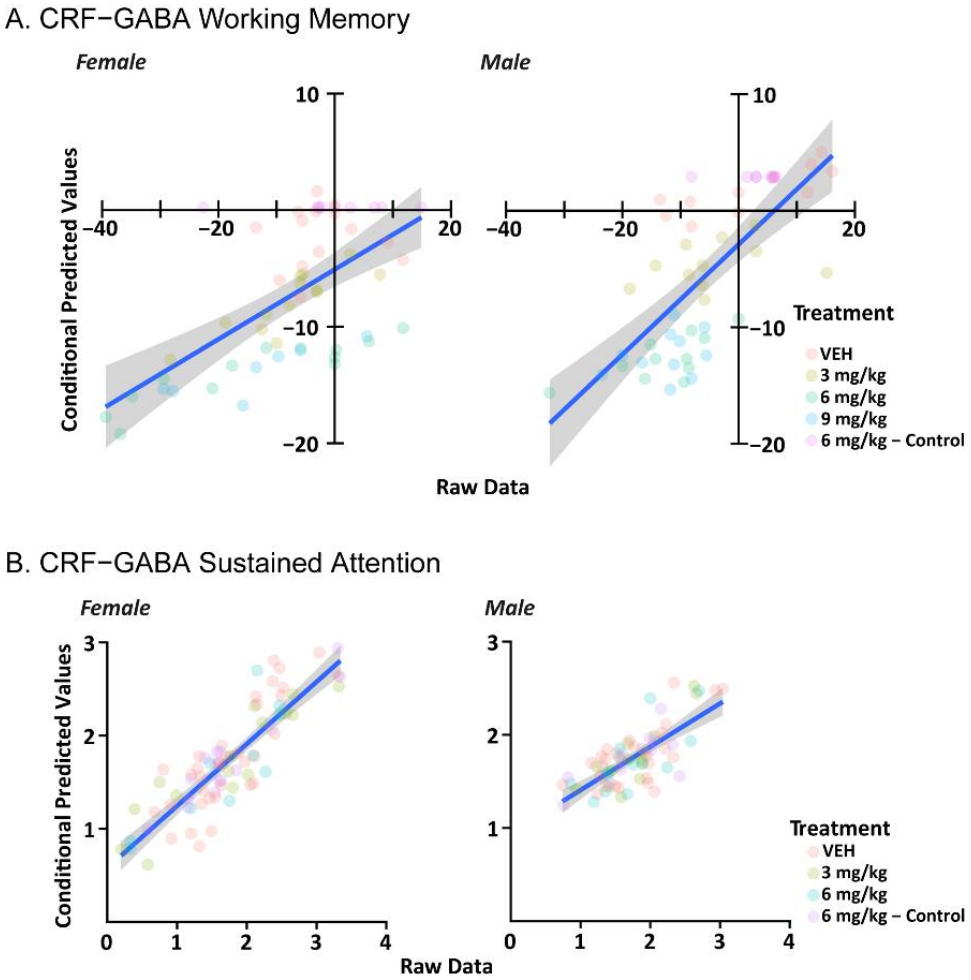

Figure S2. Relationship between conditional predicted and raw performance values for caudal dmPFC CRF$_{GABA}$ experiments. Scatter plots depict the relationship between raw performance data (working memory = % change baseline; sustained attention = d'; .X-axis) and model generated conditional predicted values (Y-axis) for **A)**working memory and **B)** sustained attention experiments in caudal dmPFC CRF$_{GABA}$ DREADD animals treated with vehicle and varying doses of CNO. Lines of best fit and their 95% confidence intervals (gray shading) are indicated.

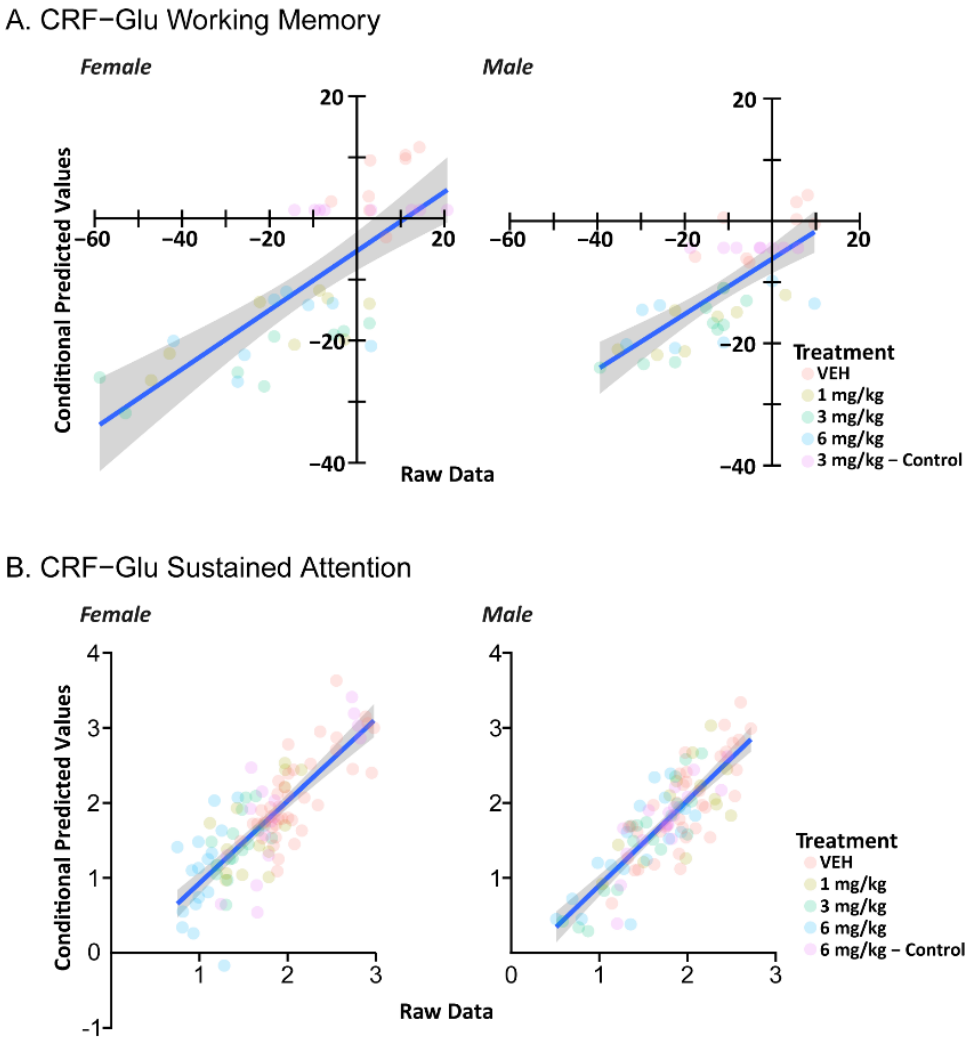

Figure S3. Relationship between model predicted and raw performance values for caudal dmPFC CRF$_{Glu}$ experiments. Scatter plots depict the relationship between raw performance data (working memory = % change baseline; sustained attention = d'; X-axis) and model generated conditional predicted values (Y-axis) for **A)** working memory and **B)** sustained attention experiments in caudal dmPFC CRF$_{Glu}$ DREADD animals treated with vehicle and varying doses of CNO. Lines of best fit and their 95% confidence intervals (gray shading) are indicated.

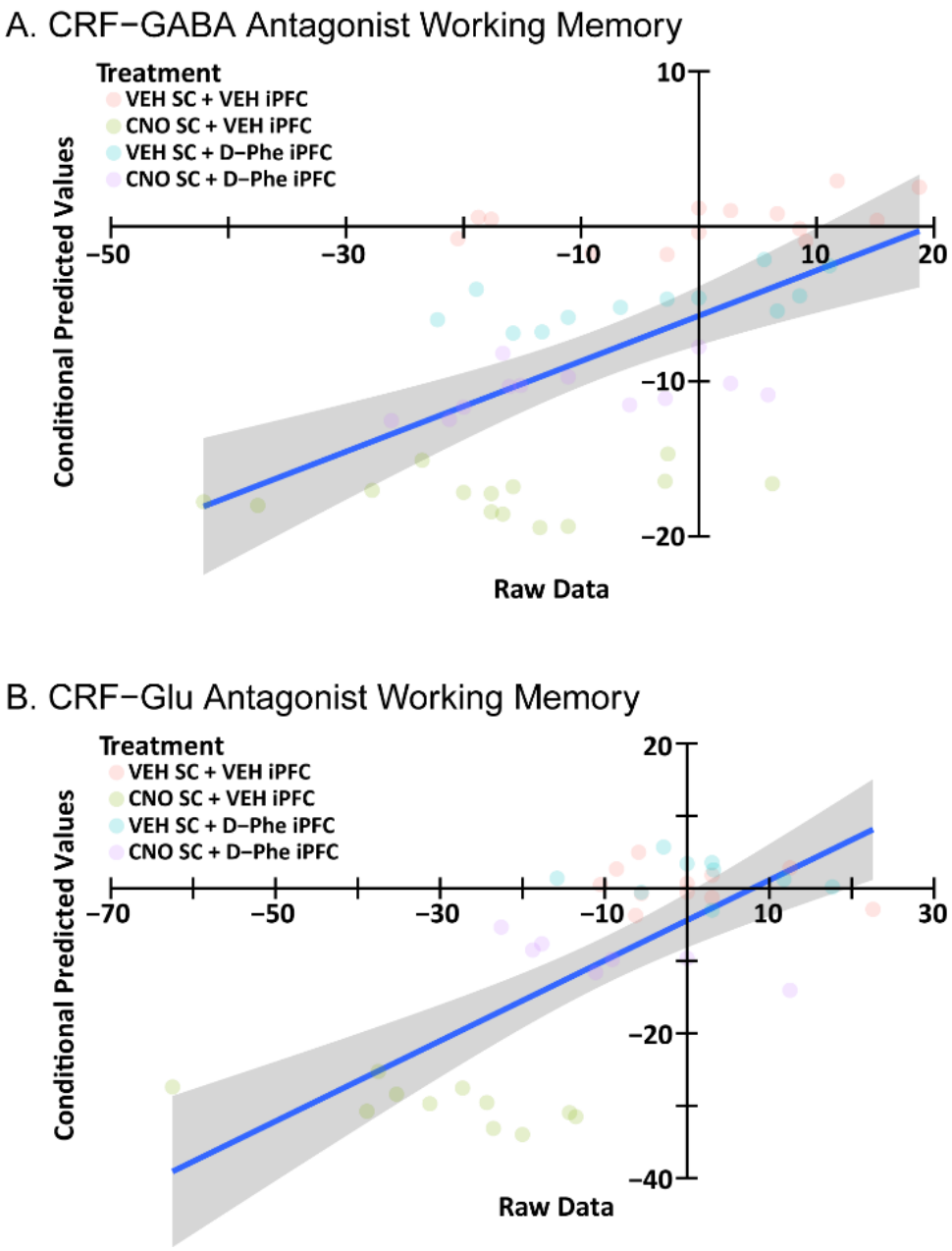

Figure S4. Relationship between model predicted and raw performance values for intra-caudal dmPFC CRF-antagonist experiments. Scatter plots depict the relationship between raw performance data (working memory = % change baseline; X-axis) and model generated conditional predicted values (Y-axis) for intra-caudal dmPFC vehicle vs. CRF antagonist in working memory tested CRF_{GABA} **A)** and CRF_{Glu} **B)** animals. The lines of best fit and their 95% confidence intervals (gray shading) are indicated.

Chapter 3

Prefrontal Cortex Corticotropin-Releasing Factor (CRF) Neurons Disrupt Sustained Attention, but Not Working Memory, Via the Mediodorsal Thalamus

Spencer Cooke, Andrea J. Martin, and Craig W. Berridge

Unpublished manuscript

Abstract

Background: The prefrontal cortex (PFC) supports higher cognitive processes that are dysregulated in multiple psychopathologies. Prior studies demonstrate the medial PFC of rats contains a dense and heterogeneous population of corticotropin-releasing factor (CRF) neurons. Activation of caudal dorsomedial PFC (dmPFC) CRF neurons disrupts both working memory and sustained attention. The working memory effects involve both glutamatergic (CRF_{Glu}) and GABAergic (CRF_{GABA}) CRF neurons that act at receptors within the caudal dmPFC. In contrast, the sustained attention actions only involve CRF_{Glu} neurons and are independent of local caudal dmPFC receptors. The neurocircuitry involved in CRF_{Glu} neuronal modulation of sustained attention is currently unknown.

Methods: Viral vectors were used to anterogradely label caudal dmPFC CRF neurons. Intra-tissue infusions of CRF or clozapine-N-oxide (CNO) in CRF-hM3Dq animals, were performed in sustained attention- and working memory-tested animals. In additional studies, electrophysiological recordings and chemogenetic activation of caudal dmPFC CRF_{Glu} neurons were used in sustained attention tested animals.

Results: The lateral mediodorsal thalamus (MD) receives a dense innervation from caudal, but not rostral, dmPFC CRF neurons. Intra-lateral MD CRF or CNO impaired sustained attention. In contrast, CRF infusions into the lateral MD had no effect on working memory. The sustained attention actions of PFC CRF_{Glu} neurons were associated with reductions in signal-related spiking activity of caudal dmPFC neurons as well as robust increases in theta/alpha oscillatory activity in the PFC-lateral MD circuit.

Conclusion: Combined, these studies provide novel insight into the neurobiology of higher cognitive function and neurocircuitry that could contribute to cognitive dysfunction.

The prefrontal cortex (PFC) and extended circuitry support executive cognitive processes, including working memory and sustained attention, that are dysregulated in multiple disorders (J. Fuster, 2015; Goldman-Rakic, 1996; Spencer & Berridge, 2019). Our incomplete understanding of the neural mechanisms supporting PFC-dependent cognition limits the development of more effective treatments for PFC-dependent cognitive dysfunction. Accruing evidence demonstrates potent cognitive actions of prefrontal corticotropin releasing factor (CRF) neurons (Berridge et al., 2022; Chen et al., 2020; Cole et al., 2016b; Cooke et al., 2025; de León Reyes et al., 2023; Hupalo et al., 2021; Hupalo, Martin, et al., 2019; Hupalo & Berridge, 2016). In particular, previous studies in outbred rats demonstrate an extremely dense population of medial PFC CRF neurons and that activation or inhibition of CRF neurons in the caudal dorsomedial PFC (dmPFC), but not other quadrants of the medial PFC, impairs or improves, respectively, both working memory and sustained attention (Berridge et al., 2022; Cooke et al., 2025; Hupalo et al., 2021; Hupalo, Martin, et al., 2019). Similar cognitive actions are observed in males and females, with the exception of proestrus, when CRF manipulations do not affect PFC-dependent cognition (Berridge et al., 2022). Interestingly, the working memory, but not sustained attention, actions of caudal dmPFC CRF neurons are dependent on local CRF receptors (Berridge et al., 2022; Hupalo et al., 2021; Hupalo, Martin, et al., 2019), indicative of heterogeneity in the projection pathways underlying the different cognitive actions of these neurons. Consistent with this, subsequent studies demonstrate that approximately 85% of PFC-CRF neurons are glutamatergic (CRF_{Glu}), while the remaining are GABAergic (CRF_{GABA}; Cooke et al., 2025). Moreover, while chemogenetic activation of CRF_{GABA} neurons impairs working memory only, CRF_{Glu} neuronal activation impairs both cognitive processes (Cooke et al., 2025). The working memory actions of both CRF subpopulations are dependent on CRF receptors in the caudal dmPFC (Cooke et al., 2025). Currently, the projection targets involved in the sustained attention actions of PFC CRF_{Glu} neurons are unknown, representing a significant lacuna in our understanding of the neurobiology of PFC-dependent cognition.

To initially address this issue, the axonal projection patterns of caudal dmPFC CRF neurons were examined using a CRF-specific viral-based anterograde labeling approach. Caudal dmPFC CRF neurons were observed to provide a remarkably dense innervation of the lateral aspect of the mediodorsal thalamus (MD), a region that plays a critical role in PFC-dependent cognition (Bolkan et al., 2017;

Broussard et al., 2006; Bucci, 2009; Mantanona et al., 2020a; Ouhaz et al., 2018; Saalmann, 2014; Sarter et al., 2001; Schmitt et al., 2017; M. Watanabe, 1989; Wolff & Halassa, 2024). Subsequent studies observed that activation of both CRF receptors and caudal dmPFC CRF neuronal axons in the lateral MD impaired sustained attention, while CRF action in the lateral MD did not influence working memory. Lastly, neuronal activity within the dmPFC-MD circuit supports higher cognitive processes (Berridge et al., 2023; Halassa & Sherman, 2019; Mailly et al., 2013; Parnaudeau et al., 2018b) and prior studies demonstrate that caudal dmPFC CRF neuronal activation robustly suppresses working memory-related neuronal activity within the dmPFC (Hupalo, Martin, et al., 2019). Therefore, additional studies examined the effects of dmPFC CRF_{Glu} neuronal activation on sustained attention-related single neuron activity and oscillatory power and synchrony within the dmPFC-lateral MD circuit.

Methods and Materials

Animals.

Male and female Sprague-Dawley rats (8-12 weeks; Charles River, Wilmington, Massachusetts) were pair-housed on a 13/11-hour light/dark cycle (lights on 0600 hours) and placed on a food restricted diet (males, 15-19 grams/day; females, 10-13 grams/day). Testing was conducted between 0800-1600 hours (5-7 days/week). Given prior observations (Berridge et al., 2022), all testing in females occurred outside proestrus. Facilities and procedures were in accordance with guidelines of the National Institutes of Health of the United States and approved by an Institutional Animal Care and Use Committee.

Immunohistochemical Analysis and Cell Counting

Animals were anesthetized and transcardially perfused, and 40-μm-thick sections collected. Immunohistochemical staining and cell counting were performed as previously described (Hupalo, Martin, et al., 2019). Washed tissue sections were incubated with guinea pig anti-CRF (1:1000; #t-5007; Bachem) then goat anti-guinea pig (1:500; #A11075, AF568; Life Technologies). Three to four 60× images were collected per section with a confocal microscope (3–5 tissue sections/animal). Cells were counted only if there was a clear nucleus and when fluorescence was clearly observed in the cytoplasm. The percentage of double-labeled cells was averaged for each animal and then averaged across animals.

Sustained Attention Testing.

Animals were trained in an operant-based visual signal detection task of sustained attention with 60dB white noise as described previously (Bushnell, 1998; Hupalo et al., 2021). Across 100 trials, animals pressed the right lever if they detected a brief LED signal of varying duration (8 lengths, range=0.125-1.0-second, with replacement) that occurred randomly on one-half of the trials (“signal trials”) and pressed the left lever if no light was detected (“no-signal trials”). Levers were projected after the signal period. Correct responses on signal trials (“hit”) and no-signal trials were rewarded (45-mg sucrose pellet/trial, Bio-Serv, Frenchtown, NJ) and followed by 5-second house light illumination. Incorrect presses on signal trials and no-signal trials (“false alarms”) resulted in lever retraction and a 5-second blackout. Upon failure to respond within 5-seconds of lever projection (“omission”), lever retraction and

a 5-second blackout ensued. Trials were separated by a variable inter-trial interval averaging 14-seconds (minimum of 5-seconds). Once animals achieved three consecutive days of ³70% correct, they underwent surgery. Following at least 4 days recovery, animals resumed testing until pre-surgery performance levels were achieved. d' (Z(N)-Z(SN), N=1-probability false alarms, SN=1-probability hits), probability of hits (number of hits/number of signal trials) and false alarms (false alarms/no-signal trials), number of omissions were analyzed. Treatments were replicated. Drug effects were assessed relative to vehicle for each replication round (Bushnell, 1998; Cooke et al., 2025; Hupalo et al., 2021).

Working Memory Testing.

Animals were trained in a delayed non-match to position T-maze task of spatial working memory in which animals alternate arm entry to receive a sucrose reward (45 mg pellet/trial) as previously described (Berridge et al., 2006; Spencer et al., 2012). External spatial cues were masked and white noise (60 dB) played above the center of the maze. Between trials, animals were placed in a start box at the base of the maze, prevented from exiting by a removable gate. Following training (10-trials/session, zero-delay) and surgery, animals were trained with 20-trials/session and the introduction of a 10-second delay between trials. As accuracy improves with repeated testing, delays were increased in 10-second intervals when needed to maintain an accuracy of 75-95% (range: 10-40 seconds). Treatments were given when accuracy across the 2 prior days did not differ by greater than 10%. Results were analyzed as percent change from baseline (average performance of the 2 prior days).

Surgery.

Stereotaxic surgery was conducted under isoflurane anesthesia (flat skull). Some animals received viral infusions (250nL/minute) into the caudal dmPFC (anteroposterior +2.5, mediolateral 0.8, ventral -2.85) or rostral dmPFC (anteroposterior +3.8, mediolateral 0.8, ventral -2.85). Injectors were left in place for 4-minutes following the infusion. Additional animals had bilateral 25ga. cannulae implanted ~200mm below the dura, targeting the lateral MD (anteroposterior -2.8; mediolateral 1.3) or adjacent regions. A subset of virus-treated animals had 8-wire linear electrode arrays (NB Labs, Dennison, TX) implanted into layer V/VI of the dmPFC (centered at anteroposterior +3.0, mediolateral 0.8, ventral -2.85) and the

lateral MD (ipsilateral to dmPFC electrodes, centered at anteroposterior -3.0, mediolateral 1.2 with 10º angle, ventral -5.4). Cannulae and electrodes were secured with skull screws and dental acrylic (Hupalo & Berridge, 2016; Spencer et al., 2012).

Viral Vectors.

To selectively target dmPFC CRF neurons, a cocktail of two viruses was utilized. The first virus was always AAV8-CRF-Cre ($1.3x10^{13}$gc/mL; Vector Biolabs, Malvern, PA; 8). The second virus varied depending on the experimental question. To anterogradely label dmPFC CRF neurons, the second virus was AAV5-hSyn-DIO-eGFP (premixed 1:2 ratio; 1.7µL/hemisphere; $2.9x10^{13}$gc/mL; Addgene). Labeled processes were examined in 40µm sections throughout the brain. To chemogenetically activate CRF axon terminals, the second virus was AAV5-DIO-hM3Dq-mCherry (premixed 1:2, 1.7µL/hemisphere, $1.5x10^{13}$gc/mL, Vector Biolabs). To chemogenetically activate CRF_{Glu} neurons the second virus was AAV8-CaMKIIα(1.3)-DIO-hM3Dq-WPRE-HA (premixed 1:2, 1.7 µL/hemisphere, $1.5x10^{13}$ gc/mL, Vector Biolabs; 11). Animals were allowed at least three weeks prior to testing for recovery and viral expression. At the end of a study, animals were transcardially perfused as previously described (Hupalo, Martin, et al., 2019). HA was visualized using a rabbit-anti hemagglutinin primary antibody (1:2000; Cell Signaling Technology, Danvers, MA, #3724s) and a donkey anti-rabbit secondary antibody (1:200; Life Technologies, #A21206, AF488). Viral controls utilized a second virus that lacked the hM3Dq transgene but were identical in all other respects.

Drugs and Treatments.

For intra-tissue infusions, CRF (human/rat, Bachem, Torrance, CA) and CNO (clozapine-N-oxide dihydrochloride, Cayman Chemical, Ann Arbor, MI) were dissolved in buffered artificial extracellular fluid (bAECF; 147mmol/L NaCl, 1.3mmol/L CaCl, 0.9mmol/L MgCl, 2.5mmol/L KCl; pH=7.4). Bilateral 0.5 nL infusions (0.25µL/minute) were made into the lateral MD via 33ga. stainless-steel infusion needles (MD, 4.8mm projection beyond a cannula). Needles were left in place for 2-minutes. For subcutaneous treatment, CNO was dissolved in 0.9% saline and injected 45-minutes prior to testing. All treatments were separated by at least 1-day and were replicated and counterbalanced.

Vaginal Cytology.

Daily vaginal cytology was used to determine estrus cycle stage as previously described (Berridge et al., 2022). Estrus was estimated from wet samples collected within 1-hour of behavioral testing. Dried samples were later stained using Harris' Hematoxylin Protocol (National Diagnostics, 2011) to confirm estrus cycle stage. Results were analyzed only if stained samples confirmed testing occurred outside proestrus.

Electrophysiological Recordings.

Experimental Design. Sustained attention testing was identical to that described above, except only a 0.5-second signal-duration was used followed by a 0.5-second interval preceding lever extension. Animals were placed in the operant chamber and tethered to a 32-channel commutator and a multichannel electrophysiology acquisition processor (MAP, Plexon, Dallas, TX). Neural activity was amplified, discriminated, and time stamped. Putative single units in the dmPFC and lateral MD exhibiting a ~3:1 signal-to-noise ratio were isolated. Multiple measures were used to ensure that sorted waveforms arose from single neurons and remained stable throughout a testing session, as described previously (Berridge et al., 2023; Hupalo, Martin, et al., 2019). After spike-sorting, a 100-trial '*pre-treatment*' testing session was conducted at ~10:30 AM followed by a second 100-trial '*post-treatment*' session 1.5-hours later. Animals remained in the testing chamber connected to the headstage between sessions. Animals received either subcutaneous vehicle or a performance impairing dose of CNO **(**6 mg/kg CNO, 11) 45-minutes prior to the post-treatment session.

Single Unit Analyses. Within the PFC, wide-spiking (WS, >200-microsecond trough-peak average), putative glutamatergic pyramidal neurons, and narrow-spiking (NS, 100-200-microsecond trough-peak average), putative inhibitory interneurons, were differentiated as previously described (Berridge et al., 2023; Hupalo, Martin, et al., 2019; Mitchell et al., 2007). Minimal NS neurons were observed, and this category was not analyzed further. Neuronal activity was analyzed for 0.5-second intervals (100-millisecond bins) following signal presentation and correct and incorrect lever press, and for a 3-second

interval associated with reward retrieval/consumption. Permutation tests were performed on 10,000 pseudo-randomly shuffled 100-millisecond bins during task events and the intertrial interval (Mohebi et al., 2019). Neurons were identified as tuned to events if the observed difference in firing rates between events and the intertrial interval was less than 5% likely to occur in the permuted (shuffled) data set (one-tailed, Holm-Bonferroni corrected).

Local Field Potential (LFP) Analyses. LFPs were recorded from all electrodes in the dmPFC and the lateral MD as previously described (Berridge et al., 2023). Signals were referenced to ground, amplified, filtered, and digitized at 1 kHz, then down sampled to 200 Hz. Offline, a differential reference with the nearest neighboring wire was performed (Meyer et al., 2018). LFP spectral density was analyzed using continuous wavelet transform (cwtft, MATLAB), with Morlet wavelets, and logarithmically increasing frequency, 4 to 100 Hz. Due to intermittent 60 Hz noise, a double-pass 59-61 Hz notch filter was applied to LFP recordings. The absolute power at each frequency was then calculated by squaring the absolute value of the wavelet coefficient (Cohen, 2014). The wire/region with the highest power and least motion artifact was selected for further analyses. Average power within distinct frequency bands (theta 4-7 Hz; alpha 7-12 Hz; beta 15-35 Hz; gamma 40-80 Hz) was calculated for each trial over the intervals of interest. To quantify synchrony, the cross-correlation as a function of frequency and time, wavelet transform coherence (wcoherence, MATLAB) with Morlet wavelets was calculated. Average synchrony per frequency band was calculated per trial.

Histology and Viral Expression.

Animals were transcardially perfused with a study-appropriate fixative, as previously described (Berridge et al., 2023; Hupalo, Martin, et al., 2019). For electrophysiological studies, animals were deeply anesthetized and cathodal current (15 μA) prior to perfusion. The placement of infusion needles, electrodes and viral expression was determined from 40μm coronal sections as previously described (Berridge et al., 2023; Cooke et al., 2025; Hupalo, Martin, et al., 2019). Double-labeled cell counting was conducted as previously described (Hupalo, Martin, et al., 2019). Data were included in the analyses only when accurate placement and minimal tissue damage were confirmed.

Statistical Analyses.

Behavioral analyses. Behavioral effects were analyzed using a linear mixed effects model. The base model used treatment as a fixed effect factor and animal as a random factor (JMP Pro Version 12.2.0, SAS Institute). For sustained attention testing, round of treatment was included as a fixed effect factor to control for increases in performance over time (Dixon, 2016). Where applicable sex was included as a fixed effect factor.

Single Unit Analyses. Unique generalized linear mixed effects models (GLMM) were utilized for each brain region (rostral PFC, caudal PFC, or MD), each event, and for the spiking of neurons that were either event-tuned or untuned (glmmTMB, R; Brooks et al., 2017). Session, treatment, and the interaction were fixed effects, and rat, date of recording, neuron id, and the interaction were random effects (Dixon, 2016). The GLMMs were run using zero-inflated gamma family distributions with inverse link function. The leverage, residuals, and Cook's distance of each point were used to determine outliers (DHARMa, R; Hartig, 2015/2026). No outlier points were identified. If significance was found, CNO effects in hM3Dq animals were directly compared to effects in viral controls using the same model but replacing treatment for virus type.

Local Field Potential Analyses. The same approach described above was used to analyze absolute power and synchrony for each frequency band (theta 4–7 Hz; alpha 7–12 Hz; beta 15–35 Hz; gamma 40-80 Hz; glmmTMB, R; 34). However, due to the lack of zero-inflation, a gamma family distribution with an inverse link function was used for GLMM analysis. No points were determined to be significant outliers for absolute power analyses. A small percentage of outliers were identified in each synchrony model. The maximum number of trials removed was for reward-beta synchrony (74 out of 6148 trials, 1.20%).

RESULTS

Anterograde Labeling of caudal dmPFC CRF neurons.

Our prior studies used an AAV8-CRF-Cre/AAV8-hM3Dq viral cocktail that did not result in robust anterograde labeling. To better determine the projection targets of caudal dmPFC-CRF neurons, we used an AAV8-CRF-Cre/AAV5-eGFP cocktail. Validation analyses demonstrated this approach results in efficient and selective labeling of PFC CRF neurons, similar to our AAV8-based approach. Specifically, out of 120 CRF-immunoreactive (ir) and 109 eGFP-positive medial PFC neurons (n=1 female/2 males), 100% of eGFP neurons colocalized with CRF-ir and 91% of CRF-ir neurons expressed eGFP (Figure 1A). Prior studies demonstrate that using this antibody there is ~99% overlap between CRF-ir and CRF mRNA expression (Cooke et al., 2025). Viral infusions were made into the caudal dmPFC (n=2 females/2 males) or rostral dmPFC (n=1 female/2 males). These infusions resulted in a light-to-moderate density of labeled fibers throughout much of the brain. In contrast, *caudal* dmPFC viral infusions resulted in an exceptionally dense innervation of the lateral portion of the MD (Figure 1B,C). These lateral MD fibers possessed dense varicosities indicative of release sites (Figure 1B). Minimal fibers were observed in the medial or central MD in these animals. Conversely, infusions into the *rostral* dmPFC, resulted in a dense innervation of the medial and ventral, but not lateral MD (Figure 1C).

Does CRF act in the lateral MD to affect sustained attention?

Additional studies examined whether CRF receptor activation in the lateral MD influences sustained attention. Animals received infusions of vehicle or varying doses of CRF (100ng, 250ng) into the lateral MD (male n=7; female n=7). There was a significant effect of treatment on performance as measured by d' ($F_{2,58}$=3.544, p=0.035), but not a significant effect of sex ($F_{1,12}$=0.249, p=0.627) or a sex*treatment interaction ($F_{2,58}$=0.5978, p=0.553). Maximal decreases were observed at the highest dose relative to vehicle (t_{32}=2.39, p=0.02; Figure 2B). These effects of CRF were not associated with significant changes in other measures of performance, including omissions (see Table 1A). Infusions of 250ng CRF into regions immediately outside the lateral MD, including the medial MD, did not impact d' (Figure 2C; medial, n=5, -5±5%; lateral, n=5, 3±16%; dorsal, n =3, 5±9%, ventral, n=3, 9±9%).

Lastly, to test whether the lateral MD is necessary for this sustained attention task, intra-lateral MD infusions of the GABA-A agonist, muscimol, were made in a subset of animals (n=7 males). These infusions elicited very large decreases in d' relative to vehicle treatment (t_{23}=7.43, p<0.001; Table 1A) that were associated with large reductions in task engagement (64±9% omissions).

Do caudal dmPFC CRF projections to MD affect sustained attention?

Given our prior observations that caudal dmPFC CRF neurons impair sustained attention via CRF release outside the PFC (Berridge et al., 2022; Cooke et al., 2025; Hupalo et al., 2021), additional studies examined whether projections from caudal dmPFC CRF neurons to the lateral MD affect sustained attention performance. Animals received infusions of the AAV8-pCRF/AAV5-DIO-hM3Dq cocktail into the caudal dmPFC (n=10) and subsequently received infusions of either 150ng CNO or vehicle into the lateral MD. Dose of CNO was based on prior observations (Hupalo, Martin, et al., 2019) and limited pilot studies. The occasional mistiming of treatments relative to proestrus leads to repeated treatments that increase risk for infection and/or tissue damage, which when observed requires removal of all data from that animal from the study. To minimize animal usage, only males were used for this study. In contrast to our earlier chemogenetic studies (Berridge et al., 2022; Cooke et al., 2025; Hupalo et al., 2021; Hupalo, Martin, et al., 2019), the current studies used an AAV5 serotype for the second virus to maximize anterograde hM3Dq expression and to align with the anatomical studies described above. We first confirmed that systemic CNO impairs sustained attention similar to our AAV8-based cocktail (Hupalo et al., 2021). Dose of CNO was based on prior observations (Hupalo et al., 2021) and limited pilot studies. When administered subcutaneously, 0.3 mg/kg CNO significantly decreased sustained attention as measured by d', relative to vehicle (n=6; t_5=5.97, p=0.0019; Figure 3C; Table 1B). CNO infusion into the lateral MD of AAV5-hM3Dq animals similarly decreased performance as measured by d', relative to both vehicle (n=10; t_{23}=2.76, p=0.0112; Figure 3C; Table 1B) and CNO infusions in viral controls (n=7; t_{13}=2.6, p=0.0224; Figure 3C; Table 1B).

Does CRF action in the lateral MD affect working?

Extensive evidence demonstrates the MD plays a crucial role in working memory (Bolkan et al., 2017; Ouhaz et al., 2018; Saalmann, 2014; M. Watanabe, 1989; Wolff & Halassa, 2024). Given caudal dmPFC CRF neurons potently modulate working memory (Berridge et al., 2022; Hupalo, Martin, et al., 2019), we hypothesized that CRF action in the lateral MD would influence working memory. To test this, we examined the effects of bilateral intra-lateral MD infusion of vehicle or CRF (100ng, 250ng) on working memory (n=12). In contrast to that observed for sustained attention, neither dose of CRF significantly affected working memory performance ($F_{2,22}$=0.85, p=0.440; Figure 4B). Nonetheless, as with sustained attention, inactivation of this region via muscimol (n=6) elicited large impairments in performance (-73±8%; Vehicle, ; t_5=7.85, p=0.0005) that were associated with decreased task engagement (35±13% omissions), though not as severe as in sustained attention.

Does PFC CRF_{Glu} neuronal activation affect sustained attention-related dmPFC-lateral MD neural coding?

PFC-dependent cognition is supported by neuronal activity across the PFC-MD circuit (Bolkan et al., 2017; Broussard et al., 2006; Bucci, 2009; Mantanona et al., 2020a; Ouhaz et al., 2018; Saalmann, 2014; Sarter et al., 2001; Schmitt et al., 2017; M. Watanabe, 1989; Wolff & Halassa, 2024). Additional studies examined the effects of activation of caudal dmPFC CRF_{Glu} neurons on task-related neuronal spiking and LFP oscillatory activity in the dmPFC and lateral MD (Figure 5). Animals received AAV8 hM3Dq/CRF_{Glu} (n=14) or control (n=8) viral cocktails bilaterally into the caudal dmPFC and recording electrodes were implanted into the dmPFC and lateral MD. Sustained attention-related single-unit and LFP activity were recorded in a pre-treatment 100-trial morning session and in a post-treatment 100-trial afternoon testing session following subcutaneous treatment with vehicle or 6 mg/kg CNO. As observed previously (Cooke et al., 2025), CNO treatment impaired sustained attention as measured by d' in hM3Dq animals relative to both vehicle-treated animals (t_{96}=4.60, p<0.0001) and viral controls (t_{23}=3.27, p=0.003; Figure 6A; Table 1C).

Single unit activity. Across all animals, 1,273 single neurons were recorded in the PFC and 575 in the MD. In the PFC, 1,225 (96%) were classified as WS and 27 (2%) as NS. Given the low numbers of NS

neurons, only wide-spiking neurons were analyzed. Permutation analyses indicated that under pre-treatment conditions 456 PFC WS neurons (37%) displayed event-related firing. Among these, 243 (53%) were tuned to reward, 181 (40%) were tuned to correct lever press, 116 (25%) were tuned to signal, and 91 (20%) were tuned to incorrect lever press. Of the 575 MD neurons, only 108 (19%) displayed event-related tuning. Among these, 75 (69%) were tuned to reward, 34 (31%) were tuned to correct trial lever press, 22 (20%) were tuned to incorrect trial lever press, and 16 (15%) were tuned to signal.

Activation of caudal dmPFC CRF_{Glu} neurons did not alter the activity of any event-related neuronal activity in dmPFC or lateral MD. However, in the PFC there was a trend for a decrease in signal-related activity. Given the virus was placed in the caudal dmPFC and given prior research demonstrating a rostrocaudal functional topography within the dmPFC (Alsene et al., 2011; Hupalo & Berridge, 2016), we analyzed signal-related neuronal activity across rostral and caudal subfields of the dmPFC. As shown in Figure 6B, caudal dmPFC CRF_{Glu} neuronal activation robustly suppressed signal-related activity of caudal dmPFC neurons relative to vehicle-treated animals (n=52; $F_{2,97}$=8.79, p=0.003) and viral controls ($F_{2,67}$=6.28, p=0.012). This was not observed in the rostral dmPFC (n=36; $F_{2,65}$=0.22, p=0.853). There were no significant effects of caudal dmPFC CRF_{Glu} neuronal activation on single-unit activity across rostral vs. caudal subdivisions of the dmPFC for other task-related events (Table 2). Given curvature of the lateral MD, it was not possible to position all 8 wires of the linear recording array within the rostrocaudal extent of this region. As such, it was not possible to analyze neural activity across rostral vs. caudal portions of this region.

Oscillatory activity. Within the dmPFC and across all events, activation of caudal dmPFC CRF_{Glu} neurons led to large increases in theta and alpha power and more modest decreases in beta and gamma power relative to vehicle-treated animals and viral controls (Figure 7A; Table 3A,C). Within the lateral MD, smaller and somewhat more varied effects were observed (Figure 7B; Table 3B,D). Similar to that seen in the PFC, there were significant increases in theta and alpha power for most events (excluding incorrect lever press theta). Unlike in the PFC, there were modest, yet significant, *increases* in beta power for all events and small, yet significant, increases in signal- and reward-related gamma power (Figure 7B; Table 3B,D). In the dmPFC, the effects of caudal dmPFC CRF_{Glu} neuronal activation

generally extended into the intertrial baseline period (Figure 7A; Table 3A,C). This was less consistent across frequencies in the lateral MD (Figure 7B; Table 3B,D).

Additional analyses examined the effects of caudal dmPFC CRF_{Glu} neuronal activation on oscillatory synchrony within the caudal dmPFC-lateral MD circuit. The only significant effects were moderate increases in reward-related theta and alpha synchrony and a small decrease in incorrect press-related gamma synchrony (Table 4; Table S1).

Discussion

Prior studies demonstrate that CRF neurons in the caudal dmPFC impair sustained attention (Berridge et al., 2023; Cooke et al., 2025; Hupalo et al., 2021). However, unlike the working memory actions of these neurons, the underlying circuitry remained unclear. The current study demonstrates that caudal dmPFC CRF neurons provide a remarkably dense innervation of the lateral MD and that CRF and axon terminals arising from caudal dmPFC CRF neurons act in this region to impair sustained attention. Given the previously documented critical role of the MD in working memory (Bolkan et al., 2017; Ouhaz et al., 2018; Saalmann, 2014; M. Watanabe, 1989; Wolff & Halassa, 2024) and the density of CRF fibers in the lateral MD, it was surprising that CRF action in this region had no impact on working memory. These studies further demonstrate that the impairment in sustained attention produced by caudal dmPFC CRF_{Glu} neuronal activation is associated with a complex pattern of actions on single-unit activity, oscillatory power and oscillatory synchrony within the dmPFC-lateral MD circuit. Collectively, these observations provide novel insight into the neural circuitry underlying PFC-dependent cognition and identify a critical role of the MD in the sustained attention actions of PFC CRF neurons.

Distinct Mechanisms Underlie CRF Modulation of Differing PFC-Dependent Cognitive Processes.

Prior studies demonstrate that the working memory, but not sustained attention, actions of caudal dmPFC CRF neurons involve CRF receptors in the caudal dmPFC (Berridge et al., 2023; Hupalo et al., 2021; Hupalo, Martin, et al., 2019; Hupalo & Berridge, 2016). Additional studies demonstrate that medial PFC CRF neurons are comprised of both CRF_{Glu} and CRF_{GABA} subtypes, in differing proportions (Cooke et al., 2025). Both CRF_{GABA} and CRF_{Glu} neurons impair working memory, while only CRF_{Glu} impair sustained attention (Cooke et al., 2025). Consistent with our earlier observations, the working memory, but not sustained attention, actions of both CRF neuronal subtypes were dependent on caudal dmPFC receptors. The current studies provide the first demonstration that CRF and CRF axons arising from caudal dmPFC CRF neurons act within the lateral MD to impair sustained attention but not working memory.

Tests of working memory and sustained attention used in these studies both require motivation, an understanding of task rules, the ability to spatially alternate responding, and the need to detect and attend to sensory information, including response outcome information. The above observations indicate that caudal dmPFC-lateral MD CRF neurotransmission does not significantly disrupt processes that are common to both tasks. A key difference between working memory and sustained attention tasks is the former requires holding information online in the absence of sensory signals. PFC neurons play a critical role in the maintenance of mental representations required for working memory (J. Fuster, 2015; Goldman-Rakic, 1996; Spencer & Berridge, 2019) and CRF neurotransmission in the caudal dmPFC degrades the neural activity associated with these representations (Hupalo, Martin, et al., 2019). The MD plays an important role in the maintenance of working memory-related neural coding within the PFC (Bolkan et al., 2017; Cardoso-Cruz et al., 2013; Floresco et al., 1999; Parnaudeau et al., 2013). Nonetheless, CRF action in the lateral MD did not interfere with working memory performance. The signal detection test of sustained attention requires directing attention to a spatially restricted region over a relatively large number of trials to detect a relatively brief sensory event. While there is an inter-trial interval during which attention to the LED panel is not required, the interval is variable, and thus the animal cannot predict when to resume attending. This contrasts with the working memory task in which an animal need only attend to the response selection made on the prior trial and its associated outcome. Thus, it is possible that CRF action in the lateral MD interferes with the sustained and effortful direction of attention towards weak sensory events, something not required in working memory testing.

Caudal dmPFC Neurons Disrupt dmPFC-Lateral MD Neural Coding of Sustained Attention

The current studies identified subpopulations of dmPFC and lateral MD neurons that responded to key task events in sustained attention testing. The PFC observations are consistent with that observed previously for this task (Gill et al., 2000). To our knowledge, this is the first examination of sustained attention-related activity of MD neurons. Interestingly, relative to the dmPFC there were lower proportions of lateral MD neurons tuned to specific events. In prior studies in working memory tested animals, activation of caudal dmPFC CRF neurons robustly suppressed delay- and reward-tuned neurons (Hupalo, Martin, et al., 2019). In contrast, chemogenetic activation of caudal dmPFC CRF_{Glu} neurons

had minimal effects across the majority of sustained attention-related events, including reward. The one exception to this was a robust suppression of the activity of signal-tuned neurons in the caudal, but not rostral, dmPFC. Suppression of signal-related neuronal activity may contribute to poor attention to or detection of key sensory information. The lack of effects on reward-related activity of PFC neurons could reflect differences in manipulations given our prior studies activated both CRF subtypes and not only CRF_{Glu} neurons. Additionally, there are differences between tasks regarding how response outcome is signaled. Specifically, in sustained attention testing a correct response elicits near-simultaneous feedback (house light activation) while in working memory testing there is a short lag between correct maze arm entry and hand delivery of reward. Prior studies suggest that the PFC contributes to dopamine signaling during unknown reward states (Starkweather et al., 2018). In the sustained attention task, the certainty of outcome associated with correct responding may not require PFC-dependent encoding of reward-related information.

Chemogenetic activation of caudal dmPFC CRF neurons resulted in large increases in dmPFC and lateral MD theta and alpha oscillatory power across all events. At least within the PFC, these effects were largely event-independent, as they extended into the intertrial interval. These changes in absolute power were generally not associated with changes in oscillatory synchrony within this circuit, with the exception of increases in reward-related theta and alpha synchrony. In humans, increases in theta and alpha activity are associated with impaired attentional function due to fatigue or distractors (Arnau et al., 2021; Lal & Craig, 2001; Tran et al., 2020; Wascher et al., 2014). This could suggest that CRF-dependent increases in theta/alpha activity contribute to impaired sustained attention via cognitive fatigue and/or increased sensitivity to distractors.

Translational Relevance

Dysregulated sustained attention is associated with a variety of behavioral conditions, including attention deficit hyperactivity disorder (ADHD). The current observations provide novel insight into the neural mechanisms regulating this cognitive process that may provide a better understanding of the origins of, and/or the treatment of, dysregulated attention. Of relevance, systemically administered CRF antagonists improve sustained attention (Berridge et al., 2022; Hupalo et al., 2021) and working memory

(Berridge et al., 2022; Hupalo & Berridge, 2016), similar to all approved drugs for ADHD treatment (Spencer et al., 2015). Evidence that caudal dmPFC CRF receptors bidirectionally regulate working memory suggested a likely role of these receptors in the working memory improving actions of systemic CRF antagonists. The current study additionally suggests that CRF receptors in the lateral MD likely contribute to the ability of these drugs to improve sustained attention. Unlike CRF antagonists, ADHD-related psychostimulants act within the dmPFC to improve both working memory and sustained attention. Outside of ADHD, functional imaging studies have shown decreased connectivity between the PFC and MD, that is correlated with decreased PFC-dependent cognitive performance, in individuals with schizophrenia (Buchmann et al., 2014; Giraldo-Chica et al., 2018) and bipolar disorder (Anticevic et al., 2014). Further study is needed to better understand the clinical potential of CRF antagonists in the treatment of PFC-dependent cognitive dysfunction.

Acknowledgments

This work was supported by the National Institutes of Health grant MH116526 (CWB) and the Office of the Vice Chancellor for Research and Graduate Education at the University of Wisconsin-Madison with funding from the Wisconsin Alumni Research Foundation (CWB). SKC was partially supported by NINDS T32NS105602 through the Neuroscience Training Program at the University of Wisconsin-Madison. CWB, AJM, and SKC designed the study. AJM and SKC collected the data and analyzed the data, with input from CWB. CWB and SKC wrote the manuscript. AJM assisted in editing. Incomplete versions of the data were presented in an abstract and poster presentation at Society for Neuroscience in 2021 and 2024. We gratefully acknowledge the expert assistance of Shannon Nicol in immunohistochemical methodology and collection of confocal microscopic images.

Disclosures

The authors report no biomedical financial interests or potential conflicts of interest.

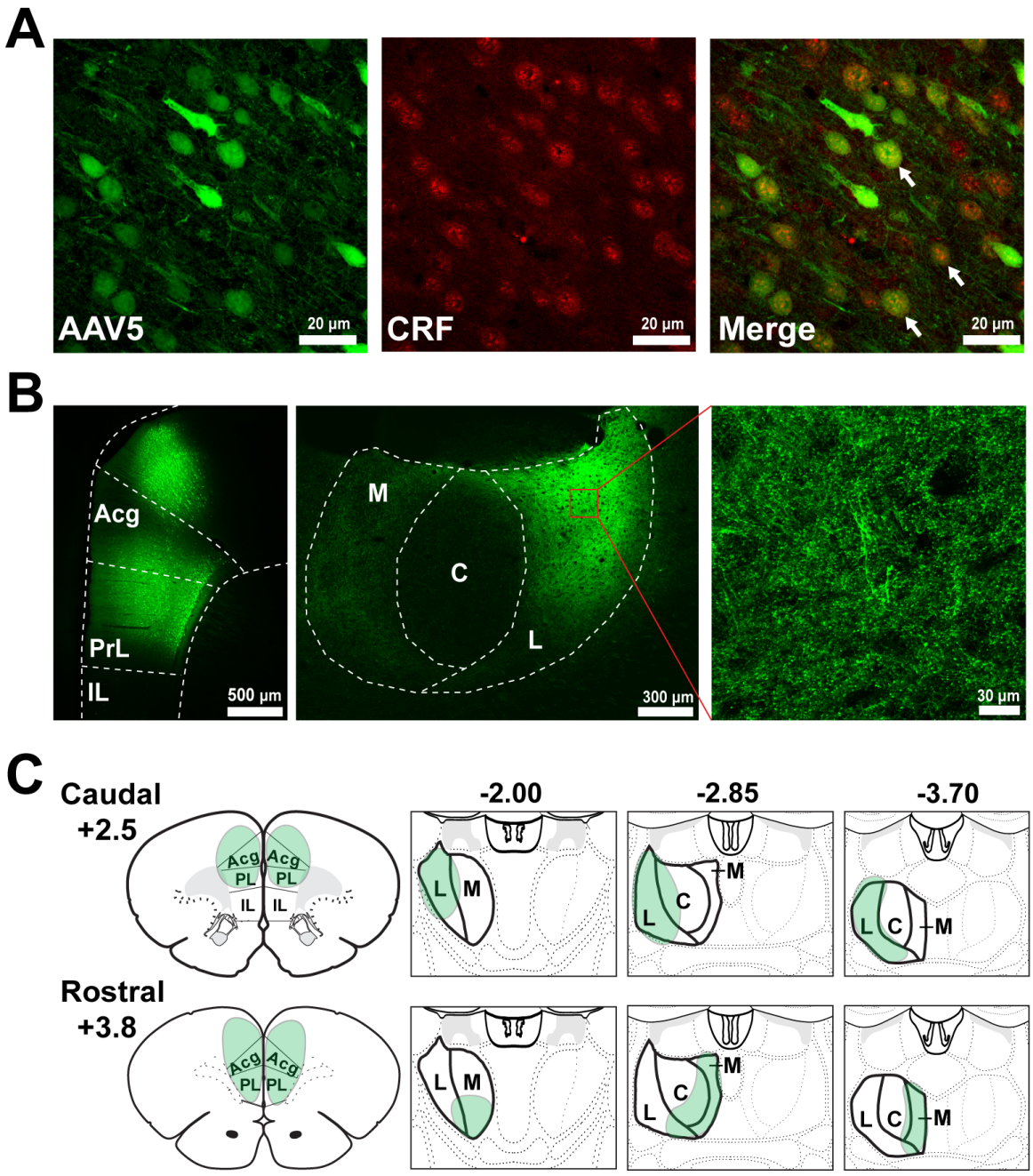

Figure 1. Anterograde labeling of dmPFC CRF neurons. A) Collapsed 2µm z-stack of photomicrographs of the dmPFC from an animal treated with the AAV8/AAV5-eGFP viral cocktail. Shown are eGFP expression (left panel, green) and CRF-ir (middle panel, red) that colocalize in a merged image (right panel). Arrows indicate examples of double-labeled neurons. **B)** Low-power photomicrographs of viral expression within the dmPFC (left panel) and the lateral MD (middle panel) and a high-power image of the lateral MD depicting labeled fibers with visible varicosities (right panel). **C)** Schematics depict the average spread of viral expression within either the caudal (top row) or rostral (bottom row) dmPFC and densest terminal fields within the MD associated with these viral infusions. Numbers correspond to anterior-posterior coordinates. Acg, anterior cingulate cortex; C, central MD; IL, infralimbic cortex; L, lateral MD; M, medial MD; PrL, prelimbic cortex.

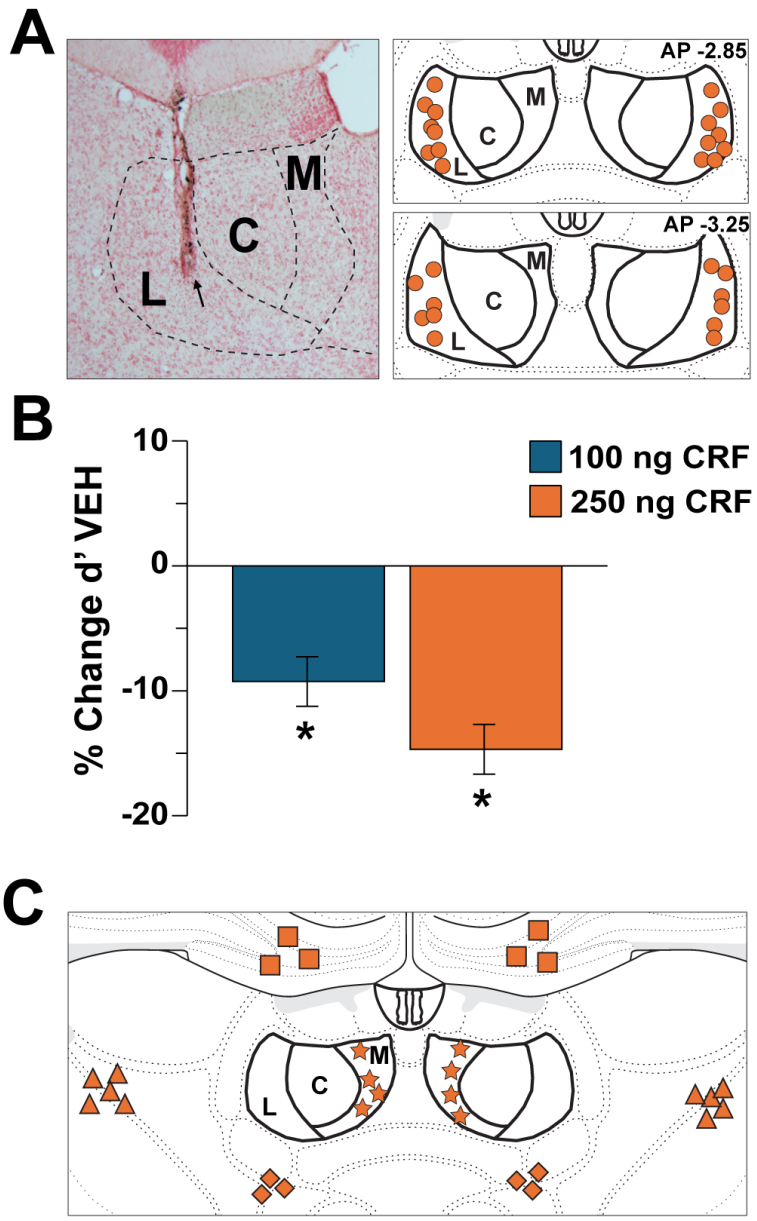

Figure 2. CRF acts within the lateral MD to impair sustained attention. Animals received bilateral vehicle or CRF infusions into or outside the lateral MD prior to sustained attention testing. **A)** Representative photomicrograph (left panel) depicting the ventral-most extent of a needle track in one hemisphere of the lateral MD and schematics (right panel) depicting lateral MD CRF infusion sites for all animals. **B)** Effects of bilateral 100ng and 250ng CRF infusions on sustained attention as measured by percent change in d' from vehicle (VEH) treatment (± SEM). **C)** Schematic depiction of 250ng/hemisphere CRF infusion sites outside the lateral MD. These infusions did not affect sustained attention performance (see Results for details). *p<0.05 vs. vehicle.

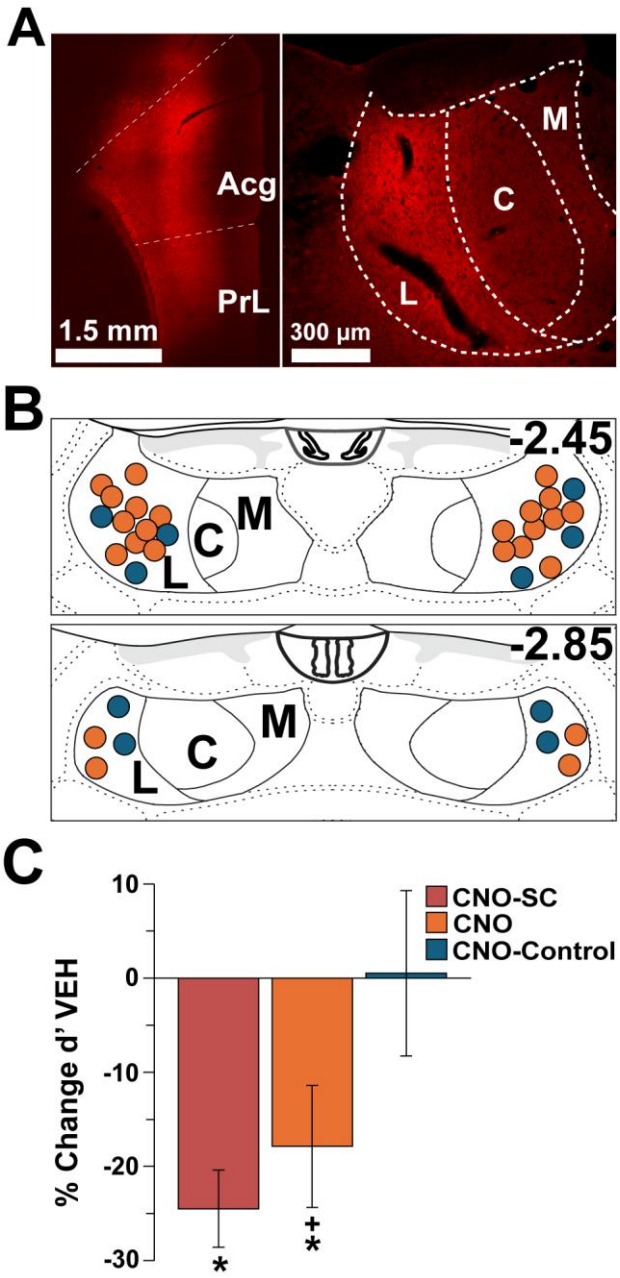

Figure 3. Chemogenetic activation of caudal dmPFC CRF axon terminals within the lateral MD impairs sustained attention. Animals received AAV8/AAV5-CRF-hM3dq (hM3Dq) or control viral cocktail infusions bilaterally into the caudal dmPFC and then received 0.3 mg/kg subcutaneous (SC) CNO or bilateral intra-lateral MD infusions of CNO (150 ng/500 nL/hemisphere) prior to testing. **A)** Low-power photomicrographs of viral expression (mCherry) within the caudal dmPFC (left panel) and lateral MD (right panel). **B)** Schematic depicts lateral MD CNO infusion sites in hM3Dq (orange) or control-virus (blue) animals. Numbers correspond to anterior-posterior coordinates. **C)** Sustained attention effects (± SEM) of subcutaneous CNO and bilateral CNO infusions as measured by percent change in d' from vehicle (VEH) treatment in hM3Dq or viral control animals. In hM3Dq animals, systemic and intra-MD CNO elicited largely comparable impairments in performance. Intra-MD CNO did not affect sustained attention in viral controls. Prior studies demonstrate that systemic CNO does not affect sustained attention performance in control virus-treated animals of varying types (Berridge et al., 2022; Cooke et al., 2025; Hupalo et al., 2021; see also Figure 6). Acg, anterior cingulate cortex; C, central MD; IL, infralimbic cortex; L, lateral MD; M, medial MD; PrL, prelimbic cortex. *p<0.05, vs. vehicle; ^{+}p<0.5, vs. viral control.

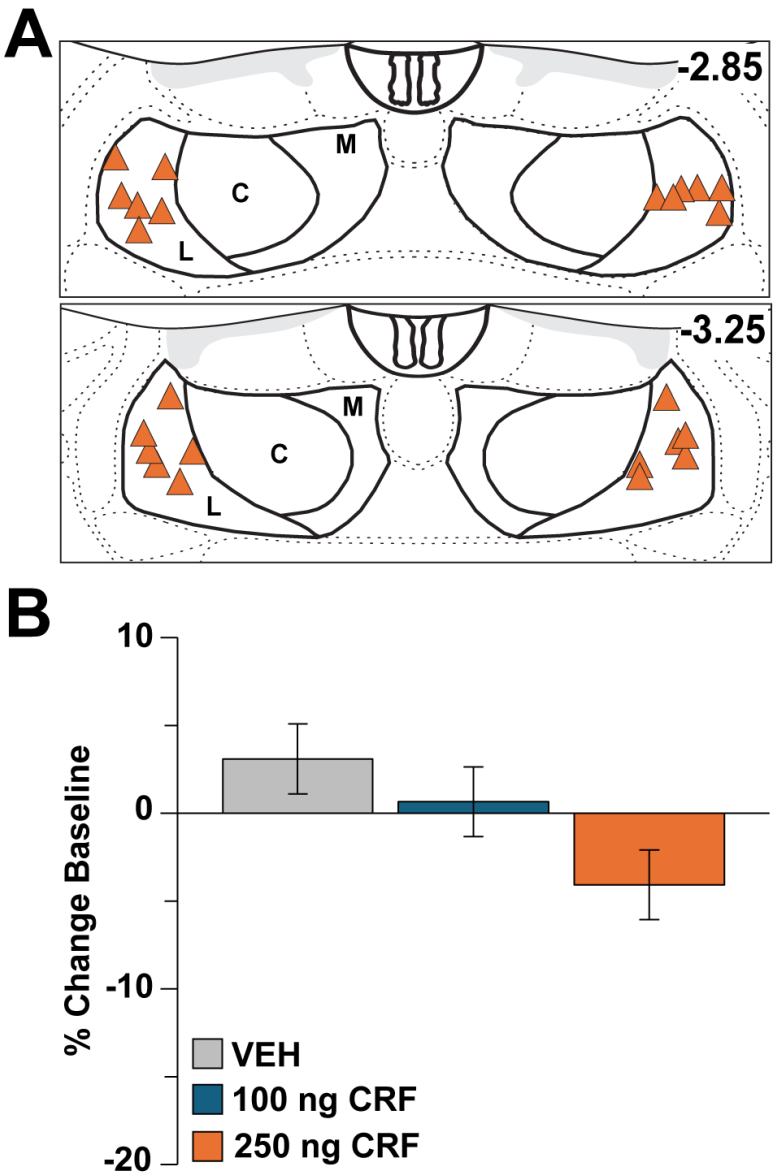

Figure 4. CRF action in the lateral MD does not impair working memory. Animals received bilateral infusions of vehicle or varying doses of CRF (100ng, 250ng) into the lateral MD prior to testing in the working memory task. **A)** Schematic depiction of the location of all infusion sites within the lateral MD. **B)** Working memory effects of bilateral infusion of vehicle (VEH) or CRF as measured by percent change from baseline (± SEM). Intra-lateral MD CRF had no influence on working memory performance. C, central MD; L, lateral MD; M, medial MD.

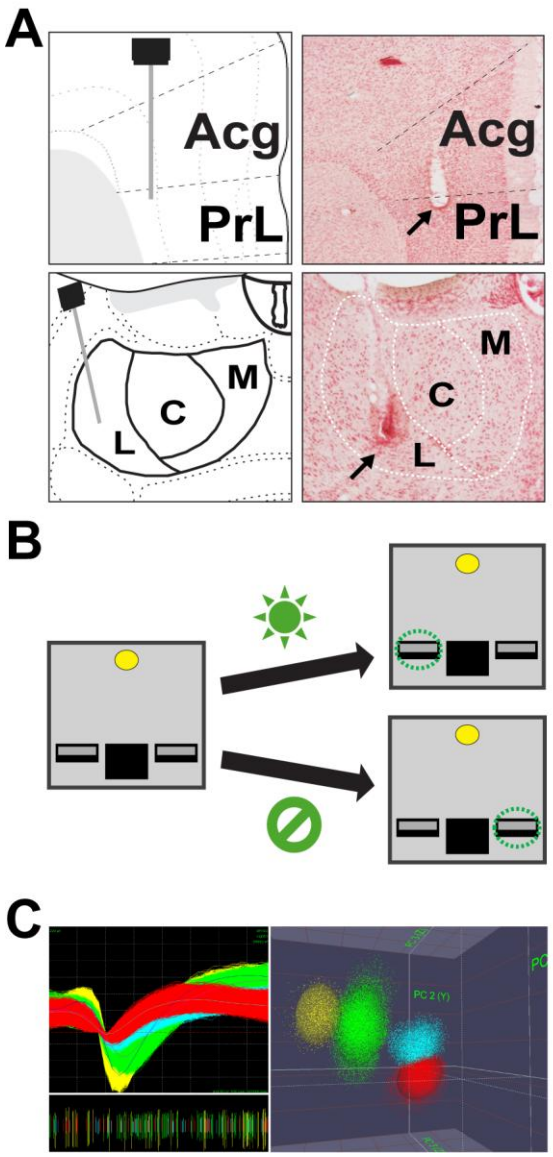

Figure 5. Experimental approach for the electrophysiological studies. A) Animals received bilateral infusions of the CRF_{Glu} viral cocktail into the caudal dmPFC and 8-wire recording ensembles were implanted into layer V/VI of the dmPFC (top row) and the lateral MD (bottom row). Accurate electrode placement was confirmed in Nissl-stained tissue sections. **B)** Schematic of the operant sustained attention task. Animals were rewarded for pressing the left lever following a signal presentation (hit) or the right lever following the absence of a signal (correct rejection). **C)** Action potential waveforms of 4 discriminated wide-spiking dmPFC neurons from a single wire (top left panel), raster of waveforms of these same neurons over time (bottom left panel), and waveforms from these units exhibit separable clusters in 3D-principal component space (right panel). Analyses ensured the same neurons were recorded across pre-treatment and post-treatment sessions. Acg, anterior cingulate cortex; C, central MD; IL, infralimbic cortex; L, lateral MD; M, medial MD; PrL, prelimbic cortex.

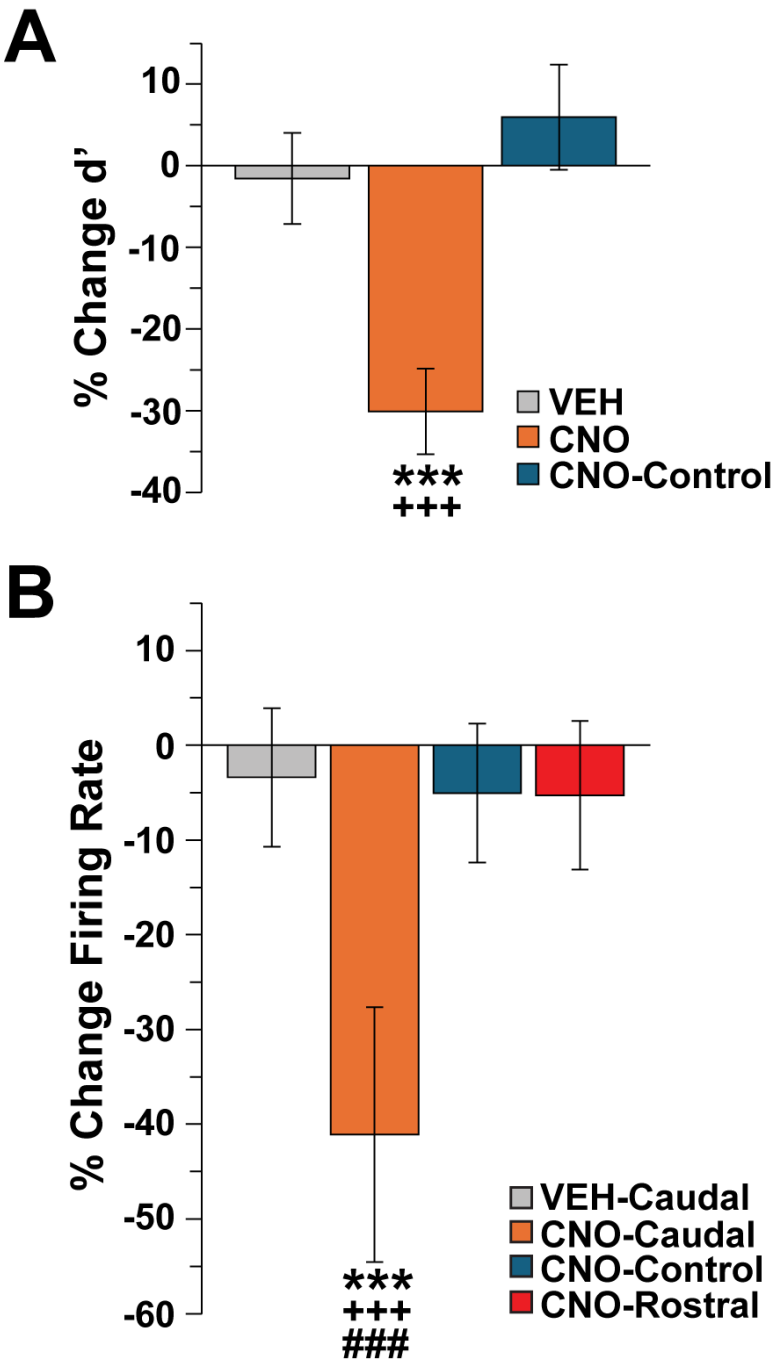

Figure 6. Chemogenetic activation of caudal dmPFC CRF_{Glu} neurons impairs sustained attention performance and reduces the activity of caudal dmPFC signal-tuned neurons. Animals received bilateral infusions of the CRF_{Glu}-hM3Dq or control viral cocktails into the caudal dmPFC and were subsequently tested before (pre-treatment) and after (post-treatment) subcutaneous vehicle (VEH) or 6mg/kg CNO. **A)** Shown are the mean (± SEM) percent change in d' from the pre-treatment testing session. CNO impaired sustained attention performance in hM3Dq animals, but not viral controls. Vehicle treatment in hM3Dq did not significantly affect performance. **B)** Chemogenetic activation of caudal dmPFC CRF_{Glu} neurons significantly decreased activity of signal-tuned neurons in the caudal, but not rostral, dmPFC. $^{***}p<0.001$, vs. vehicle; $^{+++}p<0.001$, vs. viral control; $^{###}p<0.001$, vs. rostral dmPFC.

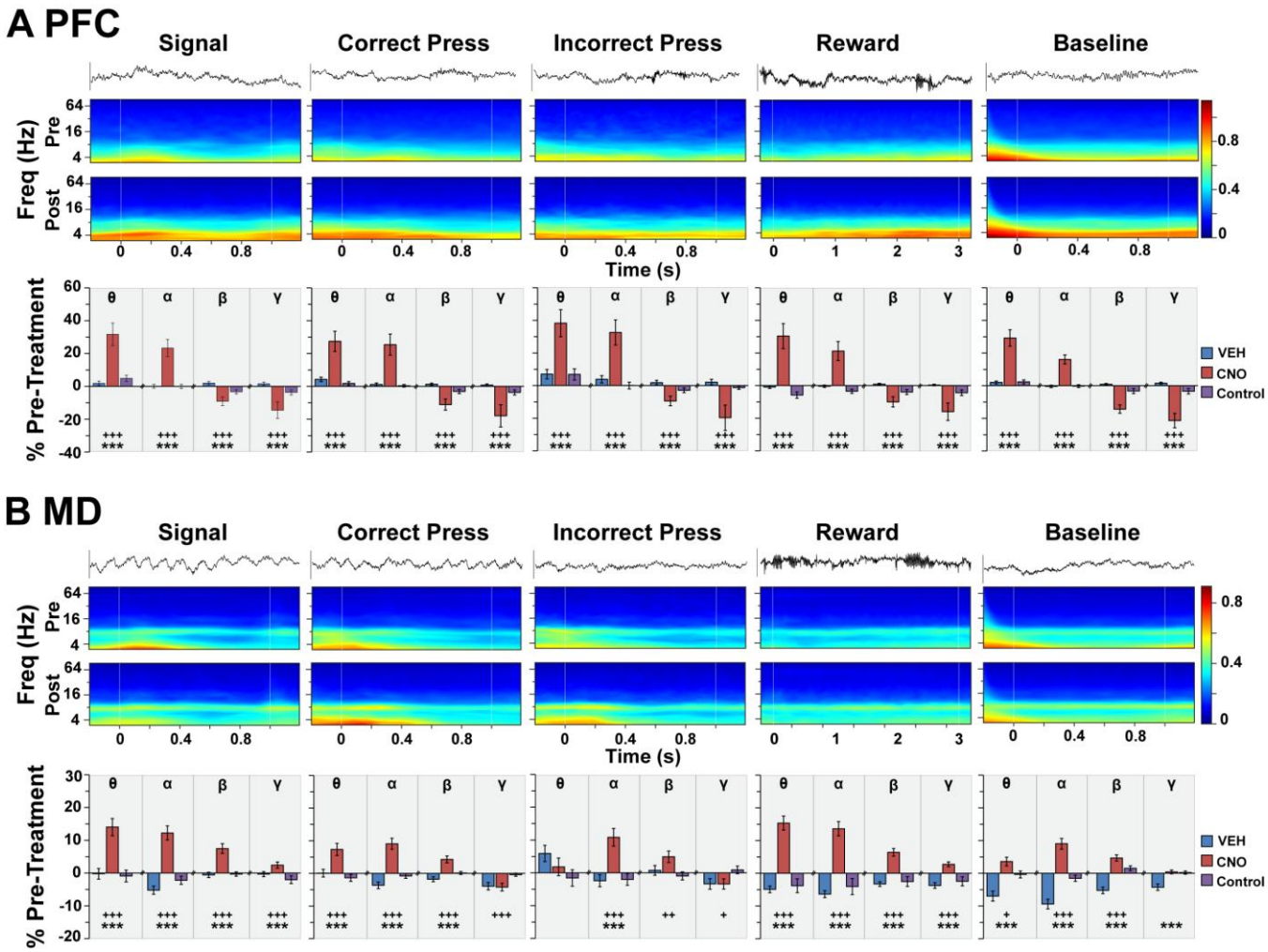

Figure 7. Chemogenetic activation of caudal dmPFC CRF_{Glu} neurons alters event-related oscillatory power in the dmPFC and lateral MD. Animals received bilateral infusions of the hM3Dq or control virus into the caudal dmPFC were subsequently treated subcutaneously with vehicle or CNO. Shown are analyses of event-related LFP oscillatory activity in **A)** the dmPFC and **B)** the lateral MD. For each region and task event, shown are a segment of an LFP recording trace from the relevant event interval of a single trial (top) and time-frequency spectrograms (middle) for the event interval averaged across all trials of an individual animal during both pre-treatment (Pre) and post-treatment (Post) recording sessions. White vertical lines indicate beginning and end of event intervals. Color scale bar reflects absolute power of LFP. Bar graphs (bottom) depict the mean (± SEM) effects of treatments on distinct frequency bands as percent change from pre-treatment conditions. θ, theta (4-7 Hz); α, alpha (7-12 Hz); β, beta (15-35 Hz); γ, gamma (40-80 Hz). $^{***}p<0.001$, vs. vehicle; $^{+}p<0.05$, $^{++}p<0.01$, $^{+++}p<0.001$, vs. viral control.

Table 1. Effects of Intra-Lateral-MD Infusions and Chemogenetic Activation of Caudal dmPFC CRF_{Glu} Neurons on Sustained Attention Performance.

A. Intra lateral-MD CRF and muscimol

Treatment	d'	Proportion Hit	Proportion False Alarm	Omission
Vehicle	1.78 ± 0.15	0.60 ± 0.04	0.08 ± 0.02	1.52 ± 0.82
100ng CRF	1.58 ± 0.15*	0.58 ± 0.04	0.10 ± 0.02	1.77 ± 0.82
250ng CRF	1.54 ± 0.15*	0.57 ± 0.04	0.10 ± 0.02	3.37 ± 0.90
Muscimol	1.73 ± 0.22***	0.37 ± 0.10*	0.36 ± 0.06**	63.19 ± 8.98***

B. Intra lateral-MD CNO

	Treatment	d'	Proportion Hit	Proportion False Alarm	Omission
hM3Dq	Vehicle	2.17 ± 0.19	0.66 ± 0.05	0.06 ± 0.02	0.15 ± 0.38
	CNO	1.82 ± 0.19*	0.61 ± 0.05	0.08 ± 0.02	0.61 ± 0.37
Control	Vehicle	1.40 ± 0.16	0.47 ± 0.06	0.09 ± 0.02	0.57 ± 0.30
	CNO	1.40 ± 0.16	0.48 ± 0.06	0.09 ± 0.02	0.57 ± 0.30
hM3Dq	Vehicle	2.44 ± 0.11	0.70 ± 0.04	0.03 ± 0.01	0.17 ± 0.27
Subcutaneous	CNO	1.85 ± 0.11**	0.64 ± 0.04	0.07 ± 0.01	0.50 ± 0.27

C. Subcutaneous CNO in Electrophysiology-Tested Animals

	Treatment	d'	Proportion Hit	Proportion False Alarm	Omission
CRF_{Glu}-hM3Dq	Pre-Vehicle	2.20 ± 0.12	0.83 ± 0.03	0.13 ± 0.02	1.41 ± 1.56
	Post-Vehicle	2.17 ± 0.12	0.77 ± 0.03	0.12 ± 0.02	1.52 ± 1.56

	Pre-CNO	2.30 ± 0.12	0.84 ± 0.03	0.12 ± 0.02	0.96 ± 1.54
	Post-CNO	1.61 ± 0.12***	0.76 ± 0.02**	0.20 ± 0.02**	8.92 ± 1.54***
CRF_{Glu}-Control	Pre-Vehicle	2.10 ± 0.19	0.81 ± 0.03	0.14 ± 0.02	0.26 ± 0.22
	Post-Vehicle	2.05 ± 0.19	0.81 ± 0.03	0.15 ± 0.02	0.69 ± 0.22
	Pre-CNO	2.07 ± 0.20	0.82 ± 0.03	0.15 ± 0.02	0.33 ± 0.23
	Post-CNO	2.21 ± 0.20	0.84 ± 0.03	0.14 ± 0.02	0.20 ± 0.23

Shown are the mean (± SEM) effects on d', proportion of hit responses, proportion of false alarm responses, and omissions in animals that received intra lateral-MD infusions of vehicle, CRF, or muscimol (A), AAV5 viral cocktail expressing animals that received intra lateral-MD or subcutaneous infusions of CNO (B), and AAV8-CRF_{Glu} viral cocktail expressing animals that received subcutaneous CNO injections (C). *, **, *** p<0.05,0.01,0.0001 vs vehicle.

Table 2. Statistical Analyses for Caudal PFC, Rostral PFC, and MD Spiking Activity.

A. Caudal PFC

		Tuned	**Untuned**
Signal	SESS	$F_{1,97}$=10.87, p=0.001	$F_{1,730}$=0.19, p=0.665
	TRT	$F_{1,97}$=10.45, p=0.001	$F_{1,730}$=2.01, p=0.156
	SESS*TRT	$F_{1,97}$=8.79, p=0.003	$F_{1,730}$=0.55, p=0.460
Correct Press	SESS	$F_{1,144}$=4.31, p=0.038	$F_{1,698}$=0.003, p=0.954
	TRT	$F_{1,144}$=0.19, p=0.663	$F_{1,698}$=0.06, p=0.814
	SESS*TRT	$F_{1,144}$=0.08, p=0.775	$F_{1,698}$=0.01, p=0.905
Incorrect Press	SESS	$F_{1,62}$=0.01, p=0.938	$F_{1,734}$=0.06, p=0.809
	TRT	$F_{1,62}$=0.75, p=0.386	$F_{1,734}$=0.003, p=0.958
	SESS*TRT	$F_{1,62}$=0.01, p=0.915	$F_{1,734}$=0.08, p=0.771

Reward	SESS	$F_{1,170}$=0.08, p=0.774	$F_{1,694}$=1.02, p=0.312
	TRT	$F_{1,170}$=0.0001, p=0.991	$F_{1,694}$=0.74, p=0.391
	SESS*TRT	$F_{1,170}$=0.06, p=0.814	$F_{1,694}$=0.43, p=0.512

B. Rostral PFC

		Tuned	**Untuned**
Signal	SESS	$F_{1,65}$=0.03, p=0.853	$F_{1,253}$=0.06, p=0.802
	TRT	$F_{1,65}$=0.47, p=0.492	$F_{1,253}$=0.21, p=0.647
	SESS*TRT	$F_{1,65}$=0.22, p=0.641	$F_{1,253}$=0.27, p=0.606
Correct Press	SESS	$F_{1,59}$=1.91, p=0.167	$F_{1,251}$=0.635, p=0.425
	TRT	$F_{1,59}$=0.90, p=0.343	$F_{1,251}$=0.003, p=0.959
	SESS*TRT	$F_{1,59}$=0.21, p=0.645	$F_{1,251}$=0.06, p=0.813
Incorrect Press	SESS	$F_{1,35}$=0.08, p=0.775	$F_{1,257}$=0.01, p=0.921
	TRT	$F_{1,35}$=1.41, p=0.235	$F_{1,257}$=0.69, p=0.405
	SESS*TRT	$F_{1,35}$=0.31, p=0.581	$F_{1,257}$=1.07, p=0.302
Reward	SESS	$F_{1,73}$=1.78, p=0.278	$F_{1,263}$=1.67, p=0.196
	TRT	$F_{1,73}$=0.82, p=0.366	$F_{1,263}$=1.58, p=0.209
	SESS*TRT	$F_{1,73}$=0.29, p=0.592	$F_{1,263}$=0.321, p=0.571

C. MD

		Tuned	**Untuned**
Signal	SESS	$F_{1,15}$=0.32, p=0.570	$F_{1,728}$=1.09, p=0.295
	TRT	$F_{1,15}$=1.31, p=0.253	$F_{1,728}$=0.23, p=0.628
	SESS*TRT	$F_{1,15}$=0.82, p=0.366	$F_{1,728}$=0.16, p=0.689
Correct Press	SESS	$F_{1,34}$=0.81, p=0.367	$F_{1,708}$=1.47, p=0.226
	TRT	$F_{1,34}$=1.11, p=0.291	$F_{1,708}$=2.80, p=0.094
	SESS*TRT	$F_{1,34}$=0.88, p=0.349	$F_{1,708}$=1.32, p=0.251

Incorrect Press	SESS	$F_{1,16}$=0.21, p=0.649	$F_{1,726}$=0.40, p=0.525
	TRT	$F_{1,16}$=2.01, p=0.156	$F_{1,726}$=2.42, p=0.120
	SESS*TRT	$F_{1,16}$=1.87, p=0.171	$F_{1,726}$=0.80, p=0.372
Reward	SESS	$F_{1,72}$=0.02, p=0.887	$F_{1,670}$=1.90, p=0.168
	TRT	$F_{1,72}$=0.48, p=0.488	$F_{1,670}$=7.25, p=0.007
	SESS*TRT	$F_{1,72}$=0.74, p=0.391	$F_{1,670}$=0.82, p=0.365

Results of general linear mixed model statistical analyses of neural spiking within the caudal (A) or rostral (B) dorsomedial PFC (dmPFC) and lateral mediodorsal thalamus (C; lateral MD) for event-tuned and untuned neurons during the signal, correct press, incorrect press, and reward. TRT, treatment (CNO vs. VEH control); SESS, session (pre-treatment vs. post-treatment).

Table 3. Statistical Analyses of PFC and MD Oscillatory Power in Sustained Attention.

A. hM3Dq-dmPFC

		Theta	**Alpha**	**Beta**	**Gamma**
Signal	SESS	$F_{1,3735}$=12.37, p<0.0001	$F_{1,3735}$=6.29, p=0.012	$F_{1,3735}$=4.82, p=0.028	$F_{1,3735}$=6.05, p=0.014
	TRT	$F_{1,3735}$=452.09, p<0.0001	$F_{1,3735}$=298.55, p<0.0001	$F_{1,3735}$=218.77, p<0.0001	$F_{1,3735}$=866.48, p<0.0001
	SESS* TRT	$F_{1,3735}$=180.58, p<0.0001	$F_{1,3735}$=144.94, p<0.0001	$F_{1,3735}$=176.08, p<0.0001	$F_{1,3735}$=614.78, p<0.0001
Correct Press	SESS	$F_{1,7668}$=2.66, p=0.103	$F_{1,7668}$=1.49, p=0.222	$F_{1,7668}$=4.27, p=0.039	$F_{1,7668}$=5.85, p=0.016
	TRT	$F_{1,7668}$=542.65, p<0.0001	$F_{1,7668}$=628.23, p<0.0001	$F_{1,7668}$=549.36, p<0.0001	$F_{1,7668}$=2,144.73, p<0.0001
	SESS* TRT	$F_{1,7668}$=173.07, p<0.0001	$F_{1,7668}$=285.79, p<0.0001	$F_{1,7668}$=389.49, p<0.0001	$F_{1,7668}$=1,443.78, p<0.0001
Incorrect Press	SESS	$F_{1,1560}$=2.12, p=0.145	$F_{1,1560}$=2.02, p=0.155	$F_{1,1560}$=3.82, p=0.051	$F_{1,1560}$=5.98, p=0.014
	TRT	$F_{1,1560}$=169.97, p<0.0001	$F_{1,1560}$=186.44, p<0.0001	$F_{1,1560}$=76.10, p<0.0001	$F_{1,1560}$=626.31, p<0.0001
	SESS* TRT	$F_{1,1560}$=51.24, p<0.0001	$F_{1,1560}$=67.29, p<0.0001	$F_{1,1560}$=57.66, p<0.0001	$F_{1,1560}$=434.02, p<0.0001
Reward	SESS	$F_{1,7317}$=3.95, p=0.047	$F_{1,7317}$=1.07, p=0.301	$F_{1,7317}$=3.85, p=0.050	$F_{1,7317}$=6.89, p=0.009
	TRT	$F_{1,7317}$=982.88, p<0.0001	$F_{1,7317}$=701.95, p<0.0001	$F_{1,7317}$=728.50, p<0.0001	$F_{1,7317}$=2,047.74, p<0.0001
	SESS* TRT	$F_{1,7317}$=504.76, p<0.0001	$F_{1,7317}$=366.94, p<0.0001	$F_{1,7317}$=489.36, p<0.0001	$F_{1,7317}$=1,301.01, p<0.0001

B. hM3Dq-lateral MD

		Theta	Alpha	Beta	Gamma
Signal	SESS	$F_{1,3169}$=11.89, p=0.001	$F_{1,3169}$=5.60, p=0.018	$F_{1,3169}$=1.15, p=0.283	$F_{1,3169}$=0.49, p=0.486
	TRT	$F_{1,3169}$=60.04, p<0.0001	$F_{1,3169}$=104.11, p<0.0001	$F_{1,3169}$=75.83, p<0.0001	$F_{1,3169}$=9.80, p=0.002
	SESS* TRT	$F_{1,3169}$=26.76, p<0.0001	$F_{1,3169}$=109.66, p<0.0001	$F_{1,3169}$=42.68, p<0.0001	$F_{1,3169}$=6.05, p=0.014
Correct Press	SESS	$F_{1,6470}$=4.01, p=0.045	$F_{1,6470}$=4.20, p=0.040	$F_{1,6470}$=0.98, p=0.322	$F_{1,6470}$=0.00, p=0.988
	TRT	$F_{1,6470}$=25.89, p<0.0001	$F_{1,6470}$=76.16, p<0.0001	$F_{1,6470}$=32.95, p<0.0001	$F_{1,6470}$=34.04, p<0.0001
	SESS* TRT	$F_{1,6470}$=13.19, p<0.0001	$F_{1,6470}$=81.04, p<0.0001	$F_{1,6470}$=34.19, p<0.0001	$F_{1,6470}$=0.08, p=0.781
Incorrect Press	SESS	$F_{1,1234}$=0.99, p=0.321	$F_{1,1234}$=3.37, p=0.066	$F_{1,1234}$=0.32, p=0.572	$F_{1,1234}$=0.00, p=0.981
	TRT	$F_{1,1234}$=0.46, p=0.499	$F_{1,1234}$=28.19, p<0.0001	$F_{1,1234}$=10.71, p=0.001	$F_{1,1234}$=6.08, p=0.014
	SESS* TRT	$F_{1,1234}$=1.58, p=0.208	$F_{1,1234}$=20.90, p<0.0001	$F_{1,1234}$=3.60, p=0.058	$F_{1,1234}$=0.00, p=0.989
Reward	SESS	$F_{1,6141}$=8.83, p=0.003	$F_{1,6141}$=6.25, p=0.012	$F_{1,6141}$=1.45, p=0.229	$F_{1,6141}$=0.74, p=0.390
	TRT	$F_{1,6141}$=253.53, p<0.0001	$F_{1,6141}$=307.70, p<0.0001	$F_{1,6141}$=134.14, p<0.0001	$F_{1,6141}$=25.09, p<0.0001
	SESS* TRT	$F_{1,6141}$=219.77, p<0.0001	$F_{1,6141}$=344.78, p<0.0001	$F_{1,6141}$=153.00, p<0.0001	$F_{1,6141}$=68.86, p<0.0001

C. Control-dmPFC

		Theta	Alpha	Beta	Gamma
Signal	SESS	$F_{1,3134}$=0.93, p=0.336	$F_{1,3134}$=0.39, p=0.535	$F_{1,3134}$=0.85, p=0.358	$F_{1,3134}$=2.27, p=0.132
	Virus	$F_{1,3134}$=375.40, p<0.0001	$F_{1,3134}$=264.80, p<0.0001	$F_{1,3134}$=215.11, p<0.0001	$F_{1,3134}$=848.30, p<0.0001
	SESS* Virus	$F_{1,3134}$=113.12, p<0.0001	$F_{1,3134}$=114.44, p<0.0001	$F_{1,3134}$=56.53, p<0.0001	$F_{1,3134}$=361.77, p<0.0001
Correct Press	SESS	$F_{1,6394}$=1.06, p=0.302	$F_{1,6394}$=0.65, p=0.419	$F_{1,6394}$=0.81, p=0.369	$F_{1,6394}$=2.12, p=0.146
	Virus	$F_{1,6394}$=505.54, p<0.0001	$F_{1,6394}$=619.68, p<0.0001	$F_{1,6394}$=581.74, p<0.0001	$F_{1,6394}$=2,169.09, p<0.0001
	SESS* Virus	$F_{1,6394}$=162.58, p<0.0001	$F_{1,6394}$=247.16, p<0.0001	$F_{1,6394}$=191.61, p<0.0001	$F_{1,6394}$=1,022.34, p<0.0001
Incorrect Press	SESS	$F_{1,1304}$=0.68, p=0.410	$F_{1,1304}$=1.04, p=0.308	$F_{1,1304}$=0.78, p=0.377	$F_{1,1304}$=2.46, p=0.117
	Virus	$F_{1,1304}$=143.80, p<0.0001	$F_{1,1304}$=167.53, p<0.0001	$F_{1,1304}$=72.97, p<0.0001	$F_{1,1304}$=616.98, p<0.0001
	SESS* Virus	$F_{1,1304}$=34.78, p<0.0001	$F_{1,1304}$=62.51, p<0.0001	$F_{1,1304}$=18.81, p<0.0001	$F_{1,1304}$=302.81, p<0.0001
Reward	SESS	$F_{1,6041}$=2.04, p=0.154	$F_{1,6041}$=0.80, p=0.370	$F_{1,6041}$=1.05, p=0.305	$F_{1,6041}$=2.65, p=0.104
	Virus	$F_{1,6041}$=835.94, p<0.0001	$F_{1,6041}$=630.53, p<0.0001	$F_{1,6041}$=728.23, p<0.0001	$F_{1,6041}$=1,958.05, p<0.0001
	SESS* Virus	$F_{1,6041}$=485.96, p<0.0001	$F_{1,6041}$=363.81, p<0.0001	$F_{1,6041}$=185.14, p<0.0001	$F_{1,6041}$=797.51, p<0.0001

D. Control-lateral MD

		Theta	Alpha	Beta	Gamma
Signal	SESS	$F_{1,2865}$=1.89, p=0.170	$F_{1,2865}$=2.26, p=0.133	$F_{1,2865}$=2.19, p=0.139	$F_{1,2865}$=1.43, p=0.232
	Virus	$F_{1,2865}$=52.27, p<0.0001	$F_{1,2865}$=100.21, p<0.0001	$F_{1,2865}$=96.56, p<0.0001	$F_{1,2865}$=12.99, p<0.0001
	SESS*Virus	$F_{1,2865}$=28.56, p<0.0001	$F_{1,2865}$=70.23, p<0.0001	$F_{1,2865}$=44.75, p<0.0001	$F_{1,2865}$=23.24, p<0.0001
Correct Press	SESS	$F_{1,5830}$=2.49, p=0.114	$F_{1,5830}$=2.52, p=0.112	$F_{1,5830}$=1.73, p=0.188	$F_{1,5830}$=1.06, p=0.303
	Virus	$F_{1,5830}$=26.76, p<0.0001	$F_{1,5830}$=81.06, p<0.0001	$F_{1,5830}$=39.50, p<0.0001	$F_{1,5830}$=41.17, p<0.0001
	SESS*Virus	$F_{1,5830}$=23.06, p<0.0001	$F_{1,5830}$=48.25, p<0.0001	$F_{1,5830}$=15.40, p<0.0001	$F_{1,5830}$=13.75, p<0.0001
Incorrect Press	SESS	$F_{1,1137}$=2.35, p=0.126	$F_{1,1137}$=2.27, p=0.132	$F_{1,1137}$=1.81, p=0.178	$F_{1,1137}$=0.99, p=0.320
	Virus	$F_{1,1137}$=0.37, p=0.542	$F_{1,1137}$=30.93, p<0.0001	$F_{1,1137}$=11.87, p=0.001	$F_{1,1137}$=6.54, p=0.011
	SESS*Virus	$F_{1,1137}$=0.77, p=0.381	$F_{1,1137}$=20.24, p<0.0001	$F_{1,1137}$=7.02, p=0.008	$F_{1,1137}$=4.50, p=0.034
Reward	SESS	$F_{1,5485}$=2.75, p=0.098	$F_{1,5485}$=2.65, p=0.104	$F_{1,5485}$=1.59, p=0.208	$F_{1,5485}$=1.30, p=0.254
	Virus	$F_{1,5485}$=256.01, p<0.0001	$F_{1,5485}$=343.87, p<0.0001	$F_{1,5485}$=157.14, p<0.0001	$F_{1,5485}$=35.31, p<0.0001
	SESS*Virus	$F_{1,5485}$=213.86, p<0.0001	$F_{1,5485}$=320.33, p<0.0001	$F_{1,5485}$=153.65, p<0.0001	$F_{1,5485}$=66.01, p<0.0001

Results of general linear mixed model statistical analyses of local field potential recordings within the dorsomedial PFC (dmPFC) and lateral mediodorsal thalamus (lateral MD) for hM3dq and viral-control animals during the signal, correct press, incorrect press, and reward intervals across the 4 analyzed frequency bands: theta, alpha, beta, and gamma. TRT, treatment (CNO vs. VEH control); SESS, session (pre-treatment vs. post-treatment).

Table 4. Statistical Analyses of PFC and MD Oscillatory Synchrony in Sustained Attention.

A. hM3Dq

		Theta	Alpha	Beta	Gamma
Signal	Pre-Treatment - VEH	0.34±0.03	0.33±0.02	0.27±0.01	0.29±0.001
	Post-Treatment - VEH	0.35±0.03	0.34±0.02	0.27±0.01	0.29±0.001
	Pre-Treatment - CNO	0.36±0.03	0.34±0.02	0.27±0.01	0.29±0.001
	Post-Treatment - CNO	0.36±0.03	0.35±0.02	0.27±0.01	0.29±0.001
Correct Press	Pre-Treatment - VEH	0.33±0.02	0.31±0.01	0.26±0.003	0.29±0.001
	Post-Treatment - VEH	0.33±0.02	0.31±0.01	0.27±0.003	0.29±0.001
	Pre-Treatment - CNO	0.35±0.03	0.32±0.01	0.27±0.003	0.29±0.001
	Post-Treatment - CNO	0.34±0.03	0.32±0.01	0.26±0.003	0.29±0.001
Incorrect Press	Pre-Treatment - VEH	0.34±0.03	0.32±0.02	0.27±0.005	0.29±0.002
	Post-Treatment - VEH	0.34±0.03	0.33±0.02	0.27±0.004	0.29±0.002
	Pre-Treatment - CNO	0.36±0.03	0.34±0.02	0.27±0.005	0.29±0.002
	Post-Treatment - CNO	0.35±0.03	0.34±0.02	0.27±0.004	0.29±0.002
Reward	Pre-Treatment - VEH	0.30±0.01	0.29±0.01	0.26±0.003	0.29±0.001
	Post-Treatment - VEH	0.29±0.01	0.28±0.01	0.26±0.003	0.29±0.001
	Pre-Treatment - CNO	0.30±0.01	0.29±0.01	0.26±0.003	0.29±0.001
	Post-Treatment - CNO	0.33±0.01	0.32±0.01	0.26±0.003	0.28±0.001

		Theta	Alpha	Beta	Gamma
Signal	SESS	$F_{1,3169}$=0.48, p=0.487	$F_{1,3169}$=0.30, p=0.582	$F_{1,3169}$=0.20, p=0.655	$F_{1,3169}$=0.01, p=0.906
	TRT	$F_{1,3169}$=0.36, p=0.550	$F_{1,3169}$=2.82, p=0.093	$F_{1,3169}$=0.25, p=0.616	$F_{1,3169}$=1.35, p=0.245
	SESS*TRT	$F_{1,3169}$=0.89, p=0.345	$F_{1,3169}$=0.00, p=0.994	$F_{1,3169}$=0.08, p=0.771	$F_{1,3169}$=0.14, p=0.709

Correct Press	SESS	$F_{1,6470}$=0.03, p=0.858	$F_{1,6470}$=1.52, p=0.218	$F_{1,6470}$=2.87, p=0.090	$F_{1,6470}$=0.10, p=0.756
	TRT	$F_{1,6470}$=3.71, p=0.054	$F_{1,6470}$=0.83, p=0.362	$F_{1,6470}$=6.90, p=0.009	$F_{1,6470}$=0.00, p=0.950
	SESS*TRT	$F_{1,6470}$=7.12, p=0.008	$F_{1,6470}$=0.62, p=0.430	$F_{1,6470}$=10.50, p=0.001	$F_{1,6470}$=0.37, p=0.545
Incorrect Press	SESS	$F_{1,1232}$=0.08, p=0.777	$F_{1,1233}$=0.56, p=0.454	$F_{1,1234}$=0.20, p=0.651	$F_{1,1234}$=4.10, p=0.043
	TRT	$F_{1,1232}$=0.58, p=0.448	$F_{1,1233}$=0.00, p=0.959	$F_{1,1234}$=0.18, p=0.667	$F_{1,1234}$=3.05, p=0.081
	SESS*TRT	$F_{1,1232}$=0.63, p=0.426	$F_{1,1233}$=0.31, p=0.576	$F_{1,1234}$=0.12, p=0.728	$F_{1,1234}$=8.07, p=0.004
Reward	SESS	$F_{1,6137}$=18.80, p<0.0001	$F_{1,6138}$=17.70, p<0.0001	$F_{1,6141}$=0.36, p=0.548	$F_{1,6141}$=11.62, p=0.001
	TRT	$F_{1,6137}$=65.47, p<0.0001	$F_{1,6138}$=71.04, p<0.0001	$F_{1,6141}$=7.04, p=0.008	$F_{1,6141}$=12.88, p<0.0001
	SESS*TRT	$F_{1,6137}$=70.38, p<0.0001	$F_{1,6138}$=68.44, p<0.0001	$F_{1,6141}$=2.66, p=0.103	$F_{1,6141}$=14.56, p<0.0001
Baseline	SESS	$F_{1,7667}$=1.88, p=0.171	$F_{1,7662}$=0.05, p=0.851	$F_{1,7646}$=0.01, p=0.907	$F_{1,7647}$=0.83, p=0.362
	TRT	$F_{1,7667}$=2.77, p=0.096	$F_{1,7662}$=1.69, p=0.194	$F_{1,7646}$=2.58, p=0.108	$F_{1,7647}$=0.20, p=0.656
	SESS*TRT	$F_{1,7667}$=0.62, p=0.431	$F_{1,7662}$=0.23, p=0.634	$F_{1,7646}$=0.29, p=0.593	$F_{1,7647}$=0.23, p=0.631

B. Control

	Theta	**Alpha**	**Beta**	**Gamma**

Signal	Pre-Treatment - VEH	0.39±0.03	0.37±0.04	0.28±0.01	0.29±0.001
	Post-Treatment - VEH	0.39±0.04	0.36±0.04	0.29±0.01	0.29±0.002
	Pre-Treatment - CNO	0.38±0.03	0.37±0.04	0.29±0.02	0.28±0.001
	Post-Treatment - CNO	0.37±0.03	0.37±0.04	0.29±0.01	0.29±0.001
Correct Press	Pre-Treatment - VEH	0.36±0.03	0.31±0.02	0.27±0.005	0.29±0.002
	Post-Treatment - VEH	0.36±0.03	0.31±0.02	0.27±0.005	0.29±0.002
	Pre-Treatment - CNO	0.36±0.03	0.32±0.02	0.27±0.005	0.29±0.002
	Post-Treatment - CNO	0.36±0.03	0.32±0.02	0.27±0.005	0.29±0.002
Incorrect Press	Pre-Treatment - VEH	0.37±0.03	0.35±0.03	0.29±0.003	0.28±0.01
	Post-Treatment - VEH	0.36±0.03	0.35±0.03	0.28±0.003	0.27±0.01
	Pre-Treatment - CNO	0.37±0.03	0.34±0.02	0.29±0.003	0.27±0.01
	Post-Treatment - CNO	0.36±0.03	0.34±0.02	0.29±0.003	0.27±0.01
Reward	Pre-Treatment - VEH	0.31±0.01	0.30±0.01	0.29±0.001	0.26±0.004
	Post-Treatment - VEH	0.30±0.01	0.29±0.01	0.29±0.001	0.26±0.004
	Pre-Treatment - CNO	0.32±0.01	0.31±0.01	0.29±0.001	0.27±0.004
	Post-Treatment - CNO	0.31±0.01	0.31±0.01	0.29±0.001	0.27±0.004

		Theta	**Alpha**	**Beta**	**Gamma**
Signal	SESS	$F_{1,2865}$=0.18, p=0.671	$F_{1,2865}$=0.31, p=0.575	$F_{1,2865}$=0.70, p=0.402	$F_{1,2865}$=1.28, p=0.257
	Virus	$F_{1,2865}$=0.35, p=0.554	$F_{1,2865}$=3.08, p=0.079	$F_{1,2865}$=0.37, p=0.546	$F_{1,2865}$=1.32, p=0.251
	SESS*Virus	$F_{1,2865}$=0.02, p=0.895	$F_{1,2865}$=1.70, p=0.192	$F_{1,2865}$=0.72, p=0.395	$F_{1,2865}$=4.61, p=0.032
Correct Press	SESS	$F_{1,5830}$=0.23, p=0.633	$F_{1,5830}$=0.01, p=0.932	$F_{1,5830}$=0.81, p=0.368	$F_{1,5830}$=1.98, p=0.159

	Virus	$F_{1,5830}$=3.70, p=0.054	$F_{1,5830}$=0.85, p=0.355	$F_{1,5830}$=6.59, p=0.010	$F_{1,5830}$=0.01, p=0.918
	SESS*Virus	$F_{1,5830}$=0.41, p=0.524	$F_{1,5830}$=0.15, p=0.695	$F_{1,5830}$=0.18, p=0.670	$F_{1,5830}$=0.60, p=0.439
Incorrect Press	SESS	$F_{1,1135}$=0.11, p=0.741	$F_{1,1136}$=0.01, p=0.935	$F_{1,1137}$=0.23, p=0.632	$F_{1,1137}$=2.68, p=0.102
	Virus	$F_{1,1135}$=0.56, p=0.453	$F_{1,1136}$=0.00, p=0.946	$F_{1,1137}$=0.17, p=0.679	$F_{1,1137}$=3.09, p=0.079
	SESS*Virus	$F_{1,1135}$=0.13, p=0.723	$F_{1,1136}$=0.01, p=0.926	$F_{1,1137}$=0.46, p=0.499	$F_{1,1137}$=5.74, p=0.017
Reward	SESS	$F_{1,5481}$=0.52, p=0.470	$F_{1,5482}$=0.09, p=0.759	$F_{1,5484}$=1.76, p=0.185	$F_{1,5485}$=10.02, p=0.002
	Virus	$F_{1,5481}$=63.57, p<0.0001	$F_{1,5482}$=68.16, p<0.0001	$F_{1,5484}$=5.98, p=0.014	$F_{1,5485}$=12.38, p<0.0001
	SESS*Virus	$F_{1,5481}$=32.78, p<0.0001	$F_{1,5482}$=25.21, p<0.0001	$F_{1,5484}$=0.25, p=0.618	$F_{1,5485}$=0.99, p=0.320
Baseline	SESS	$F_{1,6936}$=0.30, p=0.586	$F_{1,6921}$=0.0004, p=0.984	$F_{1,6912}$=0.29, p=0.590	$F_{1,6911}$=0.18, p=0.672
	Virus	$F_{1,6936}$=2.62, p=0.106	$F_{1, 6921}$=0.01, p=0.941	$F_{1,6912}$=3.08, p=0.079	$F_{1,6911}$=0.39, p=0.532
	SESS*Virus	$F_{1, 6936}$=3.08, p=0.079	$F_{1,6921}$=3.73, p=0.054	$F_{1,6912}$=2.88, p=0.090	$F_{1,6911}$=0.06, p=0.808

Means ± SEMS and results of general linear mixed model statistical analyses of synchrony between the dorsomedial PFC (dmPFC) and lateral mediodorsal thalamus (lateral MD) for hM3dq and viral-control animals during the signal, correct press, incorrect press, and reward intervals across the 4 analyzed frequency bands: theta, alpha, beta, and gamma. CNO, clozapine-n-oxide; VEH, vehicle; TRT,

treatment (CNO vs. VEH control); SESS, session (pre-treatment vs. post-treatment); Virus (hM3Dq-CNO vs Control-CNO).

Supplemental Materials

Table S1. Mean and standard error of PFC and MD oscillatory frequencies.

A. dmPFC

		Theta	Alpha	Beta	Gamma
Signal	Pre-Treatment - VEH	0.39±0.03	0.27±0.03	0.15±0.03	0.10±0.04
	Post-Treatment - VEH	0.40±0.03	0.27±0.03	0.15±0.03	0.11±0.04
	Pre-Treatment - CNO	0.40±0.03	0.27±0.03	0.13±0.02	0.07±0.02
	Post-Treatment - CNO	0.54±0.06	0.33±0.04	0.12±0.02	0.06±0.01
Correct Press	Pre-Treatment - VEH	0.39±0.04	0.26±0.03	0.15±0.03	0.11±0.05
	Post-Treatment - VEH	0.41±0.04	0.27±0.03	0.16±0.04	0.11±0.05
	Pre-Treatment - CNO	0.38±0.04	0.24±0.03	0.13±0.02	0.08±0.02
	Post-Treatment - CNO	0.48±0.06	0.31±0.05	0.11±0.02	0.06±0.01
Incorrect Press	Pre-Treatment - VEH	0.39±0.04	0.26±0.03	0.15±0.03	0.11±0.05
	Post-Treatment - VEH	0.42±0.04	0.27±0.03	0.16±0.03	0.11±0.06
	Pre-Treatment - CNO	0.36±0.03	0.24±0.02	0.13±0.02	0.07±0.02
	Post-Treatment - CNO	0.50±0.06	0.32±0.04	0.12±0.02	0.06±0.01
Reward	Pre-Treatment - VEH	0.39±0.05	0.26±0.04	0.16±0.04	0.11±0.04
	Post-Treatment - VEH	0.38±0.04	0.26±0.04	0.16±0.04	0.11±0.04
	Pre-Treatment - CNO	0.37±0.04	0.24±0.03	0.13±0.02	0.08±0.02
	Post-Treatment - CNO	0.48±0.07	0.30±0.05	0.11±0.02	0.07±0.01

B. MD

		Theta	Alpha	Beta	Gamma
Signal	Pre-Treatment - VEH	0.32±0.02	0.29±0.02	0.11±0.01	0.07±0.01
	Post-Treatment - VEH	0.32±0.02	0.27±0.02	0.11±0.01	0.07±0.01
	Pre-Treatment - CNO	0.36±0.02	0.30±0.02	0.11±0.01	0.07±0.01
	Post-Treatment - CNO	0.41±0.03	0.34±0.03	0.12±0.01	0.07±0.01

Correct Press	Pre-Treatment - VEH	0.35±0.03	0.28±0.02	0.12±0.01	0.08±0.01
	Post-Treatment - VEH	0.36±0.03	0.27±0.02	0.11±0.01	0.07±0.01
	Pre-Treatment - CNO	0.39±0.03	0.31±0.02	0.12±0.01	0.08±0.01
	Post-Treatment - CNO	0.41±0.04	0.33±0.03	0.12±0.01	0.07±0.01
Incorrect Press	Pre-Treatment - VEH	0.34±0.03	0.28±0.02	0.11±0.01	0.07±0.01
	Post-Treatment - VEH	0.36±0.03	0.27±0.02	0.11±0.01	0.07±0.01
	Pre-Treatment - CNO	0.39±0.04	0.30±0.02	0.11±0.01	0.07±0.01
	Post-Treatment - CNO	0.39±0.04	0.33±0.03	0.12±0.01	0.07±0.01
Reward	Pre-Treatment - VEH	0.32±0.02	0.26±0.02	0.12±0.01	0.08±0.01
	Post-Treatment - VEH	0.31±0.02	0.24±0.02	0.11±0.01	0.08±0.01
	Pre-Treatment - CNO	0.34±0.02	0.27±0.02	0.12±0.01	0.08±0.01
	Post-Treatment - CNO	0.39±0.03	0.31±0.03	0.12±0.01	0.08±0.01

Means ± SEMS of oscillatory power in the dorsomedial PFC (dmPFC) and lateral mediodorsal thalamus (lateral MD) for hM3dq and viral-control animals during the signal, correct press, incorrect press, and reward intervals across the 4 analyzed frequency bands: theta, alpha, beta, and gamma. CNO, clozapine-n-oxide; VEH, vehicle; TRT, treatment (CNO vs. VEH control).

Chapter 4

Conclusions and Future Directions

Summary

Background. Decades of research have established the role of the PFC in cognitive processes necessary for goal-directed behavior (Berridge & Arnsten, 2015; Gabbott et al., 2005; Miller & Cohen, 2001; Voorn et al., 2004). Despite this known relationship, how the PFC supports cognition is not well understood. This presents a problem in the treatment of PFC-dependent cognitive dysfunction as seen in disorders such as schizophrenia, depression, and ADHD (Millan et al., 2012). While treatments exist to address PFC-dependent cognition, these treatments are not universally efficacious at addressing cognitive dysfunction across different disorders and patients. All of the current treatments used to address PFC-dependent cognitive dysfunction act on the catecholamine neurotransmitter systems in the PFC (Berridge & Arnsten, 2015). This focus on the catecholamine system for addressing dysfunction has led to a dearth of targets for improving PFC-dependent cognition. One possible novel target for addressing PFC-dependent cognitive dysfunction is through manipulation of the neuropeptide CRF. Despite early establishment of CRF peptide and receptors in the PFC (De Souza et al., 1985; Lovenberg et al., 1995b; Swanson et al., 1983b; Van Pett et al., 2000), most of the research concerning CRF has focused on the subcortical actions, leaving the role of CRF in PFC-dependent cognition largely unknown. To address this issue, recent research has begun to establish the role of PFC CRF neurons in modulating PFC-dependent cognition (Berridge et al., 2022; Hupalo et al., 2021; Hupalo, Martin, et al., 2019; Hupalo & Berridge, 2016).

The four foundational findings from these recent studies of CRF action in PFC-dependent cognition are; 1) that CRF acts within the caudal dmPFC, but not other sections of the PFC, to impair working memory, 2) that CRFR blockade improves both working memory and sustained attention comparable to clinically relevant doses of amphetamines, 3) that male and female rats do not differ in the effects of CRF outside of the proestrus phase of the estrus cycle, and 4) that dmPFC CRF neuronal activation impairs working memory via local release of CRF and sustained attention via release of CRF outside the dmPFC. Despite these findings many questions remain about how CRF modulates PFC-dependent cognition. Perhaps the most salient question raised by this research was why dmPFC CRF neurons display differential circuitry across working memory and sustained attention.

The experiments presented answer this question and make substantial strides in expanding our understanding of dmPFC CRF neurobiology. Specifically, the findings of this thesis establish the neurochemical heterogeneity of dmPFC CRF neurons, the extended circuitry of dmPFC CRF neurons, and dmPFC CRF neuronal action across a frontothalamic network in working memory and sustained attention.

Findings. One possible explanation for the differential actions of dmPFC CRF neurons across working memory and sustained attention was the neurochemical identity of dmPFC CRF neurons. CRF neurons were known to be either GABAergic or glutamatergic outside the PFC(Fudge et al., 2022; Tagliaferro & Morales, 2008; Valentino et al., 2001). As GABA neurons often project locally, whereas glutamatergic neurons project both locally and distally, if dmPFC CRF neurons were either GABAergic or glutamatergic this could explain the differential actions of these neurons across working memory and sustained attention. Previous research had established the presence of GABAergic CRF neurons within the dmPFC of mice (Chen et al., 2020; de León Reyes et al., 2023), but an extensive examination of the neurochemical identity of dmPFC CRF neurons had not been conducted.

The first experiment demonstrated novel neurochemical findings showing that dmPFC CRF neurons are either GABAergic or glutamatergic, with the majority (~85%) being glutamatergic. These neuronal subpopulations display differential action across working memory and sustained attention, with dmPFC CRF_{GABA} neurons impairing only working memory performance and dmPFC CRF_{Glu} neurons disrupting both working memory and sustained attention performance. The working memory impairing actions of both dmPFC CRF_{GABA} and dmPFC CRF_{Glu} neurons were due, at least in part, to CRF agonism within the caudal dmPFC. These findings show that dmPFC CRF neurochemical identity is at least partially explanatory for the differential actions of dmPFC CRF neurons across working memory and sustained attention.

A remaining question from previous research was where dmPFC CRF neurons project and act to impair sustained attention (Hupalo et al., 2021). In the second experiment, an anterograde viral cocktail was used to characterize the projections of dmPFC CRF neurons. Across the rostral-caudal extent of the dmPFC, these studies demonstrated dense projections of PFC CRF neurons to the lateral MD. CRF neurons in the rostral dmPFC neurons sent the majority of their projections to the ventromedial extent of

the rostral MD and moved medially in the caudal MD. CRF neurons in the caudal dmPFC sent the majority of their projections to the dorsolateral portion of the rostral MD and moved more lateral in the caudal MD. Interestingly, these projection patterns match non-selective dmPFC neural projections to the MD (Sesack et al., 1989b).

To explore whether CRF acts within the MD to impair sustained attention, subsequent infusions of CRF in the lateral MD, but not medial MD or surrounding areas, produced significant reversable impairments in sustained attention performance. Interestingly, despite the known role of the lateral MD in working memory, CRF infusions into the lateral MD did not alter working memory performance. However, the current studies demonstrate that the lateral MD is necessary for both working memory and sustained attention performance, with significant impairment in both working memory and sustained attention performance observed after inactivation of the lateral MD with the GABA-A agonist muscimol. To demonstrate that dmPFC CRF neurons that project to the lateral MD disrupt sustained attention, dmPFC CRF neuronal terminals were chemogenetically activated in the lateral MD. This activation led to decreased sustained attention performance compared to vehicle treated animals and viral controls. These experiments established a novel frontothalamic CRF circuit and suggest that the lateral MD is the likely site of action for dmPFC CRF neurons to impair sustained attention.

Finally, to understand how dmPFC CRF neurons act across this circuit to generate impairments in sustained attention, caudal dmPFC CRF_{Glu} neurons where chemogenetically activated and the effect of activating these neurons on the neural encoding of sustained attention were measured using electrophysiological recordings in the dmPFC and lateral MD of animals performing the sustained attention task. Neurons in both the dmPFC and lateral MD showed elevated firing during signal presentation, correct and incorrect lever presses, and reward. The only group of neurons that demonstrated any impact of chemogenetic activation of caudal dmPFC CRF_{Glu} neurons were caudal dmPFC signal-tuned neurons. Chemogenetic activation of caudal dmPFC CRF_{Glu} neurons led to decreases in signal-related firing relative to vehicle treatment, viral controls, and rostral signal-tuned PFC neurons. In addition to these changes in neuronal firing, chemogenetic activation of caudal dmPFC CRF_{Glu} neurons resulted in significant alterations in dmPFC and lateral MD oscillatory power and synchrony. In the dmPFC, regardless of event, chemogenetic activation of caudal dmPFC CRF_{Glu}

neurons resulted in significant increases in theta and alpha oscillatory power and decreases in beta and gamma power relative to vehicle-treated animals and viral control animals. In the lateral MD the chemogenetic activation of caudal dmPFC CRF_{Glu} neurons induced small increases of power across all frequency bands in all events (with few exceptions by event and band). Interestingly, the dmPFC and lateral MD changes in oscillatory power induced by chemogenetic activation of caudal dmPFC CRF_{Glu} neurons extended into the inter-trial period (i.e. task-independent). When examining the effect of chemogenetic activation of caudal dmPFC CRF_{Glu} neurons on frontothalamic synchrony, a significant increase in theta and alpha synchrony in reward was seen relative to vehicle-treated animals and viral controls. Collectively, these results demonstrate a complex encoding of sustained attention event-related activity in neuronal spiking, oscillatory power, and synchrony which is uniquely altered by dmPFC CRF neuronal activation that coincides with impairments of sustained attention performance.

Neurochemical Heterogeneity in dmPFC CRF Neurons and Cognitive Action

Previous research demonstrated that dmPFC CRF neurons modulate both working memory and sustained attention via local or distal release of CRF, respectively (Hupalo et al., 2021; Hupalo, Martin, et al., 2019). As CRF neurons are known to be either GABAergic or glutamatergic outside the dmPFC, one potential explanation for the difference in projection patterns was the neurochemical identity of dmPFC CRF neurons (Fudge et al., 2022; Tagliaferro & Morales, 2008; Valentino et al., 2001). The above studies demonstrated not only that there are robust populations of GABAergic and glutamatergic CRF neurons within the dmPFC, but that these neurons do indeed act differently across working memory and sustained attention performance. Previous studies additionally demonstrated that blockade of CRF receptor subtype 1 ($CRFR_1$) is sufficient to interrupt the disrupting actions of chemogenetically activating dmPFC CRF_{GABA} and CRF_{Glu} neurons on working memory. Important remaining questions concerning the actions of caudal dmPFC CRF_{GABA} and CRF_{Glu} neurons in working memory are where, and on what type of neurons, these neurons synapse in the PFC to impair working memory. Additionally, it is unclear whether caudal dmPFC CRF_{GABA} and CRF_{Glu} have differential individual actions on the encoding of working memory.

An unreported finding of our viral, immunohistochemical, and in situ hybridization experiments is that large percentages of PFC neurons co-label CRF peptide and mRNA (at least 80%). Given the consistent replication of high percentages of PFC neurons expressing CRF peptide in our animal model across a decade of experimentation and dozens of animals, these results are well supported. This high degree of overlap would suggest that PFC CRF neurons are acting in the same way as traditional understandings of GABAergic and glutamatergic PFC neurons. Whether this large presence of CRF is true in other rodent models or primates remains an open question. It is important to note that while there may be a high percentage of PFC neurons expressing CRF peptide, this does not mean that PFC neurons release CRF every time these neurons depolarize. When these neurons are active and when they release CRF remains to be seen.

Frontothalamic Circuitry and Actions of dmPFC CRF Neurons

The presented data adds to a growing body of research demonstrating the role of the lateral MD in PFC-dependent cognition. In experiments conducted both in this lab and others, it is clear that the dmPFC and lateral MD contribute to the maintenance of sustained attention (Chudasama & Robbins, 2006; Mantanona et al., 2020b; Pezze et al., 2014), as well as other PFC-dependent cognitive processes. Despite sustained attention being PFC-dependent, we demonstrated that CRF does not act in any portion of the rodent dmPFC to impair sustained attention performance (Hupalo et al., 2021). This is interesting given CRF infusion in the PFC disrupts working memory. This suggests that CRF actions in the PFC affects systems that are distinct from the processes that support sustained attention. This contrasts with the actions of catecholamines in the PFC, which modulate both working memory and sustained attention via action in the PFC. We also previously demonstrated that global blockade of $CRFR_1$ was sufficient to disruot the impairing actions of caudal dmPFC CRF neuronal activation on sustained attention (Hupalo et al., 2021). As it has been shown that $CRFR_1$ is present in the lateral MD (Van Pett et al., 2000), it is likely that CRF is acting on these receptors to disrupt lateral MD and lateral MD → dmPFC function during sustained attention performance. There is some precedence for such an action across the lateral MD → dmPFC circuit. It has been shown that lateral MD neurons support delay related activity in dmPFC neurons during working memory (Bolkan et al., 2017; Ouhaz et al., 2018; Saalmann, 2014; M.

Watanabe, 1989; Wolff & Halassa, 2024). Previous research on the neurochemical identity and projection patterns of lateral MD neurons indicate that lateral MD neurons are mostly excitatory and that the presence of certain peptides and receptors can identify the projection targets and actions of these neurons in the PFC (for review see Wolff & Halassa, 2024). Given that chemogenetic activation of caudal dmPFC CRF_{Glu} neurons decreases the firing rate of signal-tuned caudal dmPFC neurons, it is possible that these neurons are either a direct or indirect target of CRF responsive lateral MD neurons. Without more detailed anatomical information about the exact projection sites of caudal dmPFC CRF_{Glu} neurons it is difficult to understand how caudal dmPFC CRF_{Glu} produce impairments in the PFC without acting in the PFC to impair sustained attention.

Large consistent changes in oscillatory power in the dmPFC, and to a lesser degree lateral MD, were observed following chemogenetic activation of caudal dmPFC CRF_{Glu} neurons. Unlike oscillatory power, only small changes in reward theta and alpha synchrony and incorrect-press gamma synchrony between the dmPFC and lateral MD were seen. This finding is interesting given the lack of changes seen in reward- or incorrect press-related firing in either the dmPFC or lateral MD. This may suggest that, while the lateral MD is important for sustained attention performance, it does not process the same information at the same time as the dmPFC. One additional consideration is that alterations in oscillatory power and synchrony following caudal dmPFC CRF_{Glu} activation may be compensatory. This would align with human research which demonstrates increased theta and alpha oscillatory power in increasingly difficult and exhausting sustained attention tasks (Lal & Craig, 2001; Tran et al., 2020; Wascher et al., 2014). Similarly, synchrony changes may reflect a compensatory process, as previous research indicates a strong role of the lateral MD in extradimensional set shifting by supporting the PFC in rule recall (Block et al., 2007; Ouhaz et al., 2022). If chemogenetic activation of caudal dmPFC CRF_{Glu} neurons disrupts rule recall, then synchrony may be increased during reward to try and address this disruption. In support of this hypothesis, in all the presented experiments, impairments in sustained attention performance were largely driven by an increase in false alarm responses and smaller decrease in hit responses suggesting difficulty recalling the correct response in the absence of a signal. However, these results could alternatively reflect a lack of sustained attention and a bias towards the lever with an

attached signal. Further testing of CRF actions during sustained attention performance is needed to better understand these details.

An additional observation from the current studies was a lack of any changes in the firing rates of the limited number of event-tuned lateral MD neurons. This could mean that MD neurons display more complex encoding of task-related information beyond elevated firing following events. For example, in working memory in primates, delay-tuned lateral MD neurons switch from representing retrospective sensory information, like dmPFC neurons, to represent prospective motor information (Funahashi, 2013; Y. Watanabe & Funahashi, 2018). MD neurons may be performing a similar function in the rodent, especially in less visually dependent tasks (for review see Wolff & Halassa, 2024). In the current study, only retrospective coding of lateral MD neurons was examined. Two events that do contain information about an upcoming event that could have shown prospective tuning in our study were reward and lever-extend (data not shown). Given this, it is interesting that the largest number of event-tuned lateral MD neurons were tuned to the reward, though the firing of these neurons was not affected by chemogenetic activation of caudal dmPFC CRF_{Glu} neurons. Analyses of the tuning of dmPFC and lateral MD neurons following lever extension demonstrated a large overlap with lever press neurons, and no effects of chemogenetic activation of caudal dmPFC CRF_{Glu} neurons on the firing rates of these neurons (data not shown). The lack of prospective tuning in lateral MD neurons in this study may reflect a difference in tasks as the response in the current task does not include an extended delay between the signal and the response. Future analyses are needed to understand if lateral MD neurons encode future events or change coding in the current sustained attention task.

Future Directions

The studies presented in this thesis elucidate important mechanisms underlying the cognitive actions of the PFC CRF system. However, many questions remain about when CRF acts across this frontothalamic circuit to alter PFC-dependent cognition. One remaining question is when CRF is released during working memory and sustained attention performance. This could be addressed utilizing recently developed neuropeptide sensors, which release light in the presence of CRF by utilizing a G protein-coupled receptor (GCPR) with circularly permutated fluorescent proteins (H. Wang et al., 2023).

CRF is present in a large amount of PFC neurons, but it is unclear if CRF is released every time PFC neurons depolarize. Given we have observed CRF in both the cell body and terminals of dmPFC CRF neurons it is additionally possible that CRF serves certain internal cellular functions and is not released upon depolarization in every neuron that co-labels for CRF peptide. Questions also remain about how much CRF is released and how far CRF travels from the release site following neural depolarization. Future studies with CRF GPCR sensors are necessary to answer these questions.

Once it is known when CRF is released the next question that can be answered is when modulating CRF release is most impactful on working memory and sustained attention. This can be accomplished using optogenetic manipulations to target, and selectively activate or inhibit, caudal dmPFC CRF_{GABA} or CRF_{Glu} neurons at different key moments in working memory and sustained attention task performance. The presented, and previous, DREADD manipulations of caudal dmPFC CRF neurons provide long term activation caudal dmPFC CRF neurons that not only cover the testing trials, but also the time between trials, leading up to the experiment, and following behavioral testing. Through repeated testing we know that animals return to baseline performance 24 hours following chemogenetic activation, but it is unclear when this manipulation is most disruptive to performance. For example, it is possible that brief stimulation of dmPFC CRF neurons is not sufficient to modulate working memory or sustained attention because it does not raise concentrations of CRF in the extracellular space to a sufficient level to disrupt performance. Optogenetic manipulation could also allow for direct testing of the relationship between oscillatory power and task performance. For example, given the large increases in theta and alpha power seen when chemogenetically activating caudal dmPFC CRF_{Glu} neurons, an optogenetic manipulation of caudal dmPFC CRF_{Glu} neurons could activate caudal dmPFC CRF_{Glu} neurons at theta or alpha frequencies during different phases of the sustained attention task to determine if increasing power at theta or alpha frequencies impacts performance.

The above manipulations utilizing CRF GPCR sensors or optogenetics could be paired with anterograde viral cocktails to explore these questions across the dmPFC → lateral MD frontothalamic circuit. For example, CRF release across the rostral caudal extent of the lateral MD from caudal dmPFC CRF_{Glu} neurons could be examined using an anterograde labeling virus that introduces CRF sensing

GPCRs in the terminal fields of caudal dmPFC CRF_{Glu} neurons and examining release in different subfields of the lateral MD. Alternatively, optogenetic probes could be inserted into different hemifields of the dmPFC and lateral MD to temporally activate or inactivate CRF neurons within or projecting between the dmPFC or lateral MD at key moments in task performance.

To better understand how CRF alters PFC-dependent cognition, additional information is also needed concerning the neurochemical and structural details of where CRF agonism occurs in the dmPFC and lateral MD to alter cognition. We have previously demonstrated that CRF disrupts both working memory and sustained attention via $CRFR_1$, and that the working memory impairments are due to downstream protein-kinase A signaling (Hupalo, Martin, et al., 2019). However, questions remain concerning the exact location and layer distribution of $CRFR_1$ in the PFC, and other brain regions, and the neurochemical identity of the PFC neurons that express CRF receptors (CRFR). While some early brain-wide explorations of CRFRs were conducted, much of the research into both CRF peptide and receptor location has focused on subcortical distributions, ignoring the finer details of cortical CRF peptide and receptor expression (Chalmers et al., 1995; Fudge et al., 2025; Van Pett et al., 2000). More recent investigations have begun to describe the expression of CRF peptide in different neuronal classes and structures in the PFC of transgenic CRF-Cre mice (Chen et al., 2020; Lewis et al., 2008; Y. Wang et al., 2021), but these explorations have mostly focused on CRF_{GABA} neurons and have failed to fully validate these mouse models for studying CRF neurons (Cooke et al., 2025). Thus, there is a need for detailed exploration of both CRF peptide and receptor expression across neuronal class and structure in the PFC and other brain regions. Without these details, it is difficult to predict how CRF receptor activation within the PFC or other brain regions leads to disruptions in broader circuit function.

Finally, it remains to be determined whether dmPFC CRF neurons influence behavior beyond working memory and sustained attention. The PFC is known to support a diversity of behavioral processes including planning, cognitive control, cognitive flexibility, social interactions, and other forms of attention besides sustained attention. It is entirely possible that dmPFC CRF neurons regulate all these behaviors via action either in the PFC or in other connected regions. Regions such as the striatum, MD, and hippocampus, are all known projection sites of the PFC (Hoover & Vertes, 2007), and all contain CRFRs (Van Pett et al., 2000). By exploring whether CRF acts in other forms of PFC-dependent

cognition in concert with other brain regions, the fundamental purpose of the CRF system in the PFC and in cognition may become clearer.

These proposed experiments would not only further our understanding of the CRF system and PFC-dependent cognition, but could lead to novel targets useful in the treatment of PFC-dependent cognitive dysfunction.

References

Alsene, K. M., Rajbhandari, A. K., Ramaker, M. J., & Bakshi, V. P. (2011). Discrete forebrain neuronal networks supporting noradrenergic regulation of sensorimotor gating. *Neuropsychopharmacology*, *36*(5), 1003–1014.

Anticevic, A., Yang, G., Savic, A., Murray, J. D., Cole, M. W., Repovs, G., Pearlson, G. D., & Glahn, D. C. (2014). Mediodorsal and Visual Thalamic Connectivity Differ in Schizophrenia and Bipolar Disorder With and Without Psychosis History. *Schizophrenia Bulletin*, *40*(6), 1227–1243. https://doi.org/10.1093/schbul/sbu100

Aosaki, T., Kimura, M., & Graybiel, A. M. (1995). Temporal and spatial characteristics of tonically active neurons of the primate's striatum. *Journal of Neurophysiology*, *73*(3), 1234–1252.

Arnau, S., Brümmer, T., Liegel, N., & Wascher, E. (2021). Inverse effects of time-on-task in task-related and task-unrelated theta activity. *Psychophysiology*, *58*(6), e13805. https://doi.org/10.1111/psyp.13805

Arnsten, A. F. (2009a). Stress signalling pathways that impair prefrontal cortex structure and function. *Nature Reviews Neuroscience*, *10*(6), 410–422.

Arnsten, A. F. (2009b). Stress signalling pathways that impair prefrontal cortex structure and function. *Nature Reviews Neuroscience*, *10*(6), 410–422.

Arnsten, A. F., Mathew, R., Ubriani, R., Taylor, J. R., & Li, B.-M. (1999). α-1 noradrenergic receptor stimulation impairs prefrontal cortical cognitive function. *Biological Psychiatry*, *45*(1), 26–31.

Arnsten, A. F., Paspalas, C. D., Gamo, N. J., Yang, Y., & Wang, M. (2010). Dynamic network connectivity: A new form of neuroplasticity. *Trends in Cognitive Sciences*, *14*(8), 365–375.

Arnsten, A. F., & Pliszka, S. R. (2011). Catecholamine influences on prefrontal cortical function: Relevance to treatment of attention deficit/hyperactivity disorder and related disorders. *Pharmacology Biochemistry and Behavior*, *99*(2), 211–216.

Arnsten, A. F. T., & Datta, D. (2024). Characterizing the Most Vulnerable Prefrontal Cortical Neurons in Schizophrenia. *American Journal of Psychiatry*, *181*(10), 861–864. https://doi.org/10.1176/appi.ajp.20240731

Arnsten, A. F., Wang, M. J., & Paspalas, C. D. (2012). Neuromodulation of thought: Flexibilities and vulnerabilities in prefrontal cortical network synapses. *Neuron*, *76*(1), 223–239.

Arski, O. N., Young, J. M., Smith, M.-L., & Ibrahim, G. M. (2021). The Oscillatory Basis of Working Memory Function and Dysfunction in Epilepsy. *Frontiers in Human Neuroscience*, *14*, 596. https://doi.org/10.3389/fnhum.2020.612024

Auger, M. L., & Floresco, S. B. (2015). Prefrontal cortical GABA modulation of spatial reference and working memory. *International Journal of Neuropsychopharmacology*, *18*(2), pyu013.

Bale, T. L., & Vale, W. W. (2004). CRF and CRF receptors: Role in stress responsivity and other behaviors. *Annual Review of Pharmacology and Toxicology*, *44*, 525.

Bangasser, D. A., Reyes, B. A., Piel, D., Garachh, V., Zhang, X.-Y., Plona, Z. M., Van Bockstaele, E. J., Beck, S. G., & Valentino, R. J. (2013). Increased vulnerability of the brain norepinephrine system of females to corticotropin-releasing factor overexpression. *Molecular Psychiatry*, *18*(2), 166–173.

Bangasser, D. A., Zhang, X., Garachh, V., Hanhauser, E., & Valentino, R. J. (2011). Sexual dimorphism in locus coeruleus dendritic morphology: A structural basis for sex differences in emotional arousal. *Physiology & Behavior*, *103*(3–4), 342–351.

Batuev, A. S., Kursina, N. P., & Shutov, A. P. (1990). Unit activity of the medial wall of the frontal cortex during delayed performance in rats. *Behavioural Brain Research*, *41*(2), 95–102.

Benchenane, K., Tiesinga, P. H., & Battaglia, F. P. (2011). Oscillations in the prefrontal cortex: A gateway to memory and attention. *Current Opinion in Neurobiology, Behavioural and Cognitive Neuroscience*, *21*(3), 475–485. https://doi.org/10.1016/j.conb.2011.01.004

Berridge, C. W., & Arnsten, A. F. (2015). Catecholamine mechanisms in the prefrontal cortex: Proven strategies for enhancing higher cognitive function. *Current Opinion in Behavioral Sciences*, *4*, 33–40.

Berridge, C. W., Devilbiss, D. M., Andrzejewski, M. E., Arnsten, A. F., Kelley, A. E., Schmeichel, B., Hamilton, C., & Spencer, R. C. (2006). Methylphenidate preferentially increases catecholamine neurotransmission within the prefrontal cortex at low doses that enhance cognitive function. *Biological Psychiatry*, *60*(10), 1111–1120.

Berridge, C. W., Devilbiss, D. M., Martin, A. J., Spencer, R. C., & Jenison, R. L. (2023). Stress degrades working memory-related frontostriatal circuit function. *Cerebral Cortex*, *33*(12), 7857–7869.

Berridge, C. W., Martin, A. J., Hupalo, S., & Nicol, S. E. (2022). Estrus cycle-dependent working memory effects of prefrontal cortex corticotropin-releasing factor neurotransmission. *Neuropsychopharmacology*, 1–8. https://doi.org/10.1038/s41386-022-01349-7

Berridge, C. W., Shumsky, J. S., Andrzejewski, M. E., McGaughy, J. A., Spencer, R. C., Devilbiss, D. M., & Waterhouse, B. D. (2012). Differential sensitivity to psychostimulants across prefrontal cognitive tasks: Differential involvement of noradrenergic α1-and α2-receptors. *Biological Psychiatry*, *71*(5), 467–473.

Birnbaum, S., Gobeske, K. T., Auerbach, J., Taylor, J. R., & Arnsten, A. F. (1999). A role for norepinephrine in stress-induced cognitive deficits: α-1-adrenoceptor mediation in the prefrontal cortex. *Biological Psychiatry*, *46*(9), 1266–1274.

Block, A. E., Dhanji, H., Thompson-Tardif, S. F., & Floresco, S. B. (2007). Thalamic–prefrontal cortical–ventral striatal circuitry mediates dissociable components of strategy set shifting. *Cerebral Cortex*, *17*(7), 1625–1636.

Bloom, F. E., Battenberg, E. L., Rivier, J., & Vale, W. (1982). Corticotropin releasing factor (CRF): Immunoreactive neurones and fibers in rat hypothalamus. *Regulatory Peptides*, *4*(1), 43–48.

Bolkan, S. S., Stujenske, J. M., Parnaudeau, S., Spellman, T. J., Rauffenbart, C., Abbas, A. I., Harris, A. Z., Gordon, J. A., & Kellendonk, C. (2017). Thalamic projections sustain prefrontal activity during working memory maintenance. *Nature Neuroscience*, *20*(7), Article 7. https://doi.org/10.1038/nn.4568

Brooks, M. E., Kristensen, K., Benthem, K. J. van, Magnusson, A., Berg, C. W., Nielsen, A., Skaug, H. J., Mächler, M., & Bolker, B. M. (2017). glmmTMB Balances Speed and Flexibility Among Packages for Zero-inflated Generalized Linear Mixed Modeling. *The R Journal*, *9*(2), 378–400. https://doi.org/10.32614/RJ-2017-066

Broussard, J., Sarter, M., & Givens, B. (2006). Neuronal correlates of signal detection in the posterior parietal cortex of rats performing a sustained attention task. *Neuroscience*, *143*(2), 407–417.

Bucci, D. J. (2009). Posterior parietal cortex: An interface between attention and learning? *Neurobiology of Learning and Memory*, *91*(2), 114–120.

Buchmann, A., Dentico, D., Peterson, M. J., Riedner, B. A., Sarasso, S., Massimini, M., Tononi, G., & Ferrarelli, F. (2014). Reduced mediodorsal thalamic volume and prefrontal cortical spindle activity in schizophrenia. *NeuroImage*, *102*, 540–547. https://doi.org/10.1016/j.neuroimage.2014.08.017

Bushnell, P. J. (1998). Behavioral approaches to the assessment of attention in animals. *Psychopharmacology*, *138*, 231–259.

Cardoso-Cruz, H., Sousa, M., Vieira, J. B., Lima, D., & Galhardo, V. (2013). Prefrontal cortex and mediodorsal thalamus reduced connectivity is associated with spatial working memory impairment in rats with inflammatory pain. *PAIN®*, *154*(11), 2397–2406.

Chalmers, D. T., Lovenberg, T. W., & De Souza, E. B. (1995). Localization of novel corticotropin-releasing factor receptor (CRF2) mRNA expression to specific subcortical nuclei in rat brain: Comparison with CRF1 receptor mRNA expression. *Journal of Neuroscience*, *15*(10), 6340–6350.

Charlton, B. G., Nicol Ferrier, I., & Perry, R. H. (1987). Distribution of corticotropin-releasing factor-like immunoreactivity in human brain. *Neuropeptides*, *10*(4), 329–334. https://doi.org/10.1016/S0143-4179(87)90083-7

Chen, P., Lou, S., Huang, Z.-H., Wang, Z., Shan, Q.-H., Wang, Y., Yang, Y., Li, X., Gong, H., Jin, Y., Zhang, Z., & Zhou, J.-N. (2020). Prefrontal Cortex Corticotropin-Releasing Factor Neurons Control Behavioral Style Selection under Challenging Situations. *Neuron*, *106*(2), 301-315.e7. https://doi.org/10.1016/j.neuron.2020.01.033

Chiba, A., Oshio, K., & Inase, M. (2015). Neuronal representation of duration discrimination in the monkey striatum. *Physiological Reports*, *3*(2), e12283.

Chudasama, Y., & Robbins, T. W. (2006). Functions of frontostriatal systems in cognition: Comparative neuropsychopharmacological studies in rats, monkeys and humans. *Biological Psychology*, *73*(1), 19–38.

Cohen, M. X. (2014). *Analyzing neural time series data: Theory and practice*. MIT press.

Cole, R. D., Kawasumi, Y., Parikh, V., & Bangasser, D. A. (2016a). Corticotropin releasing factor impairs sustained attention in male and female rats. *Behavioural Brain Research*, *296*, 30–34. https://doi.org/10.1016/j.bbr.2015.08.023

Cole, R. D., Kawasumi, Y., Parikh, V., & Bangasser, D. A. (2016b). Corticotropin releasing factor impairs sustained attention in male and female rats. *Behavioural Brain Research*, *296*, 30–34.

Cooke, S. K., Martin, A. J., Nicol, S., Kiraly, J., & Berridge, C. W. (2022, November 16). Differential Actions of Glutamatergic and GABAergic Prefrontal Corticotropin-Releasing Factor Neurons on Working Memory and Sustained Attention. *Program No. 685.11*. Society for Neuroscience. https://www.sfn.org/-/media/SfN/Documents/NEW-SfN/Meetings/Neuroscience-2022/Abstracts/Abstract-PDFs/SFN22_Abstracts-PDF-Posters_WED_PM.pdf

Cooke, S. K., Martin, A. J., Spencer, R. C., Nicol, S. E., & Berridge, C. W. (2025). Neurochemical and Circuit Heterogeneity of Cognition-Modulating Prefrontal Corticotropin-Releasing Factor Neurons. *Biological Psychiatry*. https://www.sciencedirect.com/science/article/pii/S0006322325010996?casa_token=JPS0mAL7wssAAAAA:1TBuz7LSqFDa0YK4_gK6JQ592l0Szqkb5fsORwoicOXbXnK-B4WjOj8mHg2L29b7IducOjph9XJL

Dabrowska, J., Hazra, R., Guo, J., DeWitt, S., & Rainnie, D. (2013). Central CRF neurons are not created equal: Phenotypic differences in CRF-containing neurons of the rat paraventricular hypothalamus and the bed nucleus of the stria terminalis. *Frontiers in Neuroscience*, *7*, 156.

Das, M., Vihlen, C. S., & Legradi, G. (2007). Hypothalamic and brainstem sources of pituitary adenylate cyclase-activating polypeptide nerve fibers innervating the hypothalamic paraventricular nucleus in the rat. *Journal of Comparative Neurology*, *500*(4), 761–776.

Datta, D., & Arnsten, A. F. (2018). Unique molecular regulation of higher-order prefrontal cortical circuits: Insights into the neurobiology of schizophrenia. *ACS Chemical Neuroscience*, *9*(9), 2127–2145.

de León Reyes, N. S., Díaz, P. S., Nogueira, R., Ruiz-Pino, A., Nomura, Y., de Solis, C. A., Schulkin, J., Asok, A., & Leroy, F. (2023). Corticotropin-releasing hormone signaling from prefrontal cortex to lateral septum suppresses interaction with familiar mice. *Cell*, *186*(19), 4152–4171.

De Souza, E. B., Insel, T. R., Perrin, M. H., Rivier, J., Vale, W. W., & Kuhar, M. J. (1985). Corticotropin-releasing factor receptors are widely distributed within the rat central nervous system: An autoradiographic study. *Journal of Neuroscience*, *5*(12), 3189–3203.

Deussing, J. M., & Chen, A. (2018). The corticotropin-releasing factor family: Physiology of the stress response. *Physiological Reviews*, *98*(4), 2225–2286.

Devilbiss, D. M., Jenison, R. L., & Berridge, C. W. (2012). *Stress-induced impairment of a working memory task: Role of spiking rate and spiking history predicted discharge*.

Devilbiss, D. M., Spencer, R. C., & Berridge, C. W. (2017a). Stress degrades prefrontal cortex neuronal coding of goal-directed behavior. *Cerebral Cortex*, *27*(5), 2970–2983.

Devilbiss, D. M., Spencer, R. C., & Berridge, C. W. (2017b). Stress Degrades Prefrontal Cortex Neuronal Coding of Goal-Directed Behavior. *Cerebral Cortex*, *27*(5), 2970–2983. https://doi.org/10.1093/cercor/bhw140

Dixon, P. (2016). *Should blocks be fixed or random?* [Paper]. Conference on Applied Statistics in Agriculture, Manhattan, Kansas.

Fink, G. (1981). Has corticotropin–releasing factor finally been found? *Nature*, *294*(5841), 511–512.

Floresco, S. B., Braaksma, D. N., & Phillips, A. G. (1999). Thalamic–cortical–striatal circuitry subserves working memory during delayed responding on a radial arm maze. *Journal of Neuroscience*, *19*(24), 11061–11071.

Fudge, J. L., Kelly, E. A., & Hackett, T. A. (2022). Corticotropin Releasing Factor (CRF) Coexpression in GABAergic, Glutamatergic, and GABA/Glutamatergic Subpopulations in the Central Extended Amygdala and Ventral Pallidum of Young Male Primates. *Journal of Neuroscience*, *42*(48), 8997–9010.

Fudge, J. L., Kelly, E. A., & Mahoui, I. (2025). Translating stress systems: Corticotropin releasing factor, its receptors, and the dopamine system in nonhuman primate models. *Genomic Psychiatry*, *1*(aop), 1–16.

Funahashi, S. (2013). Thalamic mediodorsal nucleus and its participation in spatial working memory processes: Comparison with the prefrontal cortex. *Frontiers in Systems Neuroscience*, *7*, 36.

Funahashi, S., Bruce, C. J., & Goldman-Rakic, P. S. (1993). Dorsolateral prefrontal lesions and oculomotor delayed-response performance: Evidence for mnemonic" scotomas". *Journal of Neuroscience*, *13*(4), 1479–1497.

Fuster, J. (2015). *The prefrontal cortex*. Academic press.

Fuster, J. M., & Alexander, G. E. (1971). Neuron activity related to short-term memory. *Science*, *173*(3997), 652–654.

Fuster, J. M., & Alexander, G. E. (1973). Firing changes in cells of the nucleus medialis dorsalis associated with delayed response behavior. *Brain Research*, *61*, 79–91. https://doi.org/10.1016/0006-8993(73)90517-9

Gabbott, P. L., Warner, T. A., Jays, P. R., Salway, P., & Busby, S. J. (2005). Prefrontal cortex in the rat: Projections to subcortical autonomic, motor, and limbic centers. *Journal of Comparative Neurology*, *492*(2), 145–177.

Gallopin, T., Geoffroy, H., Rossier, J., & Lambolez, B. (2006). Cortical sources of CRF, NKB, and CCK and their effects on pyramidal cells in the neocortex. *Cerebral Cortex*, *16*(10), 1440–1452.

Gamo, N. J., Wang, M., & Arnsten, A. F. (2010). Methylphenidate and atomoxetine enhance prefrontal function through α2-adrenergic and dopamine D1 receptors. *Journal of the American Academy of Child & Adolescent Psychiatry*, *49*(10), 1011–1023.

George, O., Sanders, C., Freiling, J., Grigoryan, E., Vu, S., Allen, C. D., Crawford, E., Mandyam, C. D., & Koob, G. F. (2012). Recruitment of medial prefrontal cortex neurons during alcohol withdrawal predicts cognitive impairment and excessive alcohol drinking. *Proceedings of the National Academy of Sciences*, *109*(44), 18156–18161.

Gill, T. M., Sarter, M., & Givens, B. (2000). Sustained Visual Attention Performance-Associated Prefrontal Neuronal Activity: Evidence for Cholinergic Modulation. *Journal of Neuroscience*, *20*(12), 4745–4757. https://doi.org/10.1523/JNEUROSCI.20-12-04745.2000

Giraldo-Chica, M., Rogers, B. P., Damon, S. M., Landman, B. A., & Woodward, N. D. (2018). Prefrontal-Thalamic Anatomical Connectivity and Executive Cognitive Function in Schizophrenia. *Biological Psychiatry, Novel Mechanisms in Schizophrenia Pathophysiology*, *83*(6), 509–517. https://doi.org/10.1016/j.biopsych.2017.09.022

Goldman-Rakic, P. S. (1995). Cellular basis of working memory. *Neuron*, *14*(3), 477–485.

Goldman-Rakic, P. S. (1996). The prefrontal landscape: Implications of functional architecture for understanding human mentation and the central executive. *Philosophical Transactions of the Royal Society of London. Series B, Biological Sciences*, *351*(1346), 1445–1453. https://doi.org/10.1098/rstb.1996.0129

Goldman-Rakic, P. S. (1999). The physiological approach: Functional architecture of working memory and disordered cognition in schizophrenia. *Biological Psychiatry*, *46*(5), 650–661.

Gorelova, N., & Yang, C. R. (1996). The course of neural projection from the prefrontal cortex to the nucleus accumbens in the rat. *Neuroscience*, *76*(3), 689–706. https://doi.org/10.1016/S0306-4522(96)00380-6

Grammatopoulos, D. K., Randeva, H. S., Levine, M. A., Kanellopoulou, K. A., & Hillhouse, E. W. (2001). Rat cerebral cortex corticotropin-releasing hormone receptors: Evidence for receptor coupling to multiple G-proteins. *Journal of Neurochemistry*, *76*(2), 509–519.

Halassa, M. M., & Sherman, S. M. (2019). Thalamocortical Circuit Motifs: A General Framework. *Neuron*, *103*(5), 762–770. https://doi.org/10.1016/j.neuron.2019.06.005

Hartig, F. (2026). *DHARMa: Residual Diagnostics for Hierarchical (Multi-Level / Mixed) Regression Models.* [R]. https://github.com/florianhartig/DHARMa (Original work published 2015)

Helmeke, C., Ovtscharoff Jr, W., Poeggel, G., & Braun, K. (2008). Imbalance of immunohistochemically characterized interneuron populations in the adolescent and adult rodent medial prefrontal cortex after repeated exposure to neonatal separation stress. *Neuroscience*, *152*(1), 18–28.

Hoover, W. B., & Vertes, R. P. (2007). Anatomical analysis of afferent projections to the medial prefrontal cortex in the rat. *Brain Structure and Function*, *212*(2), 149–179.

Hupalo, S., & Berridge, C. W. (2016). Working Memory Impairing Actions of Corticotropin-Releasing Factor (CRF) Neurotransmission in the Prefrontal Cortex. *Neuropsychopharmacology*, *41*(11), Article 11. https://doi.org/10.1038/npp.2016.85

Hupalo, S., Bryce, C. A., Bangasser, D. A., Berridge, C. W., Valentino, R. J., & Floresco, S. B. (2019). Corticotropin-Releasing Factor (CRF) circuit modulation of cognition and motivation.

Neuroscience & Biobehavioral Reviews, *103*, 50–59. https://doi.org/10.1016/j.neubiorev.2019.06.010

Hupalo, S., Martin, A. J., Green, R. K., Devilbiss, D. M., & Berridge, C. W. (2019). Prefrontal Corticotropin-Releasing Factor (CRF) Neurons Act Locally to Modulate Frontostriatal Cognition and Circuit Function. *The Journal of Neuroscience*, *39*(11), 2080–2090. https://doi.org/10.1523/JNEUROSCI.2701-18.2019

Hupalo, S., Spencer, R. C., & Berridge, C. W. (2021). Prefrontal corticotropin-releasing factor neurons impair sustained attention via distal transmitter release. *European Journal of Neuroscience*, *54*(1), 4182–4196.

Jung, M. W., Qin, Y., McNaughton, B. L., & Barnes, C. A. (1998). Firing characteristics of deep layer neurons in prefrontal cortex in rats performing spatial working memory tasks. *Cerebral Cortex (New York, NY: 1991)*, *8*(5), 437–450.

Klavdieva, M. M. (1995). The history of neuropeptides I. *Frontiers in Neuroendocrinology*, *16*(4), 293–321.

Kojima, S., & Goldman-Rakic, P. S. (1982). Delay-related activity of prefrontal neurons in rhesus monkeys performing delayed response. *Brain Research*, *248*(1), 43–50.

Kostich, W. A., Chen, A., Sperle, K., & Largent, B. L. (1998). Molecular identification and analysis of a novel human corticotropin-releasing factor (CRF) receptor: The CRF2γ receptor. *Molecular Endocrinology*, *12*(8), 1077–1085.

Lal, S. K. L., & Craig, A. (2001). A critical review of the psychophysiology of driver fatigue. *Biological Psychology*, *55*(3), 173–194. https://doi.org/10.1016/S0301-0511(00)00085-5

Lapiz, M. D. S., & Morilak, D. A. (2006). Noradrenergic modulation of cognitive function in rat medial prefrontal cortex as measured by attentional set shifting capability. *Neuroscience*, *137*(3), 1039–1049.

Lewis, D. A., Cho, R. Y., Carter, C. S., Eklund, K., Forster, S., Kelly, M. A., & Montrose, D. (2008). Subunit-Selective Modulation of GABA Type A Receptor Neurotransmission and Cognition in Schizophrenia. *American Journal of Psychiatry*, *165*(12), 1585–1593. https://doi.org/10.1176/appi.ajp.2008.08030395

Lovenberg, T. W., Liaw, C. W., Grigoriadis, D. E., Clevenger, W., Chalmers, D. T., De Souza, E. B., & Oltersdorf, T. (1995a). Cloning and characterization of a functionally distinct corticotropin-releasing factor receptor subtype from rat brain. *Proceedings of the National Academy of Sciences*, *92*(3), 836–840.

Lovenberg, T. W., Liaw, C. W., Grigoriadis, D. E., Clevenger, W., Chalmers, D. T., De Souza, E. B., & Oltersdorf, T. (1995b). Cloning and characterization of a functionally distinct corticotropin-releasing factor receptor subtype from rat brain. *Proceedings of the National Academy of Sciences*, *92*(3), 836–840.

Mailly, P., Aliane, V., Groenewegen, H. J., Haber, S. N., & Deniau, J.-M. (2013). The rat prefrontostriatal system analyzed in 3D: Evidence for multiple interacting functional units. *Journal of Neuroscience*, *33*(13), 5718–5727.

Maltese, F., Pacinelli, G., Monai, A., Bernardi, F., Capaz, A. M., Niello, M., Walle, R., de Leon, N., Managò, F., & Leroy, F. (2025). Self-experience of a negative event alters responses to others in similar states through prefrontal cortex CRF mechanisms. *Nature Neuroscience*, *28*(1), 122–136.

Mantanona, C. P., Božič, T., Chudasama, Y., Robbins, T. W., Dalley, J. W., Alsiö, J., & Pienaar, I. S. (2020a). Dissociable contributions of mediodorsal and anterior thalamic nuclei in visual attentional performance: A comparison using nicotinic and muscarinic cholinergic receptor antagonists. *Journal of Psychopharmacology (Oxford, England)*, *34*(12), 1371–1381. https://doi.org/10.1177/0269881120965880

Mantanona, C. P., Božič, T., Chudasama, Y., Robbins, T. W., Dalley, J. W., Alsiö, J., & Pienaar, I. S. (2020b). Dissociable contributions of mediodorsal and anterior thalamic nuclei in visual attentional performance: A comparison using nicotinic and muscarinic cholinergic receptor antagonists. *Journal of Psychopharmacology (Oxford, England)*, *34*(12), 1371–1381. https://doi.org/10.1177/0269881120965880

Meng, Q.-Y., Chen, X.-N., Tong, D.-L., & Zhou, J.-N. (2011a). Stress and glucocorticoids regulated corticotropin releasing factor in rat prefrontal cortex. *Molecular and Cellular Endocrinology*, *342*(1), 54–63. https://doi.org/10.1016/j.mce.2011.05.035

Meng, Q.-Y., Chen, X.-N., Tong, D.-L., & Zhou, J.-N. (2011b). Stress and glucocorticoids regulated corticotropin releasing factor in rat prefrontal cortex. *Molecular and Cellular Endocrinology*, *342*(1–2), 54–63. https://doi.org/10.1016/j.mce.2011.05.035

Meyer, G., Carponcy, J., Salin, P. A., & Comte, J.-C. (2018). Differential recordings of local field potential: A genuine tool to quantify functional connectivity. *PloS One*, *13*(12), e0209001.

Millan, M. J., Agid, Y., Brüne, M., Bullmore, E. T., Carter, C. S., Clayton, N. S., Connor, R., Davis, S., Deakin, B., DeRubeis, R. J., Dubois, B., Geyer, M. A., Goodwin, G. M., Gorwood, P., Jay, T. M., Joëls, M., Mansuy, I. M., Meyer-Lindenberg, A., Murphy, D., … Young, L. J. (2012). Cognitive dysfunction in psychiatric disorders: Characteristics, causes and the quest for improved therapy. *Nature Reviews. Drug Discovery*, *11*(2), 141–168. https://doi.org/10.1038/nrd3628

Miller, E. K., & Cohen, J. D. (2001). An integrative theory of prefrontal cortex function. *Annual Review of Neuroscience*, *24*(1), 167–202.

Mitchell, J. F., Sundberg, K. A., & Reynolds, J. H. (2007). Differential Attention-Dependent Response Modulation across Cell Classes in Macaque Visual Area V4. *Neuron*, *55*(1), 131–141. https://doi.org/10.1016/j.neuron.2007.06.018

Mohebi, A., Pettibone, J. R., Hamid, A. A., Wong, J.-M. T., Vinson, L. T., Patriarchi, T., Tian, L., Kennedy, R. T., & Berke, J. D. (2019). Dissociable dopamine dynamics for learning and motivation. *Nature*, *570*(7759), 65–70. https://doi.org/10.1038/s41586-019-1235-y

Mohila, C. A., & Onn, S.-P. (2005). Increases in the density of parvalbumin-immunoreactive neurons in anterior cingulate cortex of amphetamine-withdrawn rats: Evidence for corticotropin-releasing factor in sustained elevation. *Cerebral Cortex*, *15*(3), 262–274.

Niki, H., & Watanabe, M. (1979). Prefrontal and cingulate unit activity during timing behavior in the monkey. *Brain Research*, *171*(2), 213–224.

O'Callaghan, C., Bertoux, M., & Hornberger, M. (2014). Beyond and below the cortex: The contribution of striatal dysfunction to cognition and behaviour in neurodegeneration. *Journal of Neurology, Neurosurgery & Psychiatry*, *85*(4), 371–378.

Olschowka, J. A., O'Donohue, T. L., Mueller, G. P., & Jacobowitz, D. M. (1982). The distribution of corticotropin releasing factor-like immunoreactive neurons in rat brain. *Peptides*, *3*(6), 995–1015. https://doi.org/10.1016/0196-9781(82)90071-7

Ouhaz, Z., Fleming, H., & Mitchell, A. S. (2018). Cognitive functions and neurodevelopmental disorders involving the prefrontal cortex and mediodorsal thalamus. *Frontiers in Neuroscience*, *12*, 33.

Ouhaz, Z., Perry, B. A., Nakamura, K., & Mitchell, A. S. (2022). Mediodorsal thalamus is critical for updating during extradimensional shifts but not reversals in the attentional set-shifting task. *Eneuro*, *9*(2). https://www.eneuro.org/content/9/2/ENEURO.0162-21.2022.abstract

Panichello, M. F., & Buschman, T. J. (2021). Shared mechanisms underlie the control of working memory and attention. *Nature*, *592*(7855), 601–605.

Parnaudeau, S., Bolkan, S. S., & Kellendonk, C. (2018a). The Mediodorsal Thalamus: An Essential Partner of the Prefrontal Cortex for Cognition. *Biological Psychiatry, Circuits and Symptoms in Schizophrenia*, *83*(8), 648–656. https://doi.org/10.1016/j.biopsych.2017.11.008

Parnaudeau, S., Bolkan, S. S., & Kellendonk, C. (2018b). The mediodorsal thalamus: An essential partner of the prefrontal cortex for cognition. *Biological Psychiatry*, *83*(8), 648–656.

Parnaudeau, S., O'neill, P.-K., Bolkan, S. S., Ward, R. D., Abbas, A. I., Roth, B. L., Balsam, P. D., Gordon, J. A., & Kellendonk, C. (2013). Inhibition of mediodorsal thalamus disrupts thalamofrontal connectivity and cognition. *Neuron*, *77*(6), 1151–1162.

Paspalas, C. D., Wang, M., & Arnsten, A. F. (2013). Constellation of HCN channels and cAMP regulating proteins in dendritic spines of the primate prefrontal cortex: Potential substrate for working memory deficits in schizophrenia. *Cerebral Cortex*, *23*(7), 1643–1654.

Passingham, R. (1975). Delayed matching after selective prefrontal lesions in monkeys (Macaca mulatta). *Brain Research*, *92*(1), 89–102.

Perrin, M., Donaldson, C., Chen, R., Blount, A., Berggren, T., Bilezikjian, L., Sawchenko, P., & Vale, W. (1995). Identification of a second corticotropin-releasing factor receptor gene and characterization of a cDNA expressed in heart. *Proceedings of the National Academy of Sciences*, *92*(7), 2969–2973.

Pezze, M., McGarrity, S., Mason, R., Fone, K. C., & Bast, T. (2014). Too little and too much: Hypoactivation and disinhibition of medial prefrontal cortex cause attentional deficits. *Journal of Neuroscience*, *34*(23), 7931–7946.

Phillips, J. M., Kambi, N. A., Redinbaugh, M. J., Mohanta, S., & Saalmann, Y. B. (2021). Disentangling the influences of multiple thalamic nuclei on prefrontal cortex and cognitive control. *Neuroscience & Biobehavioral Reviews*, *128*, 487–510.

Potter, E., Sutton, S., Donaldson, C., Chen, R., Perrin, M., Lewis, K., Sawchenko, P. E., & Vale, W. (1994). Distribution of corticotropin-releasing factor receptor mRNA expression in the rat brain and pituitary. *Proceedings of the National Academy of Sciences*, *91*(19), 8777–8781. https://doi.org/10.1073/pnas.91.19.8777

Rajbhandari, A. K., Baldo, B. A., & Bakshi, V. P. (2015). Predator stress-induced CRF release causes enduring sensitization of basolateral amygdala norepinephrine systems that promote PTSD-like startle abnormalities. *Journal of Neuroscience*, *35*(42), 14270–14285.

Rao, S. G., Williams, G. V., & Goldman-Rakic, P. S. (2000). Destruction and creation of spatial tuning by disinhibition: GABAA blockade of prefrontal cortical neurons engaged by working memory. *Journal of Neuroscience*, *20*(1), 485–494.

Rikhye, R. V., Gilra, A., & Halassa, M. M. (2018). Thalamic regulation of switching between cortical representations enables cognitive flexibility. *Nature Neuroscience*, *21*(12), 1753–1763. https://doi.org/10.1038/s41593-018-0269-z

Ritchie, J. L., Qi, S., Soto, D. A., Swatzell, S. E., Grenz, H. I., Pruitt, A. Y., Artimenia, L. M., Cooke, S. K., Berridge, C. W., & Fuchs, R. A. (2024). Dorsal raphe to basolateral amygdala corticotropin-releasing factor circuit regulates cocaine-memory reconsolidation. *Neuropsychopharmacology*, *49*(13), 2077–2086. https://doi.org/10.1038/s41386-024-01892-5

Rivier, J., Spiess, J., & Vale, W. (1983). Characterization of rat hypothalamic corticotropin-releasing factor. *Proceedings of the National Academy of Sciences*, *80*(15), 4851–4855. https://doi.org/10.1073/pnas.80.15.4851

Runyan, J. D., Moore, A. N., & Dash, P. K. (2005). A role for prefrontal calcium-sensitive protein phosphatase and kinase activities in working memory. *Learning & Memory*, *12*(2), 103–110.

Saalmann, Y. B. (2014). Intralaminar and medial thalamic influence on cortical synchrony, information transmission and cognition. *Frontiers in Systems Neuroscience*, *8*, 83.

Saffran, M., Schally, A. V., & Benfey, B. G. (1955). Stimulation of the release of corticotropin from the adenohypophysis by a neurohypophysial factor. *Endocrinology*, *57*(4), 439–444.

Sakanaka, M., Shibasaki, T., & Lederis, K. (1987). Corticotropin releasing factor-like immunoreactivity in the rat brain as revealed by a modified cobalt-glucose oxidase-diaminobenzidine method. *Journal of Comparative Neurology*, *260*(2), 256–298. https://doi.org/10.1002/cne.902600209

Sakurai, Y., & Takahashi, S. (2006). Dynamic synchrony of firing in the monkey prefrontal cortex during working-memory tasks. *Journal of Neuroscience*, *26*(40), 10141–10153.

Sarter, M., Givens, B., & Bruno, J. P. (2001). The cognitive neuroscience of sustained attention: Where top-down meets bottom-up. *Brain Research Reviews*, *35*(2), 146–160.

Schmidt, R., Ruiz, M. H., Kilavik, B. E., Lundqvist, M., Starr, P. A., & Aron, A. R. (2019). Beta Oscillations in Working Memory, Executive Control of Movement and Thought, and Sensorimotor Function. *Journal of Neuroscience*, *39*(42), 8231–8238. https://doi.org/10.1523/JNEUROSCI.1163-19.2019

Schmitt, L. I., Wimmer, R. D., Nakajima, M., Happ, M., Mofakham, S., & Halassa, M. M. (2017). Thalamic amplification of cortical connectivity sustains attentional control. *Nature*, *545*(7653), 219–223. https://doi.org/10.1038/nature22073

Sesack, S. R., Deutch, A. Y., Roth, R. H., & Bunney, B. S. (1989a). Topographical organization of the efferent projections of the medial prefrontal cortex in the rat: An anterograde tract-tracing study with Phaseolus vulgaris leucoagglutinin. *Journal of Comparative Neurology*, *290*(2), 213–242. https://doi.org/10.1002/cne.902900205

Sesack, S. R., Deutch, A. Y., Roth, R. H., & Bunney, B. S. (1989b). Topographical organization of the efferent projections of the medial prefrontal cortex in the rat: An anterograde tract-tracing study with Phaseolus vulgaris leucoagglutinin. *Journal of Comparative Neurology*, *290*(2), 213–242. https://doi.org/https://doi.org/10.1002/cne.902900205

Skofitsch, G., & Jacobowitz, D. M. (1985). Distribution of corticotropin releasing factor-like immunoreactivity in the rat brain by immunohistochemistry and radioimmunoassay: Comparison

and characterization of ovine and rat/human CRF antisera. *Peptides*, *6*(2), 319–336. https://doi.org/10.1016/0196-9781(85)90058-0

Spencer, R. C., & Berridge, C. W. (2019). Receptor and circuit mechanisms underlying differential procognitive actions of psychostimulants. *Neuropsychopharmacology*, *44*(10), 1820–1827.

Spencer, R. C., Devilbiss, D. M., & Berridge, C. W. (2015). The cognition-enhancing effects of psychostimulants involve direct action in the prefrontal cortex. *Biological Psychiatry*, *77*(11), 940–950.

Spencer, R. C., Klein, R. M., & Berridge, C. W. (2012). Psychostimulants act within the prefrontal cortex to improve cognitive function. *Biological Psychiatry*, *72*(3), 221–227.

Starkweather, C. K., Gershman, S. J., & Uchida, N. (2018). The medial prefrontal cortex shapes dopamine reward prediction errors under state uncertainty. *Neuron*, *98*(3), 616–629.

Swanson, L. W., Sawchenko, P. E., Rivier, J., & Vale, W. W. (1983a). Organization of Ovine Corticotropin-Releasing Factor Immunoreactive Cells and Fibers in the Rat Brain: An Immunohistochemical Study. *Neuroendocrinology*, *36*(3), 165–186. https://doi.org/10.1159/000123454

Swanson, L. W., Sawchenko, P. E., Rivier, J., & Vale, W. W. (1983b). Organization of Ovine Corticotropin-Releasing Factor Immunoreactive Cells and Fibers in the Rat Brain: An Immunohistochemical Study. *Neuroendocrinology*, *36*(3), 165–186. https://doi.org/10.1159/000123454

Tagliaferro, P., & Morales, M. (2008). Synapses between corticotropin-releasing factor-containing axon terminals and dopaminergic neurons in the ventral tegmental area are predominantly glutamatergic. *Journal of Comparative Neurology*, *506*(4), 616–626.

Tanibuchi, I., & Goldman-Rakic, P. S. (2003). Dissociation of Spatial-, Object-, and Sound-Coding Neurons in the Mediodorsal Nucleus of the Primate Thalamus. *Journal of Neurophysiology*, *89*(2), 1067–1077. https://doi.org/10.1152/jn.00207.2002

Taniguchi, H., He, M., Wu, P., Kim, S., Paik, R., Sugino, K., Kvitsani, D., Fu, Y., Lu, J., Lin, Y., Miyoshi, G., Shima, Y., Fishell, G., Nelson, S. B., & Huang, Z. J. (2011). A Resource of Cre Driver Lines for Genetic Targeting of GABAergic Neurons in Cerebral Cortex. *Neuron*, *71*(6), 995–1013. https://doi.org/10.1016/j.neuron.2011.07.026

Taylor, J. R., Birnbaum, S., Ubriani, R., & Arnsten, A. F. (1999). Activation of cAMP-dependent protein kinase A in prefrontal cortex impairs working memory performance. *The Journal of Neuroscience*, *19*(18), RC23.

Tizard, B. (1958). The Psychological Effects of Frontal Lesion: A review of the evidence. *Acta Psychiatrica Scandinavica*, *33*(2), 232–250.

Tran, Y., Craig, A., Craig, R., Chai, R., & Nguyen, H. (2020). The influence of mental fatigue on brain activity: Evidence from a systematic review with meta-analyses. *Psychophysiology*, *57*(5), e13554. https://doi.org/10.1111/psyp.13554

Uribe-Mariño, A., Gassen, N. C., Wiesbeck, M. F., Balsevich, G., Santarelli, S., Solfrank, B., Dournes, C., Fries, G. R., Masana, M., Labermeier, C., Wang, X.-D., Hafner, K., Schmid, B., Rein, T., Chen, A., Deussing, J. M., & Schmidt, M. V. (2016). Prefrontal Cortex Corticotropin-Releasing Factor Receptor 1 Conveys Acute Stress-Induced Executive Dysfunction. *Biological Psychiatry, Stress, Fear, and Anxiety*, *80*(10), 743–753. https://doi.org/10.1016/j.biopsych.2016.03.2106

Vale, W., Spiess, J., Rivier, C., & Rivier, J. (1981). Characterization of a 41-residue ovine hypothalamic peptide that stimulates secretion of corticotropin and β-endorphin. *Science*, *213*(4514), 1394–1397.

Valentino, R. J., Rudoy, C., Saunders, A., Liu, X.-B., & Van Bockstaele, E. J. (2001). Corticotropin-releasing factor is preferentially colocalized with excitatory rather than inhibitory amino acids in axon terminals in the peri-locus coeruleus region. *Neuroscience*, *106*(2), 375–384. https://doi.org/10.1016/S0306-4522(01)00279-2

Valentino, R. J., Van Bockstaele, E., & Bangasser, D. (2013). Sex-specific cell signaling: The corticotropin-releasing factor receptor model. *Trends in Pharmacological Sciences*, *34*(8), 437–444.

Van Pett, K., Viau, V., Bittencourt, J. C., Chan, R. K., Li, H.-Y., Arias, C., Prins, G. S., Perrin, M., Vale, W., & Sawchenko, P. E. (2000). Distribution of mRNAs encoding CRF receptors in brain and pituitary of rat and mouse. *Journal of Comparative Neurology*, *428*(2), 191–212.

Vijayraghavan, S., Wang, M., Birnbaum, S. G., Williams, G. V., & Arnsten, A. F. (2007). Inverted-U dopamine D1 receptor actions on prefrontal neurons engaged in working memory. *Nature Neuroscience*, *10*(3), 376–384.

Voorn, P., Vanderschuren, L. J., Groenewegen, H. J., Robbins, T. W., & Pennartz, C. M. (2004). Putting a spin on the dorsal–ventral divide of the striatum. *Trends in Neurosciences*, *27*(8), 468–474.

Wang, H., Qian, T., Zhao, Y., Zhuo, Y., Wu, C., Osakada, T., Chen, P., Chen, Z., Ren, H., Yan, Y., Geng, L., Fu, S., Mei, L., Li, G., Wu, L., Jiang, Y., Qian, W., Zhang, L., Peng, W., … Li, Y. (2023). A tool kit of highly selective and sensitive genetically encoded neuropeptide sensors. *Science*, *382*(6672), eabq8173. https://doi.org/10.1126/science.abq8173

Wang, M., Ramos, B. P., Paspalas, C. D., Shu, Y., Simen, A., Duque, A., Vijayraghavan, S., Brennan, A., Dudley, A., & Nou, E. (2007). α2A-adrenoceptors strengthen working memory networks by inhibiting cAMP-HCN channel signaling in prefrontal cortex. *Cell*, *129*(2), 397–410.

Wang, M., Yang, Y., Wang, C.-J., Gamo, N. J., Jin, L. E., Mazer, J. A., Morrison, J. H., Wang, X.-J., & Arnsten, A. F. (2013). NMDA receptors subserve persistent neuronal firing during working memory in dorsolateral prefrontal cortex. *Neuron*, *77*(4), 736–749.

Wang, X.-J. (2001). Synaptic reverberation underlying mnemonic persistent activity. *Trends in Neurosciences*, *24*(8), 455–463.

Wang, Y., Hu, P., Shan, Q., Huang, C., Huang, Z., Chen, P., Li, A., Gong, H., & Zhou, J.-N. (2021). Single-cell morphological characterization of CRH neurons throughout the whole mouse brain. *BMC Biology*, *19*(1), 47. https://doi.org/10.1186/s12915-021-00973-x

Wascher, E., Rasch, B., Sänger, J., Hoffmann, S., Schneider, D., Rinkenauer, G., Heuer, H., & Gutberlet, I. (2014). Frontal theta activity reflects distinct aspects of mental fatigue. *Biological Psychology*, *96*, 57–65. https://doi.org/10.1016/j.biopsycho.2013.11.010

Watanabe, M. (1989). The appropriateness of behavioral responses coded in post-trial activity of primate prefrontal units. *Neuroscience Letters*, *101*(1), 113–117.

Watanabe, M. (1990). Prefrontal unit activity during associative learning in the monkey. *Experimental Brain Research*, *80*(2), 296–309.

Watanabe, M. (1992). Frontal units of the monkey coding the associative significance of visual and auditory stimuli. *Experimental Brain Research*, *89*(2), 233–247.

Watanabe, Y., & Funahashi, S. (2004). Neuronal Activity Throughout the Primate Mediodorsal Nucleus of the Thalamus During Oculomotor Delayed-Responses. I. Cue-, Delay-, and Response-Period Activity. *Journal of Neurophysiology*, *92*(3), 1738–1755. https://doi.org/10.1152/jn.00994.2003

Watanabe, Y., & Funahashi, S. (2012). Thalamic mediodorsal nucleus and working memory. *Neuroscience & Biobehavioral Reviews*, *36*(1), 134–142. https://doi.org/10.1016/j.neubiorev.2011.05.003

Watanabe, Y., & Funahashi, S. (2018). Change of information represented by thalamic mediodorsal neurons during the delay period. *NeuroReport*, *29*(6), 466. https://doi.org/10.1097/WNR.0000000000000998

Wolff, M., & Halassa, M. M. (2024). The mediodorsal thalamus in executive control. *Neuron*. https://doi.org/10.1016/j.neuron.2024.01.002

Woo, E., Datta, D., & Arnsten, A. F. (2022). Glutamate metabotropic receptor type 3 (mGlu3) localization in the rat prelimbic medial prefrontal cortex. *Frontiers in Neuroanatomy*, *16*, 849937.

Wu, D., Deng, H., Xiao, X., Zuo, Y., Sun, J., & Wang, Z. (2017). Persistent neuronal activity in anterior cingulate cortex correlates with sustained attention in rats regardless of sensory modality. *Scientific Reports*, *7*(1), 1–14.

Yuen, E. Y., Wei, J., Liu, W., Zhong, P., Li, X., & Yan, Z. (2012). Repeated stress causes cognitive impairment by suppressing glutamate receptor expression and function in prefrontal cortex. *Neuron*, *73*(5), 962–977.

Zhao, C., Eisinger, B., & Gammie, S. C. (2013). Characterization of GABAergic Neurons in the Mouse Lateral Septum: A Double Fluorescence In Situ Hybridization and Immunohistochemical Study Using Tyramide Signal Amplification. *PLoS ONE*, *8*(8). https://doi.org/10.1371/journal.pone.0073750